The northern Barents Sea during 1970–2016:

From seabed to surface in the Arctic warming hotspot

Sigrid Lind

Thesis for the Degree of Philosophiae Doctor (PhD)
University of Bergen, Norway
2018

UNIVERSITY OF BERGEN

The northern Barents Sea during 1970–2016:

From seabed to surface in the Arctic warming hotspot

Sigrid Lind

Thesis for the Degree of Philosophiae Doctor (PhD)
at the University of Bergen

2018

Date of defence: 09.05.2018

Year: 2018

Title: The northern Barents Sea during 1970–2016:

Name: Sigrid Lind

Print: Skipnes Kommunikasjon / University of Bergen

Year: 2018

Title: The northern Barents Sea during 1970–2016:

From seabed to surface in the Arctic warming hotspot

Author: Sigrid Lind

Print: AIT Bjerch AS / University of Bergen

Scientific environment

This work has been conducted at the Research Group of Oceanography and Climate at Havforskningsinstituttet (Institute of Marine Research, Norway) with workplace at its Tromsø department. The formal educational institution was the Geophysical Institute at the University of Bergen. The candidate has also been associated with the Bjerknes Centre for Climate Research, and a member of the Norwegian Research School in Climate Dynamics (ResClim) and the following Research school on changing climates in the coupled earth system (CHESS).

Acknowledgements

This PhD-life has been a long adventure, with many summits to climb, endless fields to endure and some very fun downhills to enjoy. On this journey, I always felt well supported by my supervisors, Tore Furevik at the Geophysical Institute, University of Bergen and Randi B. Ingvaldsen at the Institute of Marine Research. It has been a true pleasure working with you. Thank you for seeing me and believing in me, for your kindness and patience, and for your constructive, thorough criticism. I'm also thankful to co-supervisors Jofrid Skardhamar and Vigdis Tverberg for support whenever needed, to the Institute of Marine Research for the opportunity to explore the northern Barents Sea – the coolest job I could imagine, to the Norwegian Research Council for financial support, to the University of Bergen for educational support, to ResClim for valuable courses and network, to the people at the Research Group of Oceanography and Climate for the good times we've shared, to Geofysen and UNIS for very good courses and memorable cruises in the Arctic and to Tor Gammelsrød for being such an inspiring person, to friends and colleagues at IMR in Tromsø – Gin, Celia, Helene, Kristin, Benjamin, Uffe, Affe, Gunnar, Keka, Atal, Lise, Heidi and many others – life in the Arctic is great because of you! Lots of thanks also to family, friends, neighbours and Skogstua barnehage. My polar adventure started in Svalbard. It was the best of times, and I'm grateful for the good friends I found there, especially, Ane, Anne, Tore, Ilona, Johannes, Lisa and Fredrik, who we sadly lost all too soon. Svalbard was also where we connected, my dear Eirik. You brought happiness back to all of me, always believing in me, never having any doubts – not even to have three children during the PhD. Thank you for the everlasting, crucial and valuable support – we did this together! Finally, I'm immensely grateful for our wonderful, creative children – Birk, Håkon and Louise. You keep inspiring, challenging and surprising me every day, reminding me what life is truly about and why we *must* treasure our planet. *–Mamma Sigrid*

The difficult is what takes a little time,
the impossible is what takes a little longer.
–Fridtjof Nansen

Abstract

Global warming is amplified in the cold and white Arctic, where strong positive feedback mechanisms associated with, e.g., changes in surface conditions and the vertical structure of the Arctic atmosphere enhance the warming. The Arctic sea ice cover is described as a sensitive indicator for global warming, despite substantial internal climate variability in the region. The contribution to Arctic climate change from the oceanic heat source – the deep Atlantic layer – is to a large extent unknown, as there are only sparse measurements of the upward heat fluxes from the ocean, and it is not well understood which factors make the heat fluxes vary, laterally and temporally. This is perhaps one of the last big unknowns in the Arctic climate puzzle.

The Arctic warming has a distinct regional maximum where the winter sea ice decline and the surface warming are greatest. The northern Barents Sea is in this 'Arctic warming hotspot' and here the warming extends high up into the lower atmosphere and deep down into the water column. The Arctic warming hotspot has been linked to large-scale changes in the atmospheric circulation and mid-latitude weather extremes. As a consequence of the warming, structural changes are observed in the Barents Sea ecosystem, a productive and complex Arctic-boreal shelf ecosystem, inhabiting both valuable commercial fish stocks and vulnerable sea ice-associated marine mammals. The varying position of the sea ice edge in the Barents Sea is a complicating factor for activities across a range of sectors, including research, ecosystem management, fisheries, petroleum, shipping and tourism, and is therefore both a national and a geopolitical issue.

The triggering factors and governing mechanisms for the ongoing rapid warming are not well understood, although increased heat losses to the atmosphere in autumn and winter is a likely consequence of the reduced sea ice cover. It is not known what role the ocean plays in the Arctic warming hotspot, and what the ongoing processes here can tell us about how the Arctic climate will develop as the planet become warmer. The northern Barents Sea has been monitored annually in joint Norwegian-Russian ecosystem surveys since the early 1970's, resulting in unique data documenting the

changes in the Arctic. The data describes the entire water column's interannual variability and development through five decades of climate change. In this thesis, the data set is employed to investigate the interaction between the sea ice cover and the three layers of the water column, the Surface-, the Arctic and the Atlantic layers, and how changes relate to other factors such as surface air temperature, surface wind patterns, upstream Atlantic Water temperature and sea ice import from the interior Arctic Ocean. With focus on the vertical water column structure, the objectives are to identify the key factors that control the vertical heat fluxes from the deep Atlantic layer towards the surface, and the key factors that maintain the stratification of the water column. The role of the ocean for the Arctic warming hotspot, the wider Arctic, and the global climate system is further discussed.

The main findings of this thesis are that the intermediate, cold and fresh Arctic layer plays a key role in limiting the vertical heat exchange in the water column, and that the interannual variability of the Arctic layer salinity is a controlling factor for the strength of the vertical mixing and thus the upward fluxes of heat and salt from the deep Atlantic layer. The salt flux implies a freshwater input is needed to maintain the stratification. The sea ice import from the interior Arctic domain is the main freshwater input to the area, affecting the Barents Sea ice cover directly through adding ice, and indirectly through adding freshwater that maintains the stratification and makes the conditions for new sea ice growth favourable.

A sharp decline in the sea ice inflow to the Barents Sea after ~2005 has resulted in a large, significant and comprehensive shift in the water column structure in the northern Barents Sea. By 2016, the water column had lost about one meter (40 %) of its normal freshwater content and was weakly stratified, much warmer, and with a very limited winter sea ice cover. If the sea ice import does not soon recover, the stratification in the northern Barents Sea will likely break down completely, and make the entire Barents Sea ice free all year round, with unknown consequences for the circulation, the water mass distributions and the ecosystem in the Barents Sea. The exact timing of such a breakdown is hard to predict due to substantial variability in the atmospheric forcing and the sea ice import, but given the rapidly declining

Arctic sea ice thickness and extent and reduction in thick, old ice in the Eurasian Basin, sufficiently large sea ice inflows to recover the stratification in the northern Barents Sea become less and less probable.

The results of this thesis highlight the importance of the stratified boundary layers in the Arctic air-ice-sea column, limiting vertical exchange of properties. Local positive feedback mechanisms, in addition to less import of fresh water in the form of sea ice, have been found to be essential for the changes that have led to the Arctic warming hotspot. The mechanisms outlined in the thesis will continue to play a key role, when larger areas with cold, stratified and sea ice covered Arctic waters will transform to warmer, weaker stratified, seasonally ice-covered waters. The thesis shows that the present northern Barents Sea is in an unstable state that depends on regular freshwater input, and that stratification and distribution of freshwater are crucial aspects of the *new Arctic* on a warmer planet.

List of publications

Lind, S. & Ingvaldsen, R. B. (2012): Variability and impacts of Atlantic Water entering the Barents Sea from the north, Deep-Sea Research I, 62: 70–88.

Lind, S., Ingvaldsen, R. B. & Furevik, T. (2016): Arctic layer salinity controls heat loss from deep Atlantic layer in seasonally ice-covered areas of the Barents Sea, Geophysical Research Letters, 43.

Lind, S., Ingvaldsen, R. B. & Furevik, T.: Declining sea ice import and freshwater loss causes Arctic warming hotspot, *in review for Nature Climate Change*.

Contents

Scientific environment **3**

Acknowledgements **5**

Abstract **7**

List of publications **11**

----

1. Introduction **15**

2. Background **21**

3. Data and methods **31**

4. Summary of papers **35**

5. Discussion **39**

6. Future Arctic **43**

References **51**

Papers I–III attached **57**

1. Introduction

1.1 Global warming hotspot in the Arctic

Since the prehistoric transition from hunting societies to agriculture societies ten millennia ago, humans have been blessed with a very stable climate (Feynman & Ruzmaikin, 2007). Due to our emissions of greenhouse gases and global warming, this is no longer the case. In the era of human history, climate has never changed faster (e.g., Houghton et al., 2001; Root et al., 2003; Walther et al., 2002). One of the key features of the rapid on-going global warming is that it amplifies in the cold and white Arctic (Figure 1), where longer melt seasons make the Arctic darker, and more incoming solar radiation is absorbed in the soil- and ocean surfaces (e.g., Manabe & Stouffer, 1980; Holland & Bitz, 2003; Screen & Simmonds, 2010; Serreze & Barry, 2011). This so-called surface albedo feedback and temperature feedbacks related to characteristics of the Arctic atmosphere are two of many positive feedback mechanisms that causes the Arctic to warm about twice as fast as the global average (Serreze & Barry, 2011; Pithan & Mauritsen, 2014). Arctic amplification is also seen in paleoclimate records, and is recognised as an inherent characteristic of the global climate system (Serreze & Barry, 2011).

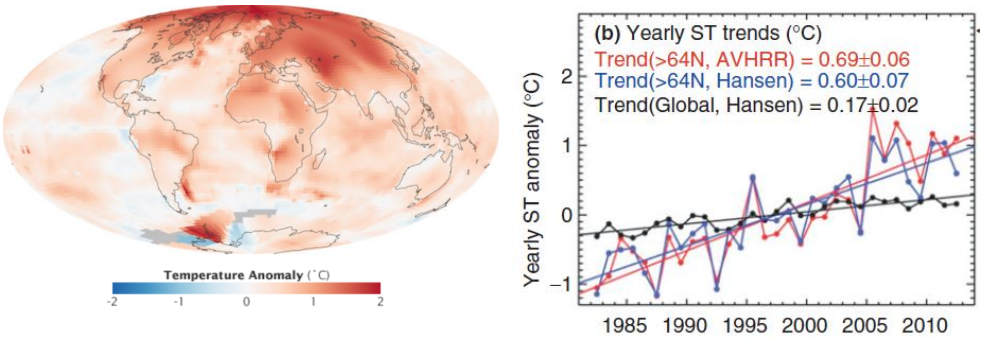

Figure 1. Left panel: Global temperature anomalies for the period 2000–2009 rel. to the 1951–1980-mean (NASA GISS). Right panel: Yearly surface temperature anomalies and trends for the Arctic (>64 °N; blue and red) and the entire globe (black) as indicated. Excerpt from Figure 2 in Comiso & Hall (2014), licensed under CC BY 3.0.

The Arctic sea ice cover is a highly sensitive climate variable that both responds to, and acts to amplify, human-induced global warming (Notz & Stroeve, 2016), but internal climate variability related to changes in the atmosphere (Ding et al., 2017) and to fluctuations in the ocean on multi-decadal time scales also significantly impacts it (Polyakov et al., 2002).The result is that the Arctic sea ice cover is rapidly becoming thinner, younger and more dynamic (e.g., Carmack et al., 2015; Figure 2), leading to increased heat flues to the atmosphere (Serreze et al., 2009) and maximum warming in autumn and winter (Screen & Simmonds, 2010; Bintanja & van der Linden, 2013). The rapid climate change in the Arctic brings large changes to Arctic indigenous societies and ecosystems adapted to the cold, harsh, light- and nutrient-limited Arctic environment (e.g., Huntington et al., 2005; Nuttall et al., 2005; Hoegh-Guldberg & Bruno, 2010). It also has socio-economic impacts across a range of sectors, including fisheries, oil and gas, shipping, tourism and research. Forecasting of the Arctic sea ice cover is therefore a matter of great interest and concern (Serreze & Stroeve, 2015).

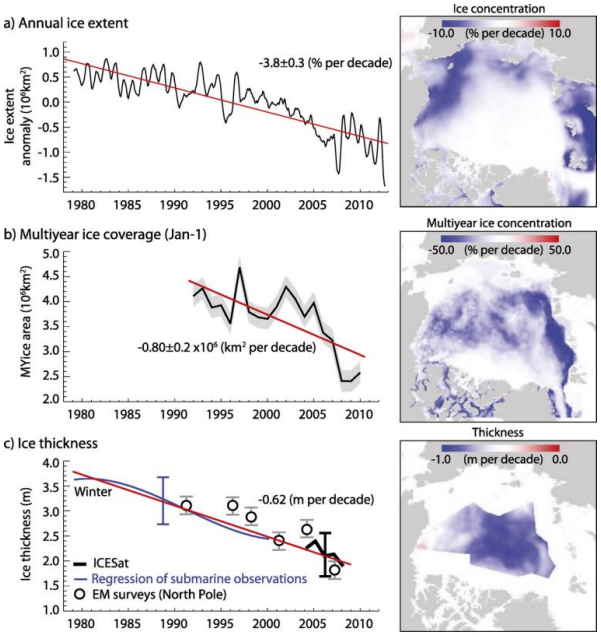

Figure 2. Linear decadal trends (red lines) and patterns of change in (a) anomalies in Arctic sea ice extent, (b) multiyear sea ice coverage on 1 Jan, and (c) sea ice thickness from submarine (blue), satellites (black), and in situ/electromagnetic surveys (circles); error bars show uncertainties in observations. Excerpt from Figure 1 in Carmack et al. (2015), ©2015 American Meteorological Society.

It is not known to which degree the poleward transports of heat in the atmosphere and the ocean are contributing to Arctic amplification (Pithan & Mauritsen, 2014). The oceanic heat import to the Arctic is with the poleward Atlantic Water flow, entering the Arctic Ocean in two branches, through the Fram Strait and via the southern Barents Sea. Both continue as subsurface flows below fresher, lighter upper layers eastwards in the Eurasian Basin (e.g., Schauer et al., 2002; Figure 3). The contribution from the oceanic heat source to the fast-declining Arctic sea ice cover is to a large extent unknown, but has been proposed to be modest or negligible owing to its subsurface presence below the cold halocline (Aagaard et al., 1981). Recently, however, considerable upward heat fluxes from the deep Atlantic layer have been observed along the Eurasian Basin margins (Polyakov et al., 2012c; Polyakov et al., 2013). The "heat in the deep" may become increasingly important in the development towards a *new Arctic* (Carmack et al., 2015; Polyakov et al., 2017), and knowledge of the factors that control variability in the upward heat fluxes in the stratified interior Arctic Ocean is needed (Carmack et al., 2015).

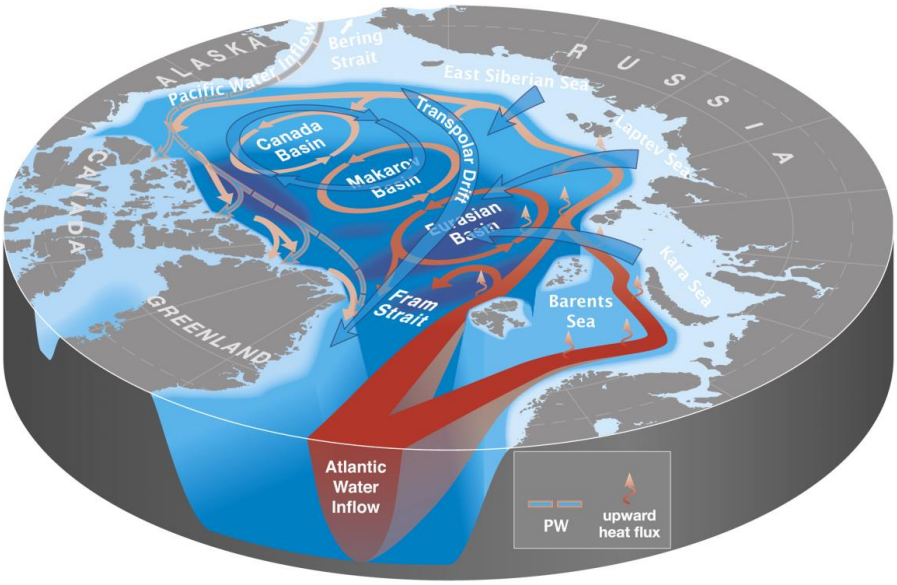

Figure 3. Schematic of the circulation in the Arctic Ocean from Carmack et al. (2015), modified from Polyakov et al. (2012a), showing the circulation of the Atlantic Water (red and pink), surface water (blue) and intermediate Pacific Water (dashed), ©2015 American Meteorological Society.

The largest decline in winter sea ice cover, and strongest increase in surface temperatures, in the Arctic are found in the northern Barents and Kara Seas (Screen & Simmonds, 2010; Comiso & Hall, 2014; Figure 4). In this 'Arctic warming hotspot', the warming extends into the lower atmosphere (Screen & Simmonds, 2010) and throughout the entire water column (Lind & Ingvaldsen, 2012; Smedsrud et al., 2013). Stretching from seabed to surface and into the lower atmosphere, the warming hotspot is evidently a strong signal in the Arctic amplification pattern, and it has been linked to changes in the large-scale atmospheric circulation (Cohen et al., 2014) and extreme mid-latitude weather (Petoukhov & Semenov, 2010), and causes structural ecosystem changes (Fossheim et al., 2015). Due to less sea ice and more absorption of heat in summer, warmer surface waters delay ice freezing and warms the lower atmosphere in autumn and winter in the northern Barents and Kara Seas, as also seen in many other areas in the Arctic (Screen & Simmonds, 2010). The mechanisms causing this region to have elevated warming are not well understood—the role of the ocean largely unknown. What is triggering the rapid change here? Can we learn from the ongoing warming to deepen our understanding of the development towards a new Arctic on a warmer planet? And, has upward heat fluxes from the deep Atlantic layer played a part in the Arctic warming hotspot?

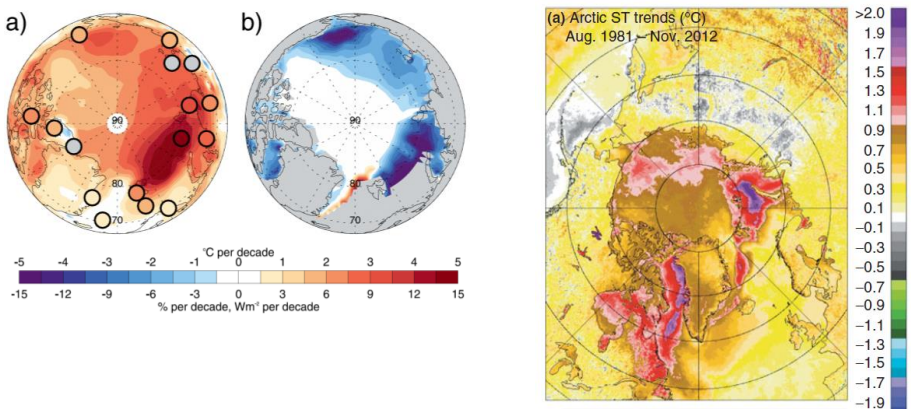

Figure 4. Right panel: (a) Surface air temperature trends (°C decade^{-1}) during Oct–Jan, 1989–2009, from observations (colored dots) and from ERA-Interim (shading). (b) Corresponding trends for sea ice concentration (% decade^{-1}). Excerpt from Figure 2 in Screen & Simmonds (2010), ©2010 American Geophysical Union. Left panel: Surface temperature trends for the entire Arctic using Aug 1981–Nov 2012 advanced very high resolution radiometer (AVHRR) data. Excerpt from Figure 2 in Comiso & Hall (2014), licensed under CC BY 3.0.

1.2 Objectives of this thesis

The Arctic Ocean is generally poorly observed, being largely inaccessible most of the year, but the northern Barents Sea is an exception, having been annually monitored since the early 1970s. The unique data set from the northern Barents Sea enables detailed studies of the interplay between the different layers of the water column and the sea ice cover during five decades of ongoing climate change in the Arctic water column, right in the centre of the Arctic warming hotspot. Here, the data set is applied to evaluate the role of the ocean in the warming, with focus on the water column structure, the processes that act to maintain or disintegrate the structure, and recent changes in it. The objectives of the thesis are (1) to describe the mean state and normal variability of the water column, (2) to identify key factors that determine the vertical heat fluxes from the deep Atlantic layer and maintenance of the stratification, and (3) to evaluate the role of the ocean and the processes that leads to the substantial changes observed in the region. The work was divided in three papers. First, the mean state, variability and distribution of water masses were described, with a focus on the deep Atlantic layer (Paper I). Next, the role of the intermediate Arctic layer was investigated (Paper II). Finally, the seasonal Surface layer, sea ice cover, heat and freshwater contents and the sea ice inflow to the region were studied, and recent disappearance of Arctic Water discussed (Paper III). Fundamental changes in the northern Barents Sea's water column structure were found, and a conceptual scheme following the Atlantic Water flow into the Arctic was proposed, linking the vertical processes with lateral inflows of sea ice above and Atlantic Water below.

2. Background

2.1 At the entrance to the Arctic

The Barents Sea is the deepest and largest shelf-sea of the Arctic Ocean, situated at the entrance to the deep polar basin (Figure 5). The Barents Sea is ~1.6 million km^2 and has an average depth of 230 m, but the bathymetry is diverse with deep trenches cutting between several banks and islands (Figure 6). It is bordered by the Norwegian and Russian mainland's in the south, the eastern steep continental shelf-slope towards the Norwegian Sea in the west, the Svalbard and Franz Josef Land archipelagos and northern continental shelf-slope in the north, and the far-stretched island Novaya Zemlya in the east. The Barents Sea is one of the two places where the poleward flowing warm and saline Atlantic Water – the main oceanic heat source in the Arctic – encounters the cold and stratified Arctic Ocean, the other direct encounter area is north of Svalbard (Figure 3).

The Arctic Ocean is largely inaccessible throughout the year due to its perennial sea ice cover, and for centuries there where large white, undiscovered areas on the Arctic map. Scientists speculated that although ice-covered at the coasts they had visited, the interior Arctic could be warmer and have open water due to the inflow of the warm Atlantic Water (Rudels, 2012). The first major successful scientific exploration of the interior Arctic Ocean was the Fram expedition in the late 19th century, led by Dr. Fridtjof Nansen. His specially designed, modern research vessel at the time, "*Fram*", was frozen into the ice-pack in the north-eastern Laptev Sea, and drifted across the Polar Basin over three years, 1893–96. Nansen found that the interior Arctic Ocean was a sea ice-covered, very cold and deep ocean, with Atlantic Water found as a subsurface layer underneath a lighter, thin layer of fresh and cold waters (Nansen, 1902). He noted that the stratification made from this thin 'Arctic layer' isolated the heat of the deeper, denser 'Atlantic layer' from direct contact with the surface, thereby enabling sea ice to cover the interior Arctic Ocean. The Arctic environment is also recognized by its cold and dense lower atmosphere having increasing temperature with height (i.e., low-level inversion; Sverdrup, 1933; Serreze et al.,

1992) and complex processes in its sea ice cover with ridging and rafting, melt ponds formation, snow cover and seasonal melt and growth cycles (e.g., Wadhams, 2000). The mean circulation of the wind-driven sea ice and surface waters are transpolar and anticyclonic, whereas the Atlantic layer has cyclonic circulations in all sub-basins (e.g., Rudels, 2012). It is less known how the intermediate Arctic- or halocline layer in the Arctic circulates (Jones, 2001).

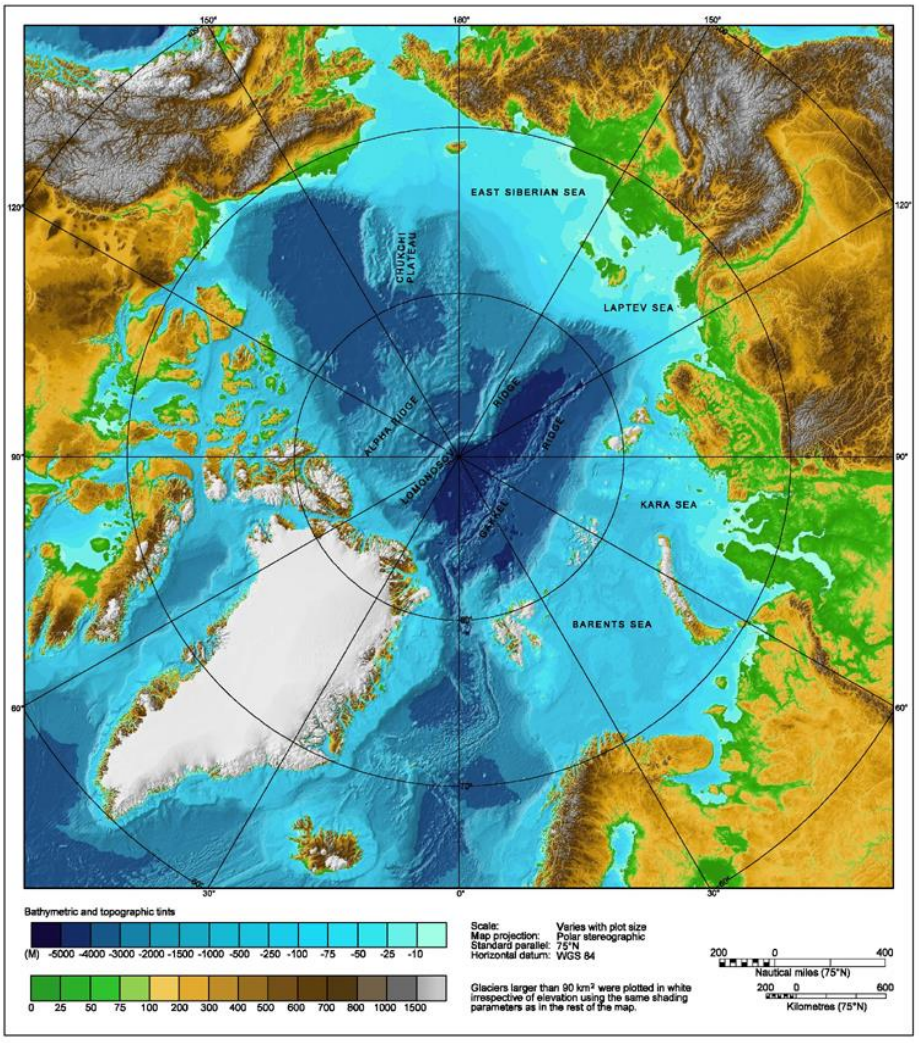

Figure 5. Bathymetry of the Arctic Ocean from the International Bathymetric Chart of the Arctic Ocean (IBCAO) Version 3.0, from Jakobsson et al. (2012), doi:10.1029/2012GL052219.

Mosby (1938) discovered that in the ice-covered northern Barents Sea, Atlantic Water enters from the north, deep in the two troughs between Svalbard and Franz Josef Land (Figure 6). The Atlantic Water is further advected south-westward in the deep trenches of the northern Barents Sea, all the time below the fresher, colder Arctic layer (Pfirman et al., 1994), and Atlantic Water has been observed year-round in Olga Basin, the innermost part of the northern Barents Sea trench-system (Abrahamsen et al., 2006). Atlantic Water does not enter the northern Barents Sea at the surface or upper layers due to the lighter Arctic water mass occupying the area. The oceanic Polar Front, separating the Arctic and Atlantic water masses, is topographically controlled and largely stationary in the western Barents Sea where the bathymetry is steep (Loeng, 1991; Gawarkiewicz & Plueddemann, 1995; Harris et al., 1998). The Arctic layer therefore becomes colder, fresher and thicker southwards in the northern Barents Sea, and in the Olga Basin just north of the Polar Front, it has its purest Arctic-type conditions (Lind & Ingvaldsen, 2012). The conditions within the interior northern Barents Sea therefore resembles the conditions in the interior Arctic Ocean, with a cold, stratified and sea ice covered water column with upward fluxes from its deep Atlantic layer.

On its eastward transfer through the southern Barents Sea, the Atlantic Water spreads out and occupies most of the area south of the Polar Front at surface in direct contact with the atmosphere and is efficiently cooled (Smedsrud et al., 2010 Figure 3). In contrast, the branch going through the Fram Strait is a narrow northward flowing current hugging the continental shelf-slope west of Svalbard, the West-Spitsbergen Current, and although some cooling and recirculation occurs in the Fram Strait, it keeps more of its heat before turning east at the northern tip of Spitsbergen (e.g., Beszczynska-Möller et al., 2012). North of Svalbard and in the south-eastern Barents Sea, Atlantic Water directly encounters and melts sea ice (Årthun et al., 2012; Onarheim et al., 2014) forming halocline waters that likely contribute to the halocline of the interior Arctic Ocean (e.g., Steele et al., 1995, Rudels et al., 2004; Rudels, 2016).

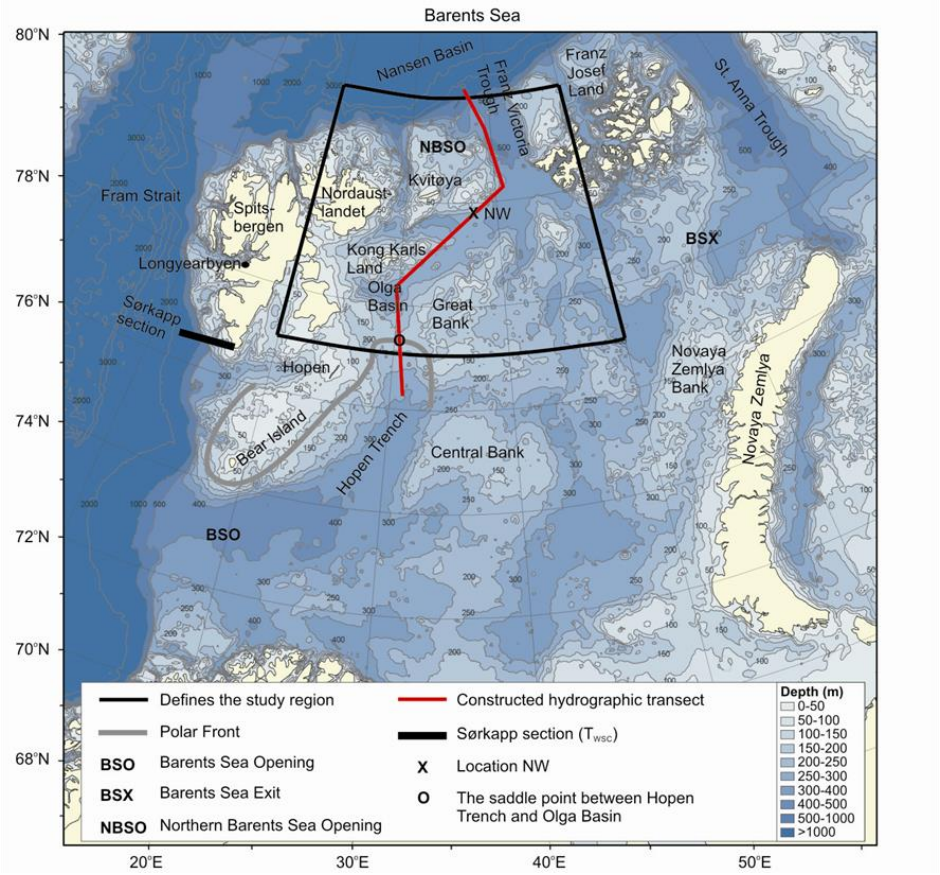

Figure 6. Detailed bathymetry of the Barents Sea showing depth (blue-coloured contours), the studied area in the northern Barents Sea (black outline) and position of the stationary, western part of the Polar Front (grey line). From Lind & Ingvaldsen (2012), ©2012 Elsevier.

The Atlantic Water continues eastward as a subsurface current below fresher halocline waters in the Arctic Ocean, via the Kara Sea for the Barents Sea branch (Figure 3). The deep Atlantic Water gradually becomes colder and fresher on its journey in the deep within the Arctic Ocean (Rudels, 2012), and within the northern Barents Sea (Mosby, 1938; Pfirman et al., 1994). This indicates that vertical mixing with the overlying Arctic layer is an important process for vertical heat fluxes up from the deep Atlantic layer into the cold and stratified Arctic regime. It has been known for more than a century that there is enough heat in the deep Atlantic layer to melt the entire sea ice cover several times (Nansen, 1902), but the vertical fluxes have for decades been considered weak and negligible (Aagaard et al., 1981). There are

only sparse measurements of the upward heat fluxes from the deep Atlantic layer, varying from negligible (0.05 Wm^{-2}; Fer, 2009) to moderate O(5−10) Wm^{-2} in stratified areas (Polyakov et al., 2012c), to very strong in areas where Atlantic Water directly encounters sea ice north of Svalbard (e.g., Carmack et al., 2015). Compared with the interior Arctic Ocean, the northern Barents Sea probably has stronger turbulence-generating forcing due to tidal effects on the shallow shelf with varying bathymetry and degree of mixing, and occasional observations of heat fluxes vary from O(10) to O(100) Wm^{-2} (Sundfjord et al., 2007). Process-studies are needed to improve the understanding of the vertical heat fluxes in the stratified interior Arctic, particularly identification of other factors that the heat fluxes depend on but that are more easily measured (Carmack et al., 2015). Given the rapid development towards a new Arctic on a warmer planet, this is perhaps one of the last important "white points" to map in the Arctic climate system.

2.2 A dynamic and complex region

The Barents Sea is essentially divided into two parts with distinctly different climate, Atlantic in the south and Arctic in the north, separated by the oceanic Polar Front (Loeng, 1991). Whereas the southern Barents Sea has been known for its large interannual to decadal fluctuations in temperature and fisheries for more than a century (Helland-Hansen & Nansen, 1909), the northern Barents Sea has in contrast been considered to have a very stable and cold climate (Mosby, 1938; Loeng, 1991). The major Atlantic Water inflow through the passage in southeast, between Fugløya and Bjørnøya, or Barents Sea Opening (BSO), has large variability in transport and properties (Ådlandsvik & Loeng, 1991; Furevik, 2001), a net inflow of 1.8 Sv (Ingvaldsen et al., 2004) and affects the climate the southern Barents Sea (e.g., Ådlandsvik & Loeng, 1991; Årthun et al., 2012). The Atlantic layer in the northern Barents Sea is renewed by advection from a branch of the Atlantic Water boundary current along the northern slope of the Barents, the continuation of the inflow to Arctic through the Fram Strait. It enters Barents Sea from the north as a deep inflow below the fresher, lighter Arctic layer through the two troughs between Svalbard and

Franz Josef Land (Mosby, 1938; Pfirman et al., 1994; Lind & Ingvaldsen, 2012; Figure 7). In addition, some Atlantic Water enters the region in the deep from the southern Barents Sea, crossing the Polar Front below the Arctic layer (Loeng, 1991).

Despite the stable climate, the northern Barents Sea is a dynamic region with a multitude of different water masses and processes active on shorter time scales. In addition to the Atlantic Water inflow, Arctic Water presence and sea ice cover, sea ice melts in spring and forms an annual surface mixed layer that warms during summer (Loeng, 1991). In winter, dense water is produced on the shallow banks from cooling and brine release during sea ice growth (Midttun, 1985), producing water with a variety of densities that fills the deep trenches of the Barents Sea and the deep polar basin at different depths (Årthun et al., 2011). Surface and Arctic Waters have been considered entering the Barents Sea from the northeast and flowing south-westward in the northern Barents Sea (Novitskiy, 1961; Tantsiura, 1973) and seem to tend to anticyclonic circulation within the Barents Sea, but there are no published volume estimates of this current system (Loeng, 1991). One of the first comprehensive studies of the hydrographic features of the Barents Sea was by Loeng (1991), and Pfirman et al. (1994) described in more detail the distribution and modification of water masses in the northern Barents Sea. The core characteristics of Pfirman et al. (1994) and extreme values found by Mosby (1938) are here combined and the water masses in the northern Barents Sea defined as surface water/melt water ($-1.9<T<4.0$°C, $S<34.0$), Arctic Water ($T<0.0$°C, $34.0<S<34.7$), Atlantic Water ($T>0.0$°C, $S>34.7$) and bottom water/Cold Dense Water ($T<0.0$°C, $S>34.75$), where salinities are practical salinity units (psu), see Sections 1 and 3 of Lind & Ingvaldsen (2012) for a more detailed literature review and description of the water masses in the northern Barents Sea.

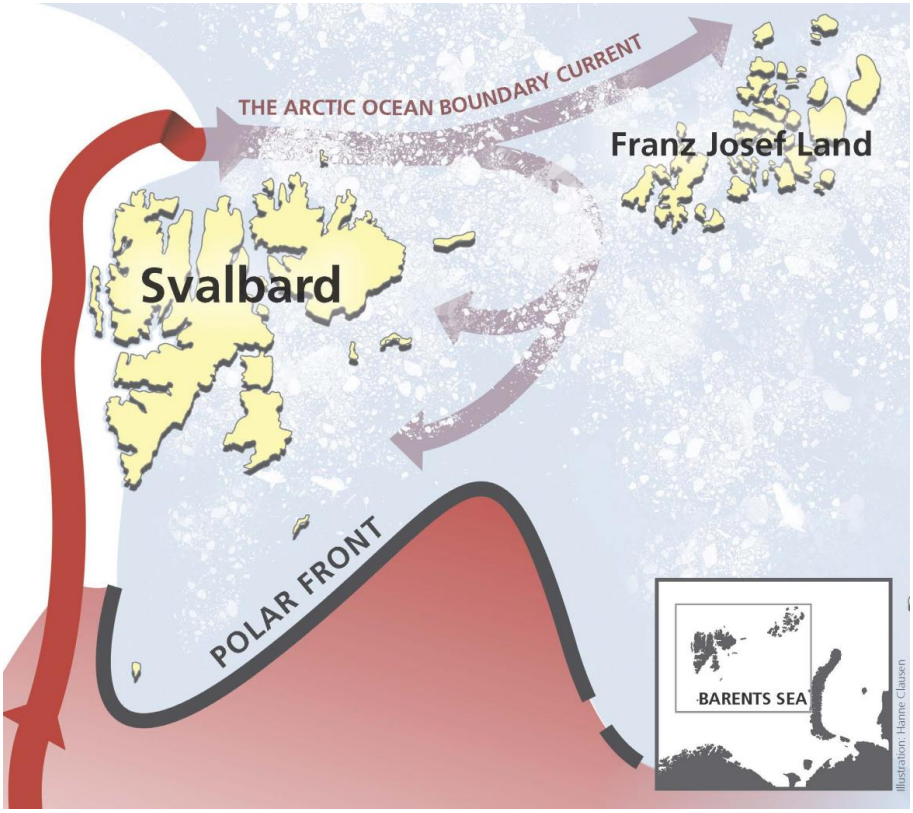

Figure 7. Schematic of the northern Barents Sea showing the subsurface inflow of Atlantic Water to the Barents Sea from the north, a branch of the Arctic Ocean Boundary Current that carries warm and saline Atlantic Water subsurface in the Arctic Ocean. ©2012 Institute of Marine Research, graphics by Hanne Clausen.

2.3 The Barents Sea marine ecosystem

The Barents Sea has a rich ecosystem inhabiting the currently greatest stock of Atlantic cod in the world (Ingvaldsen et al., 2015) and several other important commercial fish and crustacean species such as capelin, snow crab and king crab (e.g., Sakshaug et al., 2009; Alvsvåg et al., 2008). The ecosystem has two distinct food-webs, boreal and Arctic. Although adapted to each of the regimes in the southern and northern Barents Sea, there are strong interactions between them (Dalpadado et al., 2012). The marginal ice zone is an important region for such interactions, and also a productive zone where upwelling of nutrient-rich waters cause phytoplankton blooms, feeding the zooplankton and higher trophic levels (e.g.,

Sakshaug & Slagstad, 1992; Oziel, 2017). There are also seasonal migrations of several boreal species, grazing in the northern areas in summer (e.g., Haug et al., 2017). The southern, boreal part is characterized by having many species and important fish generalists that increase the connectivity and resilience of the food-web (Kortsch et al., 2015). In contrast, the northern, Arctic part is adapted to the extreme cold, light- and nutrient-limited Arctic environment. It is characterized by having few species with smaller body-sizes, and there is less connectivity in the Arctic food-web (Kortsch et al., 2015), indicating less resilience to change. The Arctic ecosystem has key species such as sea ice-algae and the amphipod *T. libellula* that are closely connected to, respectively, the sea ice cover and Arctic water mass (Dalpadado et al., 2012), and comprises polar cod and ice-associated marine mammals such as polar bear, harp seal and the rare bowhead whale (Haug et al., 2017).

Figure 8: Illustration of the Barents Sea ecosystem showing its complexity with strong interactions between the boreal (Atlantic) and Arctic food-webs. ©2006 Institute of Marine Research, graphics by Arild Sæther.

2.4 Implications of climate change in the Barents Sea

Recent warming and sea ice loss in the Barents Sea has wide-spread implications. The lower atmospheric warming has been linked to mid-latitude weather extremes (Petoukhov & Semenov, 2010) and large-scale changes in the atmospheric circulation (Cohen et al., 2014; Francis & Vavrus, 2015). The adjacent Svalbard archipelago, west of the northern Barents Sea, has experienced abnormal climate since the early 2000s, having had extreme winter temperatures, tundra melt, and more frequent storms bringing extreme precipitation, massive erosion of coastal zones, landslides and snow avalanches (Førland et al., 2011; AMAP, 2017). The changing climate in the Barents Sea is causing structural changes in the Barents Sea ecosystem as boreal fish species have started grazing in the northern areas in summer (Fossheim et al., 2015; Haug et al., 2017). This increases the competition for food for the Arctic species, that have retracted northwards to where depth might limit further migration (Fossheim et al., 2015). The conditions for marine mammals in the north have also deteriorated (Haug et al., 2017). There are wide societal impacts of changing conditions in the Barents Sea, as the highly varying sea ice cover induces large limitations for operations within several sectors, such as ecosystem management, fisheries, petroleum, shipping, research and tourism. The future development and state of the Barents Sea, particularly its sea ice edge and ecosystem state will therefore have large implications for stakeholders, policymakers, non-governmental organizations and commerce.

3. Data and methods

3.1 Data

This thesis is an observational study using an extensive data set of *in situ* ocean temperature and salinity from the northern Barents Sea. The Barents Sea has been monitored annually in joint Norwegian-Russian ecosystem surveys since the start of the 1970s (Michalsen et al., 2013). The data set now covers nearly five decades and is a true treasure in the context of polar research. The late summer situation has been monitored each year in August and September when there is a three-layer structure with the annual summer surface layer of melt water, over the winter-cooled intermediate Arctic layer and the deep Atlantic layer.

The data were interpolated horizontally at every fifth meter from 0 to 200 m depth, resulting in gridded ocean temperature and salinity maps at each vertical level, each year. This interpolation was performed on triangular finite element grids specifically designed for each of the 51 vertical levels, and accompanying error fields were applied to remove extrapolated areas (Troupin et al., 2012; Papers II and III). The gridded data were averaged over a subarea covering 85,000 km^2 for each vertical level and each year. The subarea covered both banks and troughs with different hydrography, and the spatial averaging smoothed out this local variability. The extent, diverse topography and good data coverage in the subarea ensured that the results were representative of the northern Barents Sea. The resulting annual temperature-salinity profiles were used to construct time series from each of the layers and cores in the water column.

The effect of other driving factors for the interannual variability in the northern Barents Sea were also evaluated using observational time series of atmospheric temperature, sea ice area and import, precipitation and upstream Atlantic Water temperature, reanalysis wind fields, and temperature and circulation in the Atlantic Water at 200 m in the northern Barents using a numerical general circulation model (the latter only used for descriptions in Section 3 of Paper I).

3.2 Methods

A general description of the mean hydrography in the northern Barents Sea and the inflow, variability and impact of the Atlantic Water inflow from the north was given in Paper I, showing the horizontal distribution of mean temperature and standard deviation during 1970–2009 at 0, 50, 100 and 200 m depth, and extracting time series from the area where Atlantic Water enters from the north (Figure 6-point NW). Vertical distribution of temperature and salinity were shown along a section from south of the Polar Front, following the trench out to the northern shelf-slope (Figure 6-red line). Driving factors for the temperature variability in the Atlantic Water were identified. Using observed series of surface air temperature, sea ice area and upstream Atlantic Water temperature at Svalbard, and Ekman transport and Ekman pumping velocities derived from reanalysis wind fields, spatio-temporal relationships were analysed using Empirical Orthogonal Functions.

Layer-mean time series were constructed for Papers II and III by identifying the vertical position of each feature in the water column each year, i.e., the pycnocline, Arctic core, Arctic/Atlantic-interface and Atlantic core. This procedure was chosen in preference to the classical, static water mass definitions that traditionally have been used to characterize and identify each of the water masses in the northern Barents Sea (i.e., Mosby, 1938; Loeng, 1991; Pfirman et al., 1994) because large changes in the layers were expected during the five decades with data. Capturing the actual variability and change in layer characteristics could reveal and quantify the interplay between each of the three layers and the sea ice cover, which could potentially give insight into the transfer of heat from the deep Atlantic layer to the sea ice cover and deepen the understanding of maintenance and disintegration of the cold and stratified Arctic-type conditions in the northern Barents Sea and Arctic in general.

3.3 Hypotheses

Buoyancy represents the opposing force that hinders vertical movement in the water column, and interannual variability in the stratification may therefore affect the

vertical mixing in the lower part of the water column between the Arctic and Atlantic layers. An intriguing point is that any mixing between the two layers would make them more similar in salinity and temperature, which reduces the stratification and makes the lower part of the water column more prone to vertical mixing, i.e., a positive mixing feedback. Salinity generally determines the stratification in cold waters, which implies that a positive salinity feedback in the vertical mixing may enhance the variability in mixing caused by other factors. The Arctic layer salinity has larger variability than that of the Atlantic layer, and this led to the hypothesis that the Arctic layer salinity largely controls the amount of mixing between the Arctic and Atlantic layers. Further, the salt flux and related positive feedback induces a need for a downward freshwater input to maintain the Arctic layer and stratification, thus to keep the water column in its cold, stratified and sea ice covered state. These two hypotheses made the basis for Papers II and III, respectively.

3.4 Assumptions

The residence times of the Arctic layer in the northern Barents Sea is essentially unknown. Observations of advection of Arctic waters have never been published, and it is also difficult to assess its residence times from models, since models have not been capable to simulate, with sufficient accuracy, the stratified water column structure of the northern Barents Sea (V. Lien, T. Hattermann, *personal communication*) or the Arctic Ocean (Holloway et al., 2007; Zhang & Steele, 2007). This leads to some caution when the results are interpreted, as effects of advection of Arctic Water and complete budgets could not be estimated. It was however considered a reasonable starting point to assume that local processes are primary and advection secondary in shaping the Arctic layer, since the Arctic Water is mainly being produced from cooling and brine release during sea ice growth in winter (Mosby, 1938; Rudels et al., 2004). The focus therefore was on identifying primary factors and mechanisms that drive most of the interannual variability in the different layers of the water column. *A priori* hypotheses were put forward and evaluated using the extensive observational data set, descriptive statistics and correlation analyses

(see individual papers for details). Highly significant results were considered to imply that the hypotheses could not be falsified, indicating local processes probably are primary in shaping the Arctic layer, leaving advection secondary, or that the processes found to be important in the studied region can be generalised for a larger area.

4. Summary of papers

4.1 Paper I: Variability and impacts of Atlantic Water entering the Barents Sea from the north

This paper has two main parts: The first part gives a general description of the mean state, variability and horizontal and vertical distribution of the water masses in the northern Barents Sea based on the observations from 1970–2009 and previous literature. The focus was on the Atlantic Water at 200 and 100 m depth, the Arctic Water at 50 m and the surface melt water throughout the four decades. The second part of the paper identified the primary factors that drive the interannual to multi-annual variability in the subsurface Atlantic Water inflow temperature to the Barents Sea from the north. It was found that the primary driving factor is advection of Atlantic Water, driving the general variability in Atlantic Water temperature in the whole northern Barents Sea. The second driving factor was found to be the local wind field in the northern part of the Barents Sea, causing upwelling at the shelf-slope and increased cross-shelf exchange that amplifies the inflow of Atlantic Water to the Barents Sea from the north. This weather pattern became more dominant towards the end of the time series, probably due to large-scale changes in the atmospheric circulation (Zhang et al., 2008). This probably caused a positive anomaly in the inflowing of Atlantic Water, observed as increased Atlantic Water-temperature towards the end of the time series. The temperature increase in the Atlantic Water at 200 m depth in the northern Barents Sea accelerated after the late 1990s. The Arctic Water had low and stable temperatures ~−1 °C until it started to warm rapidly in ~2000. This warming could not be explained by temperature changes in the surface water alone, but was probably caused by vertical mixing with the deeper Atlantic Water. The observed Arctic Water warming motivates for Paper II.

4.2 Paper II: Arctic layer salinity controls heat loss from deep Atlantic layer in seasonally ice-covered areas of the Barents Sea

The vertical mixing and transfer of heat between the intermediate Arctic layer and the deeper Atlantic layer is here investigated, testing the hypothesis that the Arctic layer salinity is a key controlling factor (see Chapter 3.3). The slope of the mixing line between the Arctic and Atlantic cores defines the stratification and buoyancy force in the lower part of the water column, i.e., the opposing force that vertical motion must defeat to produce mixing. This implies that the weaker the stratification is, the more vertical mixing occurs, providing that the turbulence-generating forcing is relatively stable on interannual time scales. The factors that determine the slope of the vertical mixing line could therefore determine the transfer of heat up from the deep Atlantic layer. Using a subset of the observational data set where the data coverage was good through 1970–2011, the Arctic layer salinity was found to control the stratification and amount of mixing with the Atlantic layer, as hypothesized. There is considerable variability in Arctic layer salinity and thereby vertical mixing to leave a readily traced signal in the Atlantic layer temperature—being modified from the mixing. Vertical heat fluxes from the deep Atlantic layer are therefore varying primarily due to salinity variations in the layer above, not from temperature variations in the Atlantic layer itself. For some, this may be a quite contra-intuitive result at first, given that Atlantic Water is known for having large temperature fluctuations (Helland-Hansen & Nansen, 1909). There is also a positive feedback in the salt flux since mixing brings salt up and reduces the stratification and in turn increases the salt flux (and heat flux). This ‘mixing feedback mechanism’ thus acts to enhance the variability in mixing and stratification. Overall, the findings imply that the Arctic layer salinity plays a key role in the cold, stratified and sea ice covered water column. The upward net salt flux implies that a downward freshwater input is necessary to keep the northern Barents Sea stratified and sea ice covered. This gives the motivation for Paper III.

4.3 Paper III: Declining sea ice import and freshwater loss causes Arctic warming hotspot

Paper III addresses the freshwater input to the northern Barents Sea and its effect on maintaining the stratification of the cold and stratified water column, hence limiting the upward heat and salt fluxes from the deep Atlantic layer. It also investigates the changes in water column structure due to the ongoing climate change in the Arctic warming hotspot. The sea ice import was found to be influencing the Barents Sea ice cover directly by adding ice and indirectly through being the primary freshwater input that maintains the stratification and conditions for sea ice growth in winter. The sea ice import to the Barents Sea has large interannual variability but a sharp decline after the record winter 2002/03. Comparing 2010–2016-means with the climatic reference period 1970–1999, the data set documents a large and significant water column shift towards higher Surface layer salinities and increased Arctic layer salinity, giving weaker stratification (30 and 11% reduction in the upper and lower part of the water column, respectively) and higher temperatures in the entire water column. The result has been erosion of the Arctic layer with heat input from above and below, an extreme increase in the upper ocean heat content of 3.8 ± 0.6 standard deviations above the 1970–1999-mean and a major freshwater loss of ~1 m, or 40 %. Unless the sea ice import soon recovers, the stratification will most likely break down and the northern Barents Sea become warm, well-mixed and sea ice free all year round, in all practical aspects, part of the Atlantic domain. This means removal of the habitat of the whole Arctic food-web comprising sea ice-associated marine mammals, ice-algae, Arctic amphipods and the Arctic fish species feeding on them (e.g., polar cod), with unknown consequences for the commercial species in the Barents Sea ecosystem. The interpretation also indicates a general eastward displacement of properties and conditions downstream/eastwards along the Atlantic Water-pathway as the Arctic warms.

5. Discussion

5.1 The cold, stratified and sea ice covered northern Barents Sea

This thesis confirms the general view that the northern Barents Sea used to have a remarkably stable cold and stratified, sea ice covered water column structure before the rapid climate shift event started in the early 2000s. In the stable period, the Surface- and Atlantic layers both had quite large interannual variability in temperature, but the intermediate Arctic layer was always very stable and cold with temperatures around −1 °C (Fig. 6a of Paper I; Fig. 2 of Paper III) and the winter sea ice cover kept re-freezing each autumn. The Arctic layer had, however, considerable salinity variations earlier, much larger than the Atlantic layer, and this is now known to be an important characteristic of the cold and stratified water column structure. Being formed by the annual sea ice melt water, the Surface layer usually has had a low, but varying salinity, in line with literature (Loeng, 1991; Pfirman et al., 1994).

Observations of sea ice import from the north, between Svalbard and Franz Josef Land, has been published earlier and shown to be highly varying, from import to export between years (Kwok et al., 2005). The inflow through the eastern passage, Franz Josef Land–Novaya Zemlya, is, however, shown here to be much more important, being two–three times larger and consistently giving net import (Fig. 3c of Paper III). The low auto-correlation between years in the inflow is in line with the large stochasticity in atmospheric forcing on sea ice motion (Serreze & Stroeve, 2015).

Moreover, the thesis documents that sea ice inflow from the northeast is a key factor for the Barents Sea ice cover, in addition to the already identified major driver, the Atlantic Water inflow from the southwest (Årthun et al., 2012; Onarheim et al., 2014). The effect is two-fold: First, the direct effect from adding ice (r=0.47), secondly, the indirect effect from adding freshwater that increase the stratification – a precondition for local sea ice growth (r=0.53 when the Barents Sea ice area has a one-

year time lag), see Fig. 3 of Paper III. This shows that sea ice inflow is a key variable for the Barents Sea, in line with numerical simulations (Ellingsen et al., 2009; Koenigk et al., 2009).

The deep Atlantic layer in the northern Barents Sea is continually renewed by advection of Atlantic Water entering the Barents Sea as a deep inflow from the north (Paper I). The Atlantic Water temperature varies due to temperature signals advected with the Atlantic Water flow, but also due to local winds affecting the cross-shelf exchange of Atlantic Water (Paper I) and due to varying degree of modification from mixing with the Arctic layer (Paper II). Advection in the Surface and Arctic layers are still basically unknown, but the Surface layer likely resembles the sea ice motion which is highly stochastic but net south-eastward into the Barents Sea. And, the highly significant results of Papers II and III indicate that the local processes probably are primary in determining the interannual variability of temperature and salinity in the Arctic layer, leaving advection secondary. Another possibility is that the processes found to be important can be generalised for a larger area.

There is a strong seasonal cycle in the northern Barents Sea, where winter cooling progresses downward from the surface. Brine release from sea ice growth causes the Surface layer salinity to increase, and when reaching the salinity at the base of the pycnocline, the two upper layers merge to form one winter-cooled layer (Rudels et al., 2004). Any heat stored in the Arctic layer will therefore be contributing to less sea ice growth and larger heat losses to the atmosphere in winter.

5.2 Processes that maintain or disintegrate the water column structure

There is a tight two-way connection between the sea ice cover and the Arctic layer, each of them ensuring presence of the other, as the Surface layer of melt water absorbs the incoming radiation and shelters the winter-cooled Arctic layer from warming in summer, and loses the absorbed heat to the atmosphere in autumn. The heat is thus never transferred down to the Arctic layer, ensuring the winter-cooled

water is stored through the summer, a precondition for sea ice growth in the coming winter (Paper III). The melt water also supplies the Arctic layer with freshwater and maintains the stratification in the lower part of the water column (Paper III).

There is a positive feedback mechanism in the vertical mixing between the Arctic and Atlantic layers, since mixing reduces the stratification and makes the water column more prone to vertical mixing. The mixing is largely confined by the stratification induced by the low Arctic layer salinity (Paper II), but is considerable and varying between years – dependent on the Arctic layer salinity – and causes varying upward heat fluxes from the deep Atlantic layer. The corresponding upward salt flux implies that a freshwater input is needed to maintain the stratification in the region, otherwise the stratification eventually breaks down. The sea ice import to the Barents Sea from the interior Arctic Ocean is the main freshwater input and primary factor for maintaining the northern Barents Sea in the cold, stratified and sea ice covered state. (Paper III).

5.3 Observed changes in the water column structure

Due to declining sea ice import from the interior Arctic in the 2000s, the northern Barents Sea has undergone a large and significant shift, and the 2010–2016-mean water column is significantly warmer and more saline than 1970–1999-means in all three layers, weakly stratified and less sea ice covered (Paper III). It has an extremely high upper ocean heat content and a record low freshwater content, and an abnormally warm Arctic layer after being consistently cold, stratified and sea ice covered throughout the first four decades of the observational record. The sudden decline in sea ice import has induced a rapid slowing down of the process that acts to maintain the stratification and triggered a rapid climate shift event, showing that the ocean is a major player in the Arctic warming hotspot. The dependence of regular, external freshwater inputs has made the northern Barents vulnerable to sustained low sea ice imports from the Arctic. As the Arctic sea ice cover became thinner and less compact, probabilities for high sea ice inflows to the Barents Sea dropped. The general decline in thick, old ice from the Eurasian Basin during the early 2000s

(Polyakov et al., 2012b; Carmack et al., 2015) also likely contributed to the decline. Unless the sea ice import recovers, the stratification will eventually break down and make Atlantic Water occupy the entire water column of it, causing the region to transition to a warm and sea ice free Atlantic type of climate.

5.4 Are the changes reversible?

With his process-oriented two-layer model, Stigebrandt (1981) showed that the sea ice cover vanishes abruptly when the freshwater supply is reduced below some threshold value. Building on this model, Jensen et al. (2016) found that the stratification in the model breaks down even for small freshwater inputs, before the vertical density difference vanishes, showing that a tiny stratification is not a possible solution. These findings correspond well with the mixing feedback and rapid climate shift documented in this thesis, and support that rapid climate shift events have taken place in the past climate history (Dokken et al., 2013). The process and triggering factor is, however, different from that proposed by Dokken et al. (2013). Paper III, Stigebrandt (1981), Linders & Björk (2013) and Jensen et al. (2016) all show that insufficient freshwater input at the surface is driving the change. This indicates that the Atlantic Water inflow is not a trigger, but a response variable to the "atlantification" and rapid climate shift events in the past, as discussed by Polyakov et al. (2017) and Dokken et al. (2013).

Although natural variability causes variations in the Arctic sea ice cover (e.g., Ding et al., 2017), it is highly unlikely to have caused the sudden rapid change in the northern Barents Sea after decades/centuries with a stable Arctic climate (e.g., Nansen, 1902; Mosby, 1938; Paper III). The positive mixing feedback and anticipated transition to an Atlantic climate in the northern Barents Sea (Paper III) will most likely be a permanent and irreversible change, in the sense that it would likely require extraordinary large sea ice inflows over several consecutive years to rebuild a freshwater reservoir large enough to transition back into the cold, stable Arctic climate. This is not likely to happen given the ongoing global warming and rapidly diminishing Arctic sea ice cover (Notz & Stroeve, 2016).

6. Future Arctic

6.1 In a stage of transition

The results of Paper III imply that it is the loss of freshwater, or failure to maintain the stratification that "allows" larger heat fluxes up from the Atlantic layer, showing that the freshwater is leading the game in the ongoing transition. The Arctic layer functions as the freshwater reservoir of the water column and implies there is memory in the dynamical system over several years, meaning, the larger the reserves, the larger perturbations can the water column handle without its stratification breaking down. The positive salt feedback associated with the vertical mixing opens the possibility for an instability mechanism and permanent transition to a different stable state in the dynamical system (Scheffer et al., 2009). But the timing of the shift is dependent on the stochasticity or randomness – "when a perturbation becomes large enough, it happens" (Scheffer et al., 2009). If the sea ice import should recover, the northern Barents Sea could in theory re-build its freshwater reservoir and re-establish in the cold and stratified state, after which it could endure several "bad years" with little sea ice import. But, given the present development of the Arctic this is very unlikely, as discussed above.

This is in line with a one-dimensional column model study showing Arctic ocean regions with very strong stratification can maintain their conditions, in terms of not having a decreasing thickness of their sea ice cover without external freshwater input/sea ice import, whereas areas that are weakly stratified needs an external freshwater input, otherwise, the sea ice cover thins (Linders & Björk, 2013). Hence, stratification and thickness of the sea ice cover are positively interrelated, and negatively correlated with the dependence on sea ice import/external freshwater input. Another, analytical study showed that when the stratification becomes weak enough, it breaks down abruptly before vanishing entirely (Jensen et al., 2016), showing that a "tiny" stratification is not a possible solution. Breakdown of the stratification changes the conditions entirely within short time, in coherence with rapid climate shifts in paleoclimate records, showing the Nordic Seas had Arctic

climate during cold climatic periods, but rapidly changed to Atlantic climate as the climate warmed (Dokken et al., 2013). It is a debated question whether changes in the deep Atlantic layer or changes in the freshwater input has led the game in these rapid climate shift events in the past.

How the next years will play out is open due to the stochastic nature of the atmospheric forcing and sea ice flows and dynamic ice cover (Serreze & Stroeve, 2015; Carmack et al., 2015). But, there is a high probability that the northern Barents Sea will flip over to the warm and well-mixed state and become totally sea ice free within the next decade or two. It may also occur sooner.

6.2 General remarks on possible stable states

Based on this, it appears that the water column can structurally be in two different stable states, either cold, stratified and sea ice covered or warm, well-mixed and sea ice-free, essentially the two very different dynamical regimes of the Arctic and Atlantic domains. The difference is presence, or not, of a light upper layer that suppresses heat and salt fluxes from the deeper, denser layer. Between these stable states, lays an unstable state where the water column is weakly stratified, has large upward fluxes of heat and salt and a highly seasonal sea ice cover, cf., conditions in the northern Barents Sea (Paper III). In the unstable state, the water column is sensitive to perturbations and highly dependent on regular “external” freshwater input/sea ice import to sustain its stratification. When in either of the two stable states, much larger and persistent perturbations would be needed to shift it out of its current state, cf. Scheffer et al. (2009). The change in the water column structure when following the Atlantic Water pathway from the Atlantic domain, through the frontier region and into the Arctic therefore mirror these three states (see Fig. 4 of Paper III).

The atmosphere in the Arctic domain is also distinctly different from that of the Atlantic, in that the Arctic has a cold, dense layer of air near the ground and a temperature inversion limiting vertical motion in the lower part of the atmosphere

(Serreze et al., 1992). This is an intriguing analogy to the stratification and limiting vertical exchange of properties that the oceanic boundary layer exhibits in the Arctic. Together with the sea ice cover at the surface, these three inherent characteristics of the Arctic all hinders vertical fluxes of any property, especially near the sea surface. Moreover, these characteristics are all linked to the most important positive feedback mechanisms known to give Arctic amplification (if accepting the oceanic feedback mechanism described here as important), that is, the temperature feedback related to the vertical structure of the Arctic atmosphere (Pithan & Mauritsen, 2014), the surface albedo feedback related to the sea ice cover and the oceanic mixing feedback related to the stratification in the water column. Together, these local feedbacks may be sketching a picture of an Arctic environment that is "self-sustained when healthy" with stabilizing factors in its stable cold, stratified and sea ice covered state. But positive feedback mechanisms work both ways, and when a large enough perturbation occurs, e.g., the rapid, ongoing global warming, the stratification becomes weaker, in both the ocean and the atmosphere, and the sea ice cover diminishes. In all, this picture matches Arctic amplification being an inherent characteristic of the global climate system.

6.3 The future Barents Sea

A fundamental shift to Atlantic climate in the northern Barents Sea will certainly have major consequences for the Barents Sea ecosystem, since it implies removal of the habitat of the Arctic food-web. The net effect on the commercial species is more open since capelin, a key prey for cod and other boreal fish species, feed on species that are tightly linked to the sea ice edge (Dalpadado et al., 2012). An interesting question is whether the Kara Sea will take over as the frontier region and become a new productive zone with the marginal ice zone and interactions between the boreal and Arctic ecosystems. Contrary to expectations, the Arctic warming appears to be an eastward, rather than a northward shift of climate zones, following the continental shelves eastward into the Eurasian Basin. The circulation in the Barents Sea will probably change if the northern Barents Sea becomes flushed with Atlantic Water in

a final stage of such a transition. Will the stratification break down abruptly? What will happen with the Polar Front when the fresher water mass in the north disappears? These are a few of the intriguing questions to pursue related to a new Barents Sea.

6.4 The future Arctic

The changes seen here may mirror the general tendencies in the Arctic. Several modelling studies predict that the Arctic should become more stratified due to increased runoff, but will that freshwater be distributed properly over the Arctic interior? The faith of the northern Barents Sea implies that the future Arctic becomes less stratified as it gets more seasonal characteristics with a seasonal sea ice cover, and thus may become highly dependent on regular freshwater inputs to keep being stratified. Key questions for the future Arctic are, will those inputs be sufficient to combat increasing upward fluxes of heat and salt from the deep Atlantic layer? Areas producing excess ice will likely, over years, feed other areas of the Arctic with sea ice/freshwater, but will inputs from the Siberian rivers be sufficiently distributed over the Arctic Ocean or rather follow the Arctic coast as a coastal current?

The changes observed in the Arctic warming hotspot do match the bigger picture of changes over the entire Eurasian Basin in the 2000s, with freshwater loss (Morison et al., 2012), thinning of the sea ice cover (Rothrock et al. 1999), loss of old, thick ice (Polyakov et al., 2012b), increased upward heat fluxes from the deep Atlantic layer (Polyakov et al., 2017)—particularly during winter convection of the upper layers of the water column (Polyakov et al., 2013), and the development towards a seasonal sea ice cover (Serreze et al., 2007).

Hence, a substantial proportion of the Arctic Ocean is probably heading towards a seasonal state, where it too probably becomes dependent on freshwater inputs to keep being stratified. The Arctic domain has already lost much of its sea ice cover, and the findings in Paper III implies the Arctic sea ice cover now is insufficient for sustaining the stratification of the frontier region and that the Arctic domain is about to shrink. Noteworthy, paleoclimate records indicate that the shifts towards warmer conditions

has generally been very rapid. The observed freshwater loss over the entire Eurasian Basin (Morison et al., 2012) is therefore alarming, meaning roughly half of the Arctic Ocean is moving towards the unstable, weakly stratified state where it is sensitive to perturbations.

6.5 Global consequences

The results of this thesis confirm that the northern Barents Sea is a highly pressured Arctic region, where global warming is more amplified than in the Arctic in general. This is due to its function, being the frontier region of the Arctic domain that confronts the Atlantic domain, and the interior Arctic domain must serve it with excess sea ice to sustain the stratification in its most pressured area. The failure to do so implies that the Arctic domain is shrinking in response to global warming and Arctic amplification, and the frontier region is "lost" to the Atlantic domain. This is part of the process termed "atlantification" (Polyakov et al., 2017). If the new freshwater pattern of the Arctic Ocean continues (Morison et al., 2012), the entire Eurasian Basin will likely continue the process towards increasingly seasonal conditions, in where it too probably will become dependent of and sensitive to annual freshwater inputs to sustain stratified, cf. documented process in the Arctic warming hotspot (Paper III).

This apparently is a self-magnifying process, and is perhaps a parallel to Arctic amplification and the two possible stable states, stratified or well-mixed, since they are all related to the stratified boundary layers inherent of the Arctic air-ice-sea column, limiting vertical heat exchange in the upper ocean, across the sea ice covered surface and in the lower atmosphere, the latter having cold lower layers with an inversion/temperature increasing with height. If the ongoing process of weakening stratification in the Eurasian Basin continues, larger parts of it will likely shift to Atlantic climate and reduce the relative proportion of Earth having Arctic conditions. A warmer Arctic induces weaker meridional temperature gradients and a weaker jet stream with a wavier pattern increasing the probability for extreme weather (Cohen et al., 2014; Francis & Vavrus, 2015). In depth process-studies and development of

numerical general circulation models with a proper representation of the vertical structure of the Arctic environment is needed to understand the development of the Arctic and the globe in a warmer future later in this century, cf. difficulty in simulating the halocline vertical structure of the Arctic Ocean (Holloway et al., 2007; Zhang & Steele, 2007). The Arctic system has a peculiar vertical structure limiting exchange of properties across the sea surface and within the atmospheric and oceanic boundary layers, and this is probably the most important feature of it. The dynamical vertical processes of downward freshwater input, varying stratification and responses in the upward heat and salt fluxes include important feedback processes that are key to simulate a changing Arctic moving towards a more seasonal and probably unstable state.

6.6 Final remarks

The ongoing shift has relevance not only understanding the changes occurring today, but for interpretations of rapid climate shifts in the past and future climate shifts. In general, when a dynamical system is under pressure from large perturbations and reaches a critical stage, this stage can give insight into the underlying mechanisms because variability is enhanced in such periods (Scheffer et al., 2009). The ongoing shift can therefore give insight into the Arctic system as an integrated unity, enabling detailed exploration of relations between different climate variables, functioning within the different states, threshold values, critical points and state transformations. It may also give insight into responses in the global climate system as the Arctic undergoes rapid change.

The unique observational data set collected from this special Arctic region includes a thirty-year climatological reference period, 1970–1999, and two decades of large and comprehensive climate change thereafter, with both physical and biological parameters. This is an extraordinary opportunity for studying the integrated change in physical and ecological parameters, in the ocean, on the surface and in the atmosphere due to climate change. An extended monitoring program in the northern Barents Sea covering all seasons and with extensive measurements of advection

should therefore be considered. An extraordinary research program, the Nansen Legacy—inspired by the polar pioneer Fridtjof Nansen, will take place in the coming years and hopefully provide the high-resolution advection data and year-round measurements needed to get a more complete picture of the ongoing processes.

"Happiness is the struggle towards a summit and, when it is attained,
it is happiness to glimpse new summits on the other side."
–Fridtjof Nansen

The hut on Franz Josef Land, covered in snow, in which Fridtjof Nansen and Hjalmar Johansen spent the winter of 1895–96, after trying to reach the North Pole by skis. A drawing, based on Nansen's photograph, 31st of December 1896. Source: Wikipedia Commons.

References

Aagaard, K., Coachman, L. K. & Carmack, E. (1981): "On the halocline of the Arctic Ocean", Deep-Sea Res. A, Vol. 28: 529–545.

Abrahamsen, E. P., Østerhus, S. & Gammelsrød, T. (2006): "Ice draft and current measurements from the north-western Barents Sea, 1993–96", Polar Res., Vol. 25: 25–37.

Ådlandsvik, B. & Loeng, H. (1991): "A study of the climatic system in the Barents Sea", Polar Res., Vol. 10: 45–50.

AMAP (2017): "Adaptation Actions for a Changing Arctic: Perspectives from the Barents Area. Arctic Monitoring and Assessment Programme (AMAP) ", Oslo, Norway. xiv + pp. 267.

Årthun, M., Ingvaldsen, R. B., Smedsrud, L. H. & Schrum, C. (2011): "Dense water formation and circulation in the Barents Sea", Deep-Sea Res. I, Vol. 58: 801–817.

Årthun, M., Eldevik, T., Smedsrud, L. H., Skagseth, Ø. & Ingvaldsen, R. B. (2012): "Quantifying the influence of Atlantic heat on Barents Sea ice variability and retreat", J. Clim., Vol. 25: 4736–4743.

Alvsvåg, J., Agnalt, A. L. & Jørstad, K. E. (2009): "Evidence for a permanent establishment of the snow crab (*Chionoecetes opilio*) in the Barents Sea", Biol. Invasions, Vol. 11: 587–595.

Beszczynska-Möller, A., Fahrbach, E., Schauer, U., & Hansen, E. (2012): "Variability in Atlantic water temperature and transport at the entrance to the Arctic Ocean, 1997–2010", ICES J. Mar. Sci., Vol. 69: 852–863.

Bintanja, R. & van der Linden, E. C. (2013): "The changing seasonal climate in the Arctic", Nat. Sci. Rep., Vol. 3: 1–8.

Carmack, E. et al. (2015): "Toward quantifying the increasing role of oceanic heat in sea ice loss in the new Arctic", Bull. Am. Meteorol. Soc., Vol. 96: 2079–2105.

Cohen, J. et al. (2014): "Recent Arctic amplification and extreme mid-latitude weather", Nat. Geosci., Vol. 7: 627–37.

Comiso, J. C. & Hall, D. K. (2014): "Climate trends in the Arctic as observed from space", WIREs Clim. Change, Vol. 5: 389–409.

Dalpadado, P. et al. (2012): "Climate effects on Barents Sea ecosystem dynamics", ICES J. Mar. Sci., Vol. 69: 1303–1316.

Ding, Q. et al. (2017): "Influence of high-latitude atmospheric circulation changes on summertime Arctic sea ice", Nat. Clim. Change, Vol. 7: 289–296.

Dokken, T. M., Nisancioglu, K. H., Li, C., Battisti, D. S. & Kissel, C. (2013): "Dansgaard-Oeschger cycles: Interactions between ocean and sea ice intrinsic to the Nordic Seas", Paleoceanography, Vol. 28: 491–502.

Ellingsen, I., Slagstad, D. & Sundfjord, A. (2009): "Modification of water masses in the Barents Sea and its coupling to ice dynamics: a model study", Ocean Dyn., Vol. 59: 1095–1108.

Fer, I. (2009): "Weak vertical diffusion allows maintenance of cold halocline in the central Arctic", Atmos. Ocean. Sci. Lett., Vol. 2(3): 148–152.

Feynman, J. & Ruzmaikin, A. (2007): "Climate stability and the development of agricultural societies", Climatic Change, Vol. 84: 295–311.

Førland, E. J., Benestad, R., Hanssen-Bauer, I., Haugen, J. E. & Skaugen, T. E. (2011): "Temperature and Precipitation Development at Svalbard 1900–2100", Adv. Meteorol., Vol. 2011: 893790.

Fossheim, M. et al. (2015): "Recent warming leads to rapid borealization of fish communities in the Arctic", Nat. Clim. Change, Vol. 5: 673–677.

Francis, J. A. & Vavrus, S. J. (2015): "Evidence for a wavier jet stream in response to rapid Arctic warming", Environ. Res. Lett., Vol. 10: 014005.

Furevik, T. (2001): "Annual and interannual variability of Atlantic Water temperatures in the Norwegian and Barents Seas: 1980–1996", Deep-Sea Res., Vol. 48: 383–404.

Gawarkiewicz, G. & Plueddemann, A. J. (1995): "Topographic control of thermohaline frontal structure in the Barents Sea Polar Front on the south flank of Spitsbergen Bank", J. Geophys. Res., Vol. 100(C3): 4509–4524.

Harris, C. L., Plueddemann, A. J. & Gawarkiewicz, G. G. (1998), "Water mass distribution and polar front structure in the western Barents Sea", J. Geophys. Res., Vol. 103(C2): 2905–2917.

Haug, T. et al. (2017): "Future harvest of living resources in the Arctic Ocean north of the Nordic and Barents Seas: A review of possibilities and constraints", Fish. Res., Vol. 188: 38–57.

Helland-Hansen, B. & Nansen, F. (1909): "The Norwegian Sea", Fisk. dir. Skr. Ser. Havunders., Vol. 2(2): 1–360.

Hoegh-Guldberg, O. & Bruno, J. F. (2010): "The Impact of Climate Change on the World's Marine Ecosystems", Science, Vol. 328: 1523–1528.

Holland, M. M. & Bitz, C. M. (2003): "Polar amplification of climate change in coupled models", Clim. Dynam., Vol. 21: 221–232.

Holloway, G. et al. (2007): "Water properties and circulation in Arctic Ocean models", J. Geophys. Res., Vol. 112: C04S03.

Houghton, J. T. et al. (2001): "Climate Change 2001: The scientific basis", Cambridge Univ. Press, New York.

Huntington, H. et al. (2005): "The changing Arctic: indigenous perspectives", in Arctic Climate Impact Assessment, Cambridge University Press, Cambridge, UK, chap. 3, pp. 61–98.

Ingvaldsen, R. B., Asplin, L. & Loeng, H. (2004): "Velocity field of the western entrance to the Barents Sea", J. Geophys. Res., Vol. 109: C03021.

Ingvaldsen, R. B., et al. (2015): "Sources of uncertainties in cod distribution models", Nat. Clim. Change, Vol. 5: 788–789.

Jensen, M. F., Nilsson, J. & Nisancioglu, K. H. (2016): "The interaction between sea ice and salinity-dominated ocean circulation: implications for halocline stability and rapid changes in sea ice cover", Clim. Dyn., Vol. 47: 3301–3317.

Jones, E. P. (2001): "Circulation in the Arctic Ocean", Polar Res., Vol. 20: 139–146.

Koenigk, T., Mikolajewicz, U., Jungclaus, J. H. & Kroll, A. (2009): "Sea ice in the Barents Sea: seasonal to interannual variability and climate feedbacks in a global coupled model", Clim. Dyn., Vol. 32: 1119–1138.

Kortsch, S., Primicerio, R., Fossheim, M., Dolgov, A. V. & Aschan, M. (2015): "Climate change alters the structure of arctic marine food webs due to poleward shifts of boreal generalists", Proc. R. Soc. B, Vol. 282: 20151546.

Kwok, R., Maslowski, W. & Laxon, S. W. (2005), "On large outflows of Arctic sea ice into the Barents Sea", Geophys. Res. Lett., Vol. 32: L22503.

Linders, J. & Björk, G. (2013): "The melt-freeze cycle of the Arctic Ocean ice cover and its dependence on ocean stratification", J. Geophys. Res., Vol. 118: 5963–5976.

Loeng, H. (1991): "Features of the physical oceanographic conditions in the Barents Sea", Polar. Res., Vol. 10: 5–18.

Manabe, S. & Stouffer, R. J. (1980): "Sensitivity of a global climate model to an increase of CO_2 concentration in the atmosphere", J. Geophys. Res., Vol. 85: 5529–5554.

Michalsen, K. et al. (2013): "Marine living resources of the Barents Sea – Ecosystem understanding and monitoring in a climate change perspective", Mar. Biol. Res., Vol. 9: 932–947.

Midttun, L. (1985): "Formation of dense bottom water in the Barents Sea", Deep-Sea Res. A, Vol. 32: 1233–1241.

Morison, J. et al. (2012): "Changing Arctic Ocean freshwater pathways", Nature, Vol. 481: 66–70.

Mosby, H. (1938): "Svalbard Waters", Geofys. Publ., Vol. 12: 1–86.

Nansen, F. (1902): "Oceanography of the North Polar Basin: The Norwegian North Polar Expedition", Sci. Results, Vol. 9: pp. 427.

Novitskiy, V. P. (1961): "Permanent currents of the northern Barents Sea", Tr. Gos. Okeanogr. Inst., Vol. 64: 1–32 (english translation).

Notz, D. & Stroeve, J. (2016): "Observed Arctic sea-ice loss directly follows anthropogenic CO_2 emission", Science, Vol. 354: 747–750.

Nuttall, M. et al. (2005): "Hunting, herding, fishing, and gathering: indigenous peoples and renewable resource in the Arctic", in: Arctic Climate Impact Assessment. Cambridge University Press, Cambridge, UK, chap. 12, pp. 649–690.

Onarheim, I. H., Smedsrud, L. H., Ingvaldsen, R. B. & Nilsen, F. (2014): "Loss of sea ice during winter north of Svalbard", Tellus, Vol. 66: 23933.

Onarheim, I. H., Eldevik, T., Årthun, M., Ingvaldsen, R. B. & Smedsrud, L. H. (2015): "Skillful prediction of Barents Sea ice cover", Geophys. Res. Lett., Vol. 42: 5364–5371.

Oziel, L. et al. (2017): "Role for Atlantic inflows and sea ice loss on shifting phytoplankton blooms in the Barents Sea", J. Geophys. Res., Vol. 122: 5121–5139.

Pfirman, S., Bauch, D. & Gammelsrød, T. (1994): "The northern Barents Sea: water mass distribution and modification", in: Johannesen, O. M., Muench, R. & Overland, J. (eds.): "The Polar Oceans and their Role in Shaping the Global Environment", Geophysical Monograph Series, Vol. 85: 77–94, American Geophysical Union.

Petoukhov, V. & Semenov, V. A. (2010): "A link between reduced Barents-Kara sea ice and cold winter extremes over northern continents", J. Geophys. Res., Vol. 115: D21111.

Pithan, F. & Mauritsen, T. (2014): "Arctic amplification dominated by temperature feedbacks in contemporary climate models", Nature Geosci. Vol. 7: 181–184.

Polyakov, I. V. et al. (2002): "Observationally based assessment of polar amplification of global warming", Geophys. Res. Lett., Vol. 29(18): 1878.

Polyakov, I. V., Pnyushkov, A. V. & Timokhov, L. A. (2012a): "Warming of the Intermediate Atlantic Water of the Arctic Ocean in the 2000s", J. Clim., Vol. 25(32): 8362–8370.

Polyakov, I., Walsh, J. E. & Kwok, R. (2012b): "Recent changes of Arctic multiyear sea ice coverage and the likely causes", Bull. Am. Meteorol. Soc., Vol. 93: 145–151.

Polyakov, I. V. et al. (2012c): "Mooring-based observations of double-diffusive staircases over the Laptev Sea slope", J. Phys. Oceanogr., Vol. 42, 95–109.

Polyakov, I. V. et al. (2013): "Winter convection transports Atlantic water heat to the surface layer in the Eastern Arctic Ocean", J. Phys. Oceanogr., Vol. 43: 2142–2155.

Polyakov, I. V. et al. (2017): "Greater role for Atlantic inflows on sea-ice loss in the Eurasian Basin of the Arctic Ocean", Science, 10.1126/science.aai8204.

Root, T. L. et al. (2003): "Fingerprints of global warming on wild animals and plants", Nature, Vol. 421: 57–60.

Rothrock, D. A., Yu. Y. & Maykut, G. A. (1999): "Thinning of the Arctic sea-ice cover", Geophys. Res. Lett., Vol. 26(23): 3469–3472.

Rudels, B., Jones, E. P., Schauer, U. & Eriksson, P. (2004): "Atlantic sources of the Arctic Ocean surface and halocline waters", Polar Res., Vol. 23(2): 181–208.

Rudels B. (2012): "Arctic Ocean circulation and variability – advection and external forcing encounter constraints and local processes", Ocean Sci., Vol. 8: 261–286.

Rudels, B. (2016): "Arctic Ocean stability: The effects of local cooling, oceanic heat transport, freshwater input, and sea ice melt with special emphasis on the Nansen Basin", J. Geophys. Res., Vol. 121: 4450–4473.

Sakshaug, E. & Slagstad, D. (1992): "Sea ice and wind: Effects on primary productivity in the Barents Sea", Atmos. Ocean, Vol. 30: 579–591.

Sakshaug, E., Johnsen, G. & Kovacs, K. (2009): "Ecosystem Barents Sea", Tapir Academic Press, Trondheim, Norway.

Screen, J. A. & Simmonds, I. (2010): "Increasing fall-winter energy loss from the Arctic Ocean and its role in Arctic temperature amplification", Geophys. Res. Lett., Vol. 37: L16707.

Schauer, et al. (2002): "Confluence and redistribution of Atlantic water in the Nansen, Amundsen and Makarov basins", Ann. Geophys., Vol. 20(2): 257–273.

Scheffer, M. et al. (2009): "Early-warning signals for critical transitions", Nature, Vol. 461: 53–59.

Serreze, M. C., Kahl, J. D. & Schnell, R. C. (1992): "Low-level temperature inversions of the Eurasian Arctic and comparisons with Soviet drifting station data", J. Clim., Vol. 5: 615–629.

Serreze, M. C., Holland, M. M. & Stroeve, J. (2007): "Perspectives on the Arctic's Shrinking Sea-Ice Cover", Science, Vol. 315:1533–1536.

Serreze, M. C., Barrett, A. P., Stroeve, J. C., Kindig, D. N. & Holland, M. M. (2009): "The emergence of surface-based Arctic amplification". Cryosphere, Vol. 3: 11–19.

Serreze, M. C. & Barry, R. G. (2011): "Processes and impacts of Arctic amplification: A research synthesis", Glob. Planet. Change, Vol. 77: 85–96.

Serreze, M. C. & Stroeve J. (2015): "Arctic sea ice trends, variability and implications for seasonal ice forecasting", Phil. Trans. R. Soc. A, Vol. 373: 20140159.

Smedsrud, L. H., Ingvaldsen, R., Nilsen, J. E. Ø. & Skagseth, Ø. (2010): "Heat in the Barents Sea: transport, storage, and surface fluxes", Ocean Sci., Vol. 6: 219–234.

Smedsrud, L. H. et al. (2013): "The role of the Barents Sea in the Arctic climate system", Rev. Geophys., Vol. 51: 415–449.

Steele, M., Morison, J. H. & Curtin, T. B. (1995): "Halocline water formation in the Barents Sea", J. Geophys. Res., Vol. 100(C1): 881–894.

Stigebrandt, A. (1981): "A model for the thickness and salinity of the upper layer in the Arctic Ocean and the relationship between the ice thickness and some external parameters", J. Phys. Oceanogr., Vol. 11: 1407–1422.

Sundfjord, A., Fer, I., Kasajima, Y. & Svendsen, H. (2007): "Observations of turbulent mixing and hydrography in the marginal ice zone of the Barents Sea", J. Geophys. Res., Vol. 112: C05008.

Sverdrup, H. U. (1933): "The Norwegian North Polar Expedition with the "*Maud*", 1918–1925", Scientific Res., Vol. 1a: pp. 331.

Tantsiura, A. I. (1973): "On seasonal changes in currents in the Barents Sea", Transactions of the Polar Scientific Research Institute of Marine Fisheries and Oceanography—N.M. Knipovic, english translation by the Norwegian Polar Institute, Oslo, Norway.

Troupin, C. et al. (2012): "Generation of analysis and consistent error fields using the Data Interpolating Variational Analysis (DIVA)", Ocean Model., Vol. 52: 90–101.

Wadhams, P. (2000): "Ice in the ocean", Gordon and Breach Science Publishers, Amsterdam.

Walther, G.-R. et al. (2002): "Ecological responses to recent climate change", Nature, Vol. 416: 389–395.

Zhang, J., & Steele, M. (2007): "Effect of vertical mixing on the Atlantic Water layer circulation in the Arctic Ocean", J. Geophys. Res., Vol. 112: C04S04.

Zhang, X. D., Sorteberg, A., Zhang, J., Gerdes, R., Comiso, J. C. (2008): "Recent radical shifts of atmospheric circulations and rapid changes in Arctic climate system", Geophys. Res. Lett., Vol. 35: L22701.

Deep-Sea Research I 62 (2012) 70–88

Contents lists available at SciVerse ScienceDirect

Deep-Sea Research I

journal homepage: www.elsevier.com/locate/dsri

Variability and impacts of Atlantic Water entering the Barents Sea from the north

Sigrid Lind [a,c,d,*], Randi B. Ingvaldsen [b,d]

[a] Institute of Marine Research, Sykehusveien 23, 9019 Tromsø, Norway
[b] Institute of Marine Research, Nordnesgaten 50, 5005 Bergen, Norway
[c] Geophysical Institute, University of Bergen, Allégaten 70, 5007 Bergen, Norway
[d] Bjerknes Centre for Climate Research, Allégaten 55, 5007 Bergen, Norway

ARTICLE INFO

Article history:
Received 9 March 2011
Received in revised form
9 December 2011
Accepted 16 December 2011
Available online 28 December 2011

Keywords:
Northern Barents Sea
Northwest Barents Sea
Barents Sea heat transport
Fram Strait Branch
Atlantic Water slope-current
Arctic Ocean boundary current

ABSTRACT

Branches of the submerged Atlantic Water (AW) slope-current in the Nansen Basin enter the Barents Sea from the north between Svalbard and Franz Josef Land. Using hydrographic observations from annual surveys during 1970–2009, the mean state, variability and trend of the AW in the northern Barents Sea were documented, and the dominant driving forces were identified. The AW temperature has a strong positive trend over the last 40 years that accelerated in the late 1990s. The most important driving factor is the upstream temperature in the West Spitsbergen Current, which influences the entire region occupied by AW. This driving factor has pronounced multiannual variability and has a significant increasing trend, although it cannot account for the accelerated increase since the late 1990s. The secondary forcing is associated with the wind stress curl/Ekman pumping on the shelf-break towards the Arctic Ocean, causing cross-shelf exchange between the Barents Sea and the Arctic Ocean. This process increases the penetration of AW onto the shelf and is mostly confined to the northern shelf. The signal is dominated by multidecadal variability with a notable shift in the late 1990s/early 2000s, thereby amplifying the AW temperature increase compared with the upstream conditions. Additionally, coastal upwelling along northern Svalbard and the winter-mean surface air temperature were found to impact the AW temperature variability, although they were of less importance than the wind stress curl. Variability in the sea ice cover does not appear to influence the subsurface AW temperature.

Variability in the AW temperature is transferred to the Arctic Water (ArW), and the vertical extent of the ArW varies considerably. Before the early 2000s, the ArW temperature was stable and low; afterwards, both the variability and the temperature increased. Our results indicate that the ArW in the northern Barents Sea is mainly heated from below.

1. Introduction

During the last decade, pronounced changes in the Arctic climate have been reported. These changes include an accelerating sea ice decline (Comiso et al., 2008), strong positive surface air temperature anomalies, and a dipole pattern of the near surface atmospheric pressure, which favours stronger meridional winds compared with previous decades (Overland and Wang, 2005; Overland et al., 2008; Zhang et al., 2008).

The Barents Sea also experienced large climate changes in the last decade. The winter mean surface air temperature (SAT) in the northern Barents Sea has increased by 2.5 °C since the millennial shift, and the summer sea ice concentration has decreased by 14% (Zhang et al., 2008). Both changes were linked to the near-surface atmospheric dipole pressure pattern (Zhang et al., 2008). Additionally, there has been observed increasing oceanic heat flux to the Barents Sea from the Norwegian Sea (Skagseth et al., 2008). With the rapid climatic changes observed in the Arctic as a whole and the more regional warming in the Barents Sea, significant changes are expected in the ocean climate in the northern Barents Sea. Processes in the Barents Sea may, due to the water mass exchange across the northern and eastern boundaries of the Barents Sea, influence the properties of the halocline, the Atlantic Water (AW) and the intermediate water in the Arctic Ocean (e.g., Rudels et al., 1994, 2004; Steele et al., 1995; Schauer et al., 1997; Aagard and Woodgate, 2001). Changing physical conditions in the Barents Sea will also have an impact on the Barents Sea ecosystem. In the 2000s, many species have been observed further north in the Barents Sea than previously (ICES, 2011).

* Corresponding author at: Institute of Marine Research, Sykehusveien 23, 9019 Tromsø, Norway. Tel.: +47 77609766; fax: +47 77609701.
E-mail address: sigridl@imr.no (S. Lind).

0967-0637/$ - see front matter © 2011 Elsevier Ltd. All rights reserved.
doi:10.1016/j.dsr.2011.12.007

The Barents Sea is bounded to the north by the Arctic Ocean. Following the definition used in Jakobsson et al. (2004), we use the Nansen Basin continental slope as the northern boundary of the Barents Sea (Fig. 1). This definition differs from that given by the International Hydrographic Organisation (1953) in "Limits of Oceans and Seas", which uses a line between Nordaustlandet and Franz Josef Land. We find the definition of Jakobsson et al. (2004) more appropriate as it includes the entire shallow shelf in the Barents Sea.

The Barents Sea borders the warmer Norwegian Sea in the south, and warm AW enters the Barents Sea from the Norwegian Sea in the southwest. The AW in the south is separated from the Arctic Water (ArW) in the north by the oceanic Polar Front, a dominant hydrographic feature of the near-surface waters of the Barents Sea (Fig. 1; Loeng, 1991; Pfirman et al., 1994). The Polar Front is located in the southern portion of our study area. A detailed description of our study area is given in Section 3.

The northern Barents Sea is a seasonally ice-covered marginal ice zone (Kvingedal, 2005). There is a highly fluctuating sea ice transport to/from the Arctic Ocean (Kwok et al., 2005) due to cyclone activity (Sorteberg and Kvingedal, 2006), causing strong interannual variability in the extent and concentration of the sea ice. The region also has a complex topographic structure, with deep trenches cutting between shallow banks (Fig. 1).

Information on the water masses present in the northern Barents Sea can be found in, e.g., Rudels (1986), Loeng (1991), Pfirman et al. (1994), Steele et al. (1995) and Løyning (2001). Following the definitions in Loeng (1991), the water masses in the northern Barents Sea are surface water/melt water, ArW, (modified) AW and bottom water/Cold Dense Water

AW enters the northern Barents Sea from the north through the Northern Barents Sea Opening (NBSO, Fig. 1) (Mosby, 1938; Hanzlick and Aagard, 1980; Pfirman et al., 1994; Steele et al., 1995; Matishov et al., 2009). The AW is advected south-westward below the ArW and has been observed year-round in the Olga Basin (Abrahamsen et al., 2006). The AW entering the northern Barents Sea through the NBSO is a branch of the AW slope-current, the submerged AW boundary current coming from Fram Strait and propagating eastward along the Nansen Basin continental shelf slope (Mosby, 1938; Pfirman et al., 1994; Steele et al.,

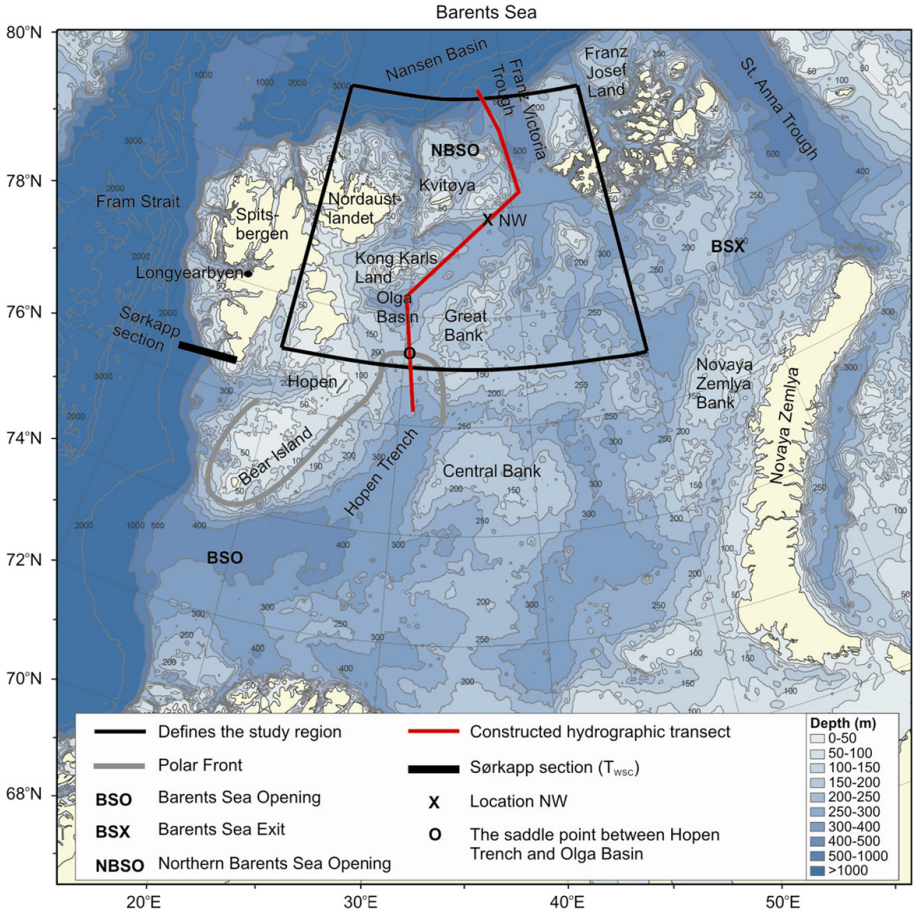

Fig. 1. Bathymetry of the Barents Sea (from Gebco—http://www.gebco.net/). The study region (black bordered region), the Polar Front (grey line), the openings of the Barents Sea (the Barents Sea Opening (BSO), the Northern Barents Sea Opening (NBSO) and the Barents Sea Exit (BSX)), the annually observed CTD transect at Sørkapp (black thick line), the constructed hydrography transect (red line), the saddle point between Hopen Trench and Olga Basin (O) and location NW (X) is denoted. (For interpretation of the references to colour in this figure legend, the reader is referred to the web version of this article.)

1995). The variability in the temperature and extent of the AW entering through the NBSO is largely unknown.

Smaller fractions of AW also enter the northern Barents Sea as a submerged flow from the south across the ~200 m deep saddle point between the Hopen Trench and the Olga Basin (Novitskiy, 1961; Loeng, 1991; Pfirman et al., 1994; Aksenov et al., 2010). This AW is cold (~0 to 0.5 °C) due to the strong atmospheric heat loss in the southern Barents Sea, but it maintains a high salinity. Thus, these waters are denser and flow below the AW entering through the NBSO, which is both freshened and cooled from mixing with ArW (Pfirman et al., 1994).

ArW usually occupies the layer between 20 and 100 m in the northern Barents Sea (Pfirman et al., 1994; Løyning, 2001) and has a temperature minimum ranging from −1.8 to −1 °C at 50–75 m (Loeng, 1991). Presently, there is no consistent understanding of the formation and advection of ArW in the Barents Sea. According to Mosby (1938), ArW develops locally due to sea ice formation and heat loss to the atmosphere in winter and is modified by mixing in summer, while Novitskiy (1961) and Tantsiura (1973) claimed that it is advected into the region from the northern Kara Sea and partly from the Arctic Ocean. Steele et al. (1995), however, argued that all the water masses in the northern Barents Sea were generated from AW by varying degrees of heat loss to the atmosphere and ice melting and that at least part of this water mass (the Cold Halocline Water) is advected from the Barents Sea toward the Arctic Ocean. ArW is subject to strong water mass modifications and vertical mixing in the regions where subsurface AW enters from the north (Pfirman et al., 1994; Sundfjord et al., 2007). Downward and upward heat fluxes of 15–20 W m^{-2} between the ArW and the surrounding water masses have been estimated (Sundfjord et al., 2007). Thus, the variability in the AW and ArW might influence each other.

Cold Dense Water is formed through heat loss to the atmosphere and brine release during winter (e.g., Midttun, 1985). This water flows along the bottom and exits the Barents Sea through the Franz-Victoria Trough (e.g., Årthun et al., 2011; Platov, 2011). Characteristics of this outflow have been addressed by, e.g., Rudels (1986), Steele et al. (1995), Schauer et al. (1997) and Rudels and Friedrich (2000).

The hydrography in the northern Barents Sea has a complex vertical structure due to the multitude of active processes, such as the AW (e.g., Mosby, 1938; Pfirman et al., 1994) and ArW inflows (Novitskiy, 1961; Tantsiura, 1973); the melting, formation and import/export of sea ice (e.g., Steele et al., 1995; Kvingedal, 2005; Kwok et al., 2005); winter convection and mixing of the components to produce Cold Dense Water with a variety of densities (e.g., Midttun, 1985; Steele et al., 1995; Rudels et al., 2004; Årthun et al., 2011); the lateral exchanges with extremely small Rossby radius (~1 km) due to the strong stratification and high latitude (e.g., Gill, 1982); and the interaction of topographically steered flows with cascading plumes (e.g., Schauer et al., 1997; Ivanov et al., 2004).

Although the water mass exchanges in the southern boundary of our study region are limited due to the Polar Front, the exchanges across the NBSO are not well known. Direct current measurements in and/or near the NBSO have only been performed twice: one east of Kvitøya (Aagaard et al., 1983) and the other in the AW slope-current north of Kvitøya (Ivanov et al., 2009). Several numerical model studies (Maslowski et al., 2004; Johansen, 2008; Aksenov et al., 2010) have provided volume and heat transports across the gateway, but the results differ considerably, ranging from −0.4 to 0.4 Sv and from 0.5 to 6 TW into the Barents Sea.

An overview of the ocean currents and circulation in the Barents Sea from model studies can be found (e.g., Maslowski et al., 2004; Aksenov et al., 2010; Postlethwaite et al., 2011). All the authors show the AW slope-current in the Nansen Basin, and Maslowski et al. (2004) and Aksenov et al. (2010) also show its branching off bringing AW into the NBSO. According to Aksenov et al. (2010), the AW makes excursions into the trenches of the NBSO, where it interacts with the water masses there before recirculating in the Franz Victoria Trough. This pattern is consistent with a recent model study by Platov (2011), although his main focus was on dense water flow from the Barents Sea toward the Arctic Ocean. However, all the published studies focus on the entire Barents Sea (or even larger regions) or on specific processes. Thus, inferring details on the ocean currents of the northern Barents Sea from these studies is difficult. Consequently, the general circulation of the northern Barents Sea is not well known.

At the current stage, basic knowledge of the distribution (both horizontal and vertical) and the temporal variability of the water masses in the northern Barents Sea is lacking. Details on vertical structure, vertical heat fluxes and other parameters in the region can be found in recent publications (e.g., Sundfjord et al., 2007, 2008; Matishov et al., 2009). However, all of these studies are based upon and focus on short time scales or small spatial scales. Here, we utilise vertical temperature and salinity data covering most of the sea ice-free northern Barents Sea annually over the period 1970–2009. We establish a picture of the general oceanographic conditions (“the mean state”), we investigate variability on the multiannual and decadal time scales, and we investigate the oceanographic processes and external factors important for the observed variability. The objectives of this paper are (1) to give a basic description of the AW inflow to the Barents Sea from the north and its impact on the ArW, and (2) to identify the factors driving the multiannual variability of the AW temperature. We investigate heat advected with the AW slope-current and its upstream surface heat loss, ice cover and wind stress curl/Ekman pumping as possible driving factors.

The paper is organised as follows: the data and methods are described in Section 2. In Section 3, we use descriptive methods to give a background description of the mean state, variability and processes important for the temperature variability in the northern Barents Sea. A statistical analysis of the observational data are presented and discussed in Section 4, and the findings are summarised and the implications are discussed in Section 5.

2. Data and methods

We define our study area to be bounded in the south by 77°N, in the north by the Nansen Basin continental slope, and within the zonal band 20–50°E (Fig. 1). The reason for the regional definition is threefold: (1) it covers the inflow and distribution of AW to the Barents Sea coming from the north; (2) it excludes most of the AW dominating the Barents Sea south of the Polar Front (Figs. 1 and 2); and (3) the area has reasonably good annual hydrographic data coverage. However, because the AW inflow from the north is likely to be influenced by driving factors outside the region (e.g., upstream AW temperature and large-scale atmospheric forcing), we also include forcing factors outside our main study area.

2.1. Data acquisition and processing

The data consist of hydrographic observations, numerical model results and parameterisations of driving forces (driving factors).

2.1.1. Hydrographic observations

This paper is based on Conductivity–Temperature–Depth (CTD) profiles and water bottle data sampled during annual joint

Table 1
Definitions of northern Barents Sea water masses, modified from Pfirman et al. (1994) and Mosby (1938).

Water mass	Temperature range (°C)	Salinity range (psu)
Surface waters	$-1.9 < T < 4.0$	$S < 34.0$
Arctic Water	$T < 0.0$	$34.0 < S < 34.7$
Atlantic Water	$T > 0.0$	$S > 34.7$
Cold Dense Water	$T < 0.0$	$S > 34.75$

Norwegian–Russian surveys designed to cover the entire Barents Sea in August–October. Over the study period of 1970–2009, the number of station profiles sampled varied between 128 and 914, with a total of more than 17,000 profiles. The data from Norwegian stations are available at the International Council of the Exploration of the Sea (http://www.ices.dk) and the World Ocean Database (http://www.nodc.noaa.gov/OC5/WOD/pr_wod.html). The Russian data were sampled by the Knipovich Polar Research Institute of Marine Fisheries and Oceanography (http://www.pinro.ru). Quantifying the general accuracy of the dataset is not feasible, as it spans low-accuracy water bottle samples from the early 1970s to high-accuracy Seabird CTD-data from the last decades. A subset of the dataset, the northern Barents Sea, is used here (Fig. 1). We classify the observations into water mass definitions that comprise the core characteristics given by Pfirman et al. (1994) and the extreme values found by Mosby (1938) (Table 1).

Temperature observations at 0, 50, 100 and 200 m were interpolated onto a horizontal grid with a 1/6° meridional resolution (18 km) and a 1/2° zonal resolution (10–14 km). For each separate vertical level, a two-dimensional algorithm (Taylor, 1976) combining Laplacian and cubic spline interpolation was applied. No extrapolation or smoothing was performed except for the implicit effect of the interpolation. This approach resulted in one interpolated temperature field for each autumn season at each vertical level.

Time series of observed temperature were extracted from the gridded temperature fields at northwest location (NW) (see Fig. 1 for position). The NW position was chosen to provide information about the southward flow of AW entering through the Franz Victoria Trough (excluding AW originating from the Barents Sea Opening (BSO; see Fig. 1)). Horizontal correlation fields between the temperature time series at location NW and the horizontal fields of the gridded temperature at the respective depths (not shown) revealed that the correlation coefficient exceeded 0.5 in most of the area between 78–81°N and 30–45°E at all depths, indicating that location NW is representative for the temperature variability in the northern Barents Sea.

2.1.2. Numerical ocean model

Results from a regional coupled ice-ocean model covering the Barents and Kara seas, the northern parts of the Norwegian and Greenland seas and the southern part of the Nansen Basin (see Fig. 1 in Budgell, 2005) were used in this study to describe the ocean currents and seasonality. The ocean part was a three-dimensional baroclinic general ocean model based on Regional Ocean Modelling System (ROMS) version 2.1. The model had a stretched spherical coordinate grid (Bentsen et al., 1999) with a horizontal resolution varying from 7.8 to 10.5 km and 32 generalised sigma-coordinate vertical levels, which were stretched to enhance the resolution near the surface and the bottom. The atmospheric forcing was the ERA-40 Reanalysis, and the mixing scheme was the generic length scale (GLS) *k–kl* scheme (Mellor and Yamada, 1982; Warner et al., 2005). The initial conditions were archived five-day mean fields from a large-scale model covering the North Atlantic and Arctic oceans (see Fig. 2 in Budgell, 2005). The boundaries were forced with interpolated five-day mean fields from the large-scale model and with tidal velocities and free surface heights from eight constituents of the Arctic Ocean Tidal Inverse Model (Padman and Erofeeva, 2004). The large-scale model had similar horizontal and vertical grids as the regional model, with a 50-km horizontal resolution and 30 vertical levels. This model was forced with the NCEP/NCAR Reanalysis, with surface flux corrections as developed by Bentsen and Drange (2000). The model did not simulate tides, and it had an LMD (Large et al., 1994) vertical mixing scheme. The sea ice module dynamics were based on elastic–viscous–plastic rheology after Hunke and Dukowicz (1997) and Hunke (2001), while the thermodynamics consisted of two ice layers and one snow layer and was based on Mellor and Kantha (1989) and Häkkinen and Mellor (1992). For more details about the model, see Budgell (2005).

Budgell (2005) compared the model results from the Barents Sea with sea surface temperature (from satellite), hydrographic sections, time series from long-time moored instruments (in the BSO) and sea ice concentration (from satellite). He concluded that the model setup produces realistic ice-ocean seasonal and interannual variability, and the agreement is particularly good for temperature time series in the southern Barents Sea. However, a detailed comparison of the model results with observed subsurface hydrography in the northern Barents Sea, where the vertical gradients are strong due to ArW overlaying AW, did not show consistent vertical distributions (Johansen, 2008). The inflow of AW spanned a thicker vertical layer in the model compared with the observations, with the main deficiency in the upper layers, where the model showed an inflow of AW at too shallow depths. This problem, in turn, had an impact on the modelled ArW, which was too warm and saline at the ~50 to 100 m depth (Johansen, 2008). Thus, no vertical integrated estimates, e.g., volume and heat fluxes, can be calculated from the simulation. Additionally, due to the improper representation of the upper AW boundary, and because we do not know exactly why this occurred, the model cannot be used to quantify the vertical movements in the water column.

Despite the poor representation of the vertical gradients, the horizontal distribution of the modelled AW temperature at 200 m was accurate (Johansen, 2008; and compare Fig. 2a and the temperature field in Fig. 4). Thus, we find the model to be a reasonable tool for describing the general flow and temporal variability of the seasonal cycle at 200 m, which is the depth of AW inflow in the NBSO.

2.1.3. Driving factors

2.1.3.1. AW inflow. AW in the West Spitsbergen Current (WSC) has been observed annually in August–October since 1977 in a CTD transect westward from Sørkapp, the southern tip of Spitsbergen (Fig. 1). This section gives a continuous interannual time series of the WSC summer/autumn hydrography (Blindheim et al., 2000; Saloranta and Haugan, 2001). Here, we use the mean 50–200 m AW temperature. Although the series is nearly 1000 km upstream of the NBSO, and modifications of the WSC over 1000 km can be significant (Saloranta and Haugan, 2004), the series has been found to have coherent signals with the subsurface hydrography (100–300 m layer) northwest of Svalbard at approximately 80°N in the 1980s and 1990s (Saloranta and Haugan, 2001). We therefore considered this series the most appropriate for investigating the impact of upstream temperature variations on the AW entering the northern Barents Sea from the north.

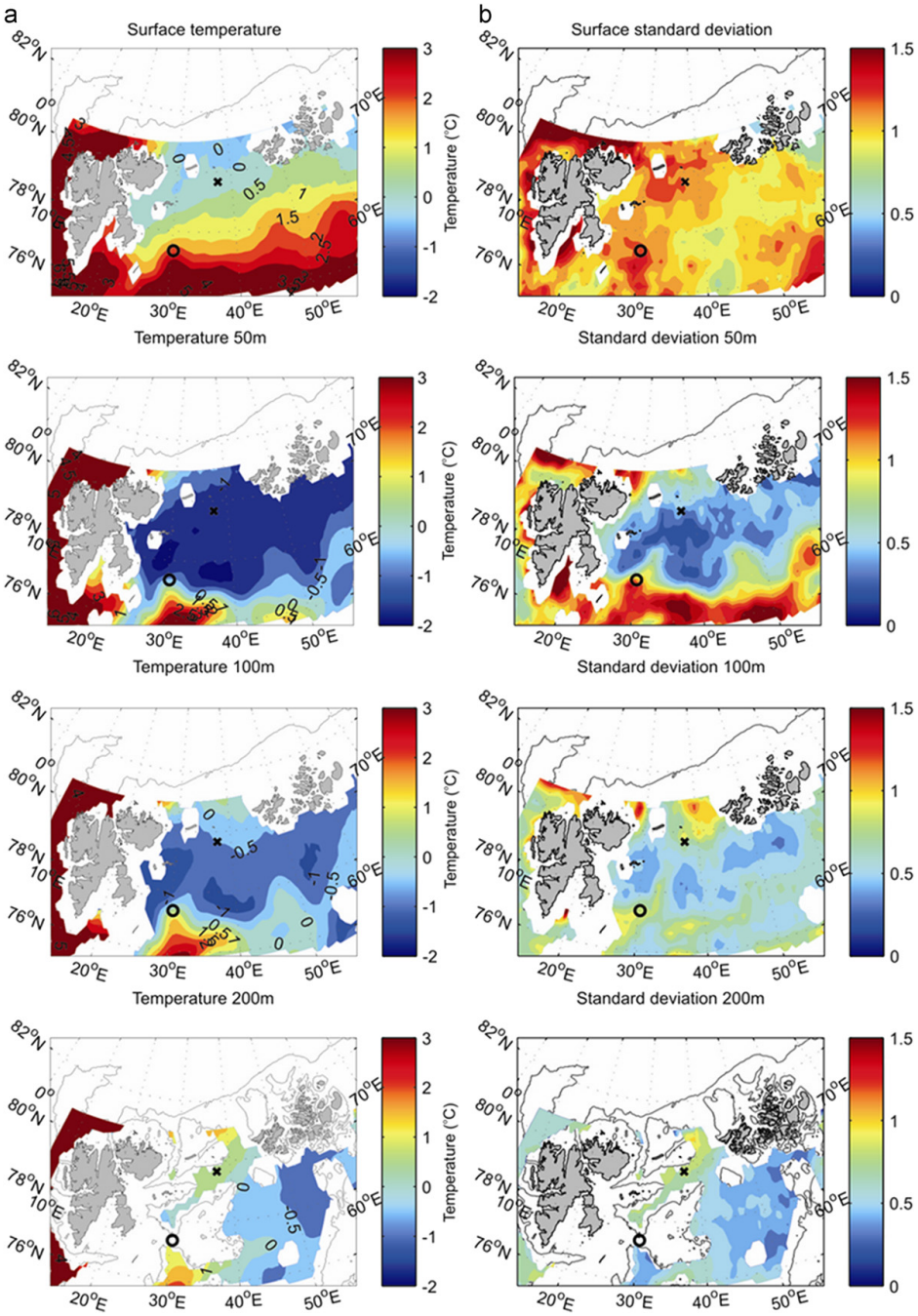

Fig. 2. (a) Mean interpolated temperature (°C) and (b) temperature standard deviation (°C) at surface, 50, 100 and 200 m depth based on observations in August–October from 1970 to 2009. For definition of O and X, see Fig. 1.

2.1.3.2. Surface air temperature. Daily values of SAT in Longyearbyen, Svalbard, available from the Norwegian Meteorological Institute, were combined into an annual time series of winter-mean (December–March) SATs. The air temperature was observed 2 m above ground in Longyearbyen from 1969 to 1975 (37 m above sea level) and at Longyearbyen Airport from 1976 to

2009 (28 m above sea level). We use the winter-mean SAT as an index for the direct heat loss from the WSC to the atmosphere. A higher SAT can decrease the local heat loss, resulting in a higher AW temperature when it enters the Arctic Ocean (e.g., Saloranta and Haugan, 2001). There is a relatively strong co-variability between the SAT in Longyearbyen and the northerly wind stress component on the Svalbard shelf (Cottier et al., 2007), indicating that the SAT in Longyearbyen is comparable with the open sea SAT. Part of the heat loss from the WSC has been shown to occur laterally (Saloranta and Haugan, 2004; Nilsen et al., 2006; Tverberg and Nøst, 2009). Our analysis did not include the variability of the lateral heat loss.

2.1.3.3. Sea ice concentration and area. We got monthly averaged sea ice concentrations derived from SMMR and SSM/I passive microwave remote sensing data from the National Snow and Ice Data Center. The final processed data were used for the period 1978–2007 (Cavalieri et al., 1996; Meier et al., 2006). Because the processing of this data set was temporarily suspended, near-real-time ice concentration data were used to cover the time period 2008–2009 (Maslanik and Stroeve, 1999).

The ice area was calculated for the region 20–50°E and 77–82°N (0.32 million km^2) and combined into winter-mean (December–March) and summer-mean (June–September) values. The northern Barents Sea is mostly ice-covered, with a mean sea ice concentration of more than 90% in winter and spring (Kvingedal, 2005), thereby isolating the ocean from the atmosphere. A decrease in sea ice concentration/area in winter can impact the ocean by increasing the heat loss. Hence, we use the winter-mean ice area to evaluate the atmospheric influence on the surface and subsurface water masses during winter. The summer-mean ice area is included for quantifying summer heating of the upper layer water masses.

2.1.3.4. Wind stress curl, Ekman transport and pumping. Monthly mean surface wind fields (10 m above sea level) were available from an atmospheric hindcast archive covering the Norwegian and Barents Seas produced by the Norwegian Meteorological Institute (Eide et al., 1985; Reistad and Iden, 1998) from 1970 to 2008. The archive data had a six-hourly temporal resolution on a 75-km evenly distributed rotated polar-stereographic grid. This source was chosen instead of the more commonly used NCEP/NCAR or ERA-40 reanalyses due to its higher resolution.

Based on the hindcast archive, we calculated monthly mean surface wind stress and the associated Ekman transport and pumping. The effects of sea ice on the ocean surface stress curl were accounted for in the analysis using two different approaches. The first approach was calculating the wind stress $\boldsymbol{\tau}=(\tau_x,\tau_y)=\rho_a C_a U_a \boldsymbol{U}_a$ using the lower threshold value for the mean air-ocean and air–ice drag coefficient ($C_a=2.7\times10^{-3}$) for outer marginal ice zones (~50% ice concentration) (Guest et al., 1995; also used by Sundfjord et al., 2007 for the northern Barents Sea). With this approach, we assume that all the momentum in the ice is transferred to the ocean. The other parameters involved in the calculation were air density $\rho_a=1.25$ kg m^{-3} and surface wind $\boldsymbol{U}_a$ referenced to 10 m above sea level.

The other approach included the sea ice concentration directly in the calculations. Drifting ice affects the momentum transfer from the atmosphere to the ocean (e.g., Wadhams, 2000; Leppäranta, 2005). Depending on its characteristics, sea ice act to either enhance or reduce the momentum transfer (Leppäranta, 2005). A detailed description of the equations and parameterisations involved in these calculations is given in Appendix A. As seen in Appendix A, it is not straightforward to include the effect of sea ice on the ocean surface layer, and several crude assumptions were made. The air–ice drag coefficient was parameterised from the sea ice concentration (Andreas et al., 2010). However, the ice-ocean drag coefficient parameterisation requires the sea ice roughness characteristics and the draft/length ratio (Lu et al., 2011), which are unknown. Additionally, calculating the sea ice drift introduces large errors, particularly because both ocean velocity and sea ice thickness are unknown.

Monthly mean Ekman transport using both the above approaches was calculated with $\boldsymbol{U}_e=(u_e,v_e)=(1/\rho_w f)(\tau_y,-\tau_x)$, where $\rho_w=1025$ kg m^{-3} is the mean ocean mixed layer density, and $f=2\Omega$ sin φ_{mean} is the Coriolis acceleration at the mean grid latitude $\varphi_{mean}=79.16$°N. The monthly mean Ekman pumping (also using both approaches) was calculated with

$$w_e=(1/\rho_w f)(\partial\tau_y/\partial x-\partial\tau_x/\partial y) \quad (1)$$

The derived monthly fields were combined to annual fields.

The wind stress curl is an important driver for ocean circulation, and Ekman pumping is an efficient process creating vertical movement in the ocean (Gill, 1982). Coastal upwelling is the most dominant and strongest Ekman pumping case, and it has been found to have a strong influence on the cross-shelf exchange of AW along the West Spitsbergen coast (Cottier et al., 2007). Ekman pumping in the open ocean is substantially weaker, but it can still be important at seasonal or longer time scales (deSzoeke, 1980). Ekman pumping has been shown to induce strong open ocean downwelling/upwelling in the northern Arabian Sea (Bauer et al., 1991). Thus, wind stress curl and Ekman pumping fields were included in the analysis to investigate their effect on the cross-shelf exchange of AW across the NBSO.

2.2. Statistical methods

To relate the observed temperature variability to relevant driving factors, an Empirical Orthogonal Function/Principal Component (EOF/PC) analysis was performed on the gridded temperature fields, and the derived PCs were correlated with the driving factors. The EOF/PC analysis provides a compact description of the spatial and temporal variability of data series by finding structures that explain the maximum variance and identify centres of action (centres of maximum variance) (Emery and Thomson, 2004). The outputs are spatial fields of variability modes (EOFs) with corresponding time series giving the temporal variability of each mode (PCs). The analysis was performed on the fields at 50 and 200 m to capture the variability in the ArW and AW least influenced by mixing (see Section 3.3.1). An analysis for 100 m showed similar results, and the PCs at 100 m were always between those for 50 and 200 m (not shown). EOF/PC analysis was also used to find the dominant modes of variability in the annual mean Ekman pumping fields.

A five-year moving average was applied to the PCs and the driving factors before correlation analysis. The reason for this approach was twofold: (1) the spatial coverage of the observations in this area varies, which may influence the estimated interannual variability when using statistical analysis. To minimise this problem, but still utilise all observations, time filtering was found to be appropriate. (2) Due to the advection and propagation of anomalies, time lags may be expected when considering upstream conditions (e.g., Pfirman et al., 1994). Due to the complexity of representing all the relevant forcing factors, we found it necessary not to include lags in the analysis.

The linear trend was removed from the filtered PCs and driving factors, and the resulting series were standardised. To adjust for autocorrelation in the series, the effective number of degrees of freedom was calculated in accord with Pyper and Peterman (1998):

$$\frac{1}{N^*}=\frac{1}{N}+\frac{2}{N}\sum_{j=1}^{N/5} r_{xx}(j)r_{yy}(j)$$

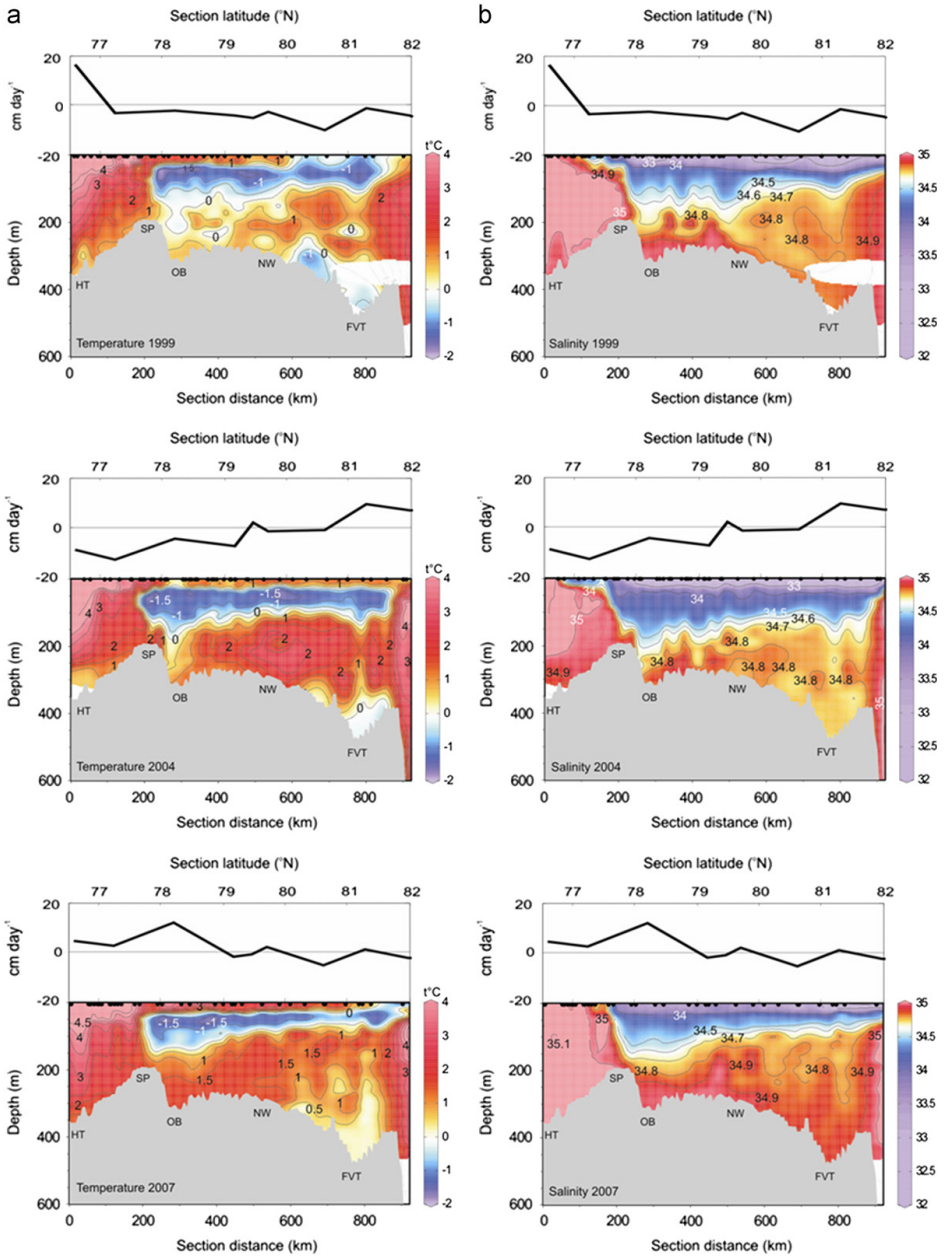

Fig. 3. (a) Temperature (°C) and (b) salinity (psu) observed in September 1999 (upper panels), September 2004 (middle panels) and September 2007 (lower panels) in a transect from northern Hopen Trench (HT), crossing over the saddle point (SP) between HT and Olga Basin, to the Franz Victoria Trough (FVT) constructed with Ocean Data View (Schlitzer, 2009). See Fig. 1 for position of transect and definition of O and X. Also shown above each panel is the annual mean Ekman pumping (cm day^{-1}) at the transect. The Ekman pumping is discussed in Section 3.3.1.

where N^* is the effective number of degrees of freedom of the time series X and Y, N is the sample size and $r_{xx}(j)$ and $r_{yy}(j)$ are the autocorrelations of X and Y at lag j. Following the recommendation by Pyper and Peterman (1998), a maximum of $N/5$ lags were included in the calculation of N^*. Linear correlation coefficients between the filtered, detrended and standardised

time series were calculated using the derived effective number of degrees of freedom. The presented correlation coefficients are significant on the 95% level unless otherwise mentioned.

3. The northern Barents Sea—water masses and processes

A thorough description of the northern Barents Sea hydrography is lacking in the literature. Thus, we find it necessary to give a general description of the northern Barents Sea hydrography and its temporal variability and to present the mean state and variability of the driving factors included in this paper.

3.1. General description

In this section, the horizontal and vertical distribution of water masses are described based on the hydrographic observations from 1970 to 2009, and the general circulation is outlined based on the numerical model results.

3.1.1. Horizontal water mass distribution (from observations)

The overall picture from the surface temperature fields is that the temperature in the northern Barents Sea is decreasing northwards (Fig. 2a). The high standard deviation shows strong interannual temperature variability (Fig. 2b), and the strongest interannual variability is found where the seasonal variability in sea ice cover is large. ArW dominates the whole study area at 50 m, with a mean temperature below -1 °C (Fig. 2a). At 100 m, ArW is evident only in the central area, being limited by AW intruding into the area both from the north and the south. The region occupied by ArW has low interannual variability compared with the surrounding areas (Fig. 2b). AW entering the area from the north through the troughs of the NBSO is clearly visible at 100 m, and this water mass fills the entire trench system of the northern Barents Sea at 200 m (Fig. 2a). Weaker indications of AW originating from the BSO and crossing the ~200-m-deep saddle point between Hopen Trench and Olga Basin can be seen in the enhanced standard deviation northeast of the saddle point at 100 m (Fig. 2b).

3.1.2. Vertical water mass distribution (from observations)

The vertical temperature and salinity transects from the northern Hopen Trench and into the Arctic Ocean through the Franz Victoria Trough (see Fig. 1) were constructed from the CTD profiles sampled in 1999, 2004 and 2007 (Fig. 3). The data were not sampled continuously, but all profiles in each transect were observed within two to three weeks. The surface layer in all three years reached down to 15–30 m (Fig. 3). The surface layer shows large lateral variability but is more homogeneous in the vertical. From 1999 to 2007, the surface layer became warmer and slightly more saline. The ArW is evident as the layer with minimum temperature between the surface layer and the (modified) AW (Fig. 3). In all three years, the layer was thickest, coldest and freshest in Olga Basin, gradually becoming thinner, warmer and more saline toward the Franz Victoria Trough. This northward thinning is probably caused by strong water mass modifications and vertical mixing in the regions where subsurface AW enters from the north (Pfirman et al., 1994; Sundfjord et al., 2007). The AW entering from the north is evident at 50–300 m in the Franz Victoria Trough (Fig. 3). This AW submerges under the ArW in the Franz Victoria Trough and shows a gradual descent southward. The temperature and extent (lateral and vertical) of AW in the northern Barents Sea varies considerably between years. In 1999 and 2007, the AW core in the Franz Victoria Trough was situated at 100–200 m, and when penetrating southward, the AW became substantially mixed from below and above. In 2004, the AW

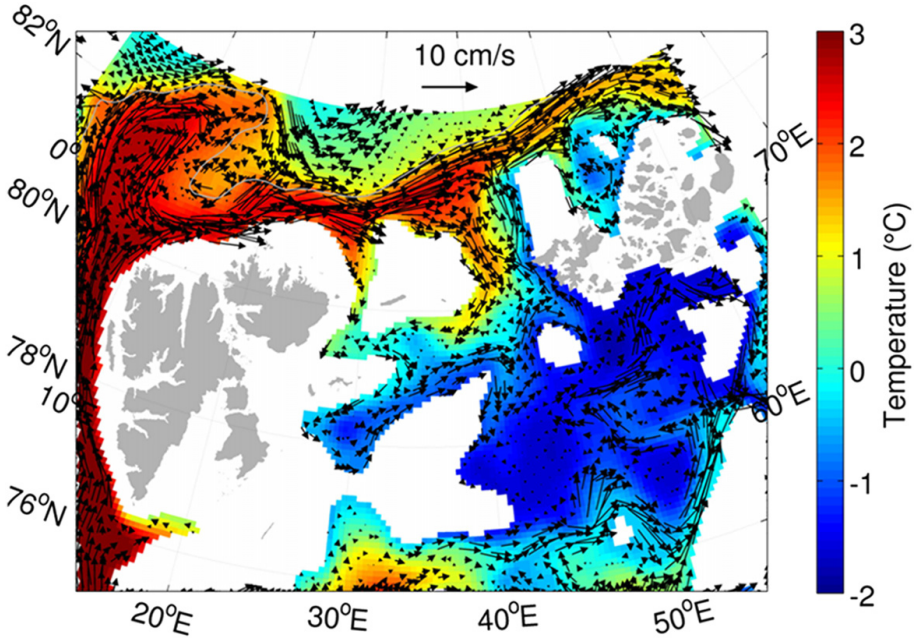

Fig. 4. Mean 1993–2001 simulated temperature (°C—filled contours) and velocity (cm s^{-1}—arrows) at 200 m depth from the regional ocean circulation ROMS model. Velocity in every fifth grid cell is shown (see reference arrow).

extended up to the surface layer on the shelf-break, there was a substantially higher temperature at the 200–400 m depth layer near the Franz Victoria Trough, and there was a stronger inflow of AW to the northern Barents Sea. Also evident in 2004 is a reduction in salinity causing a weaker stratification (not shown) and a fresher and thicker ArW layer compared with the two other years. The AW originating from the BSO and crossing the Polar Front is evident as colder, more saline water near the bottom in the Olga Basin, below the AW originating from the NBSO. Cold Dense Water is present near the bottom in the Franz Victoria Trough.

3.1.3. Ocean currents (from the numerical model)

The 1993–2001 mean model velocity and temperature at 200 m (Fig. 4) shows the AW slope-current along the shelf-slope north of the Barents Sea flowing as one single current after the remerging of the inner Svalbard Branch and the outer Yermak Branch. The slope-current has a speed of 15–20 cm s^{-1} and a temperature of ~3 °C. Part of the AW enters the Barents Sea through the troughs of the NBSO. The major inflow occurs through the Franz Victoria Trough, although there is also some recirculation in this trough. Once entering the northern Barents Sea, the AW cools substantially, and the AW temperature decreases to ~0.5 °C when reaching the south of Kvitøya. The circulation continues cyclonically in the Olga Basin, and intensifies along the northern slope of the Great Bank. Then, the strongly modified AW either exits to the Arctic Ocean through the Franz Victoria Trough or flows into the area east of the Great Bank. The model indicates a substantial cooling of the AW slope-current when passing the Franz Victoria Trough.

3.2. Temporal variability

Seasonal, interannual, and multiannual variability are investigated using time series from the NW location (see Fig. 1 and Section 2.1.1).

3.2.1. Seasonal variability (from the numerical model)

Information about the seasonal variability in the sub-surface layers in this area is sparse. To evaluate whether the CTD observations (from autumn) are suitable for studying the multiannual temperature variability of the AW, the seasonal variability of the AW layer was investigated in the numerical model results from 200 m. The annual temperature, salinity, and velocity cycles at location NW (Fig. 1) were extracted from the model fields (Fig. 5). Due to the strong high-frequency variability, a 30-day moving average was applied to the current speed to highlight the seasonal cycle.

The temperature cycles at NW (Fig. 5a) indicate that the minimum usually occurs in March (mean ~ −0.5 °C) and the maximum in late September/early October (mean ~2 °C). This result is consistent with the seasonal cycle observed in the AW in the southern Barents Sea (Loeng, 1991; Furevik, 2001), but one month earlier than the maximum observed in the AW slope-current core in the Nansen Basin (Ivanov et al., 2009). The model seasonal range is ~2.5 °C, which is substantially higher than that observed both in the southern Barents Sea and in the slope-current. The salinity cycle has the same shape as the temperature: high and relatively stable salinities throughout summer and autumn and lower and more varying salinities in winter and spring (Fig. 5b). This pattern indicates more mixing in winter and spring (consistent with Sundfjord et al., 2008, their Fig. 5). There is no clear seasonal cycle in current speed (Fig. 5c), but the model indicates a minimum in summer and early autumn. The interannual variability is large. The annual-mean current has a maximum speed of ~4 cm s^{-1} in winter, decreasing to ~3 cm s^{-1} in summer. The majority of the current directions were toward the west–southwest, reflecting a strong topographic steering (Fig. 5d).

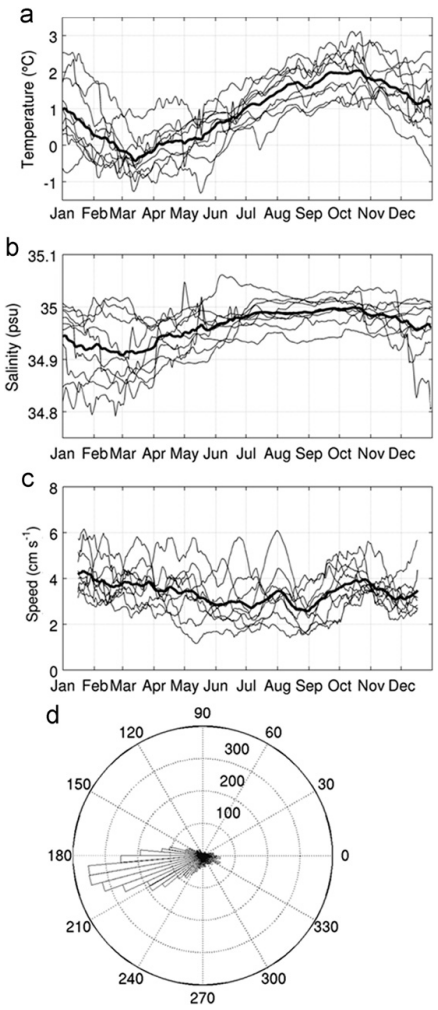

Fig. 5. Daily values of (a) temperature (°C), (b) salinity (psu) and (c) current speed (cm s^{-1}) simulated in the regional circulation ROMS model at location NW (see Fig. 1 for location) at 200 m from 1993 to 2001. The thin lines are annual cycles and the thick line is the mean annual cycle. Current speed has been filtered with a 30-day moving average. (d) Frequency distribution of simulated current directions at location NW at 200 m from 1993 to 2001 (daily values; the total number of days is 3285 days).

In summary, the model results indicate that the annual CTD observations were sampled close to the maximum in the seasonal cycle of the AW temperature and salinity, which occurred during a season with relatively slowly varying temperature and salinity. This implies that the observations had low sensitivity towards sampling time (i.e., low synoptic error). This result suggests that the interannual variability in the autumn observations is the true interannual variability and not an artificial variability due to sampling errors. Therefore, the annual autumn CTD observations

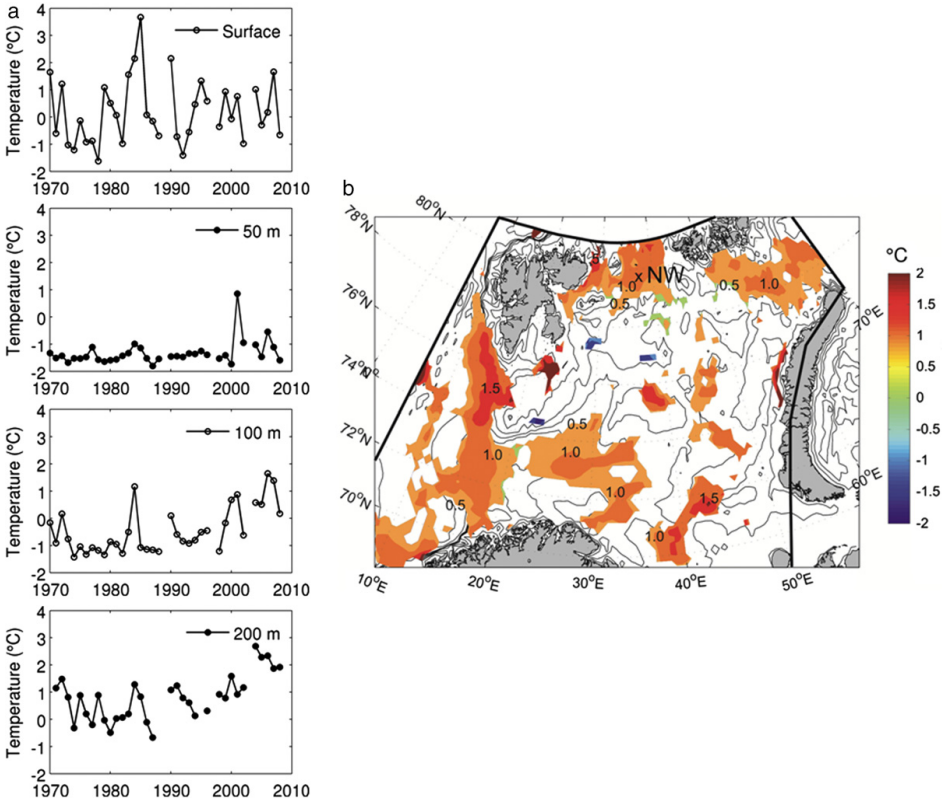

Fig. 6. (a) Time series of temperature at NW extracted from the gridded temperature fields at surface, 50, 100 and 200 m depth. (b) Estimated linear increase (during 1970–2009) in autumn temperature at 50–200 m depth, shown where the trend is statistically significant on the 95% level.

should be suitable for studying the interannual to multiannual variability of the AW.

3.2.2. *Interannual to multiannual variability and trends (from observations)*

The interannual temperature variability from observations at location NW (Fig. 1) shows that the surface water is dominated by the interannual variability and has no increasing or decreasing trend (Fig. 6a). At 50 m, however, the temperature was extremely stable, with no trend until the late 1990s; but thereafter, both the temperature and the interannual variability increased substantially. Although there has been an increase in sampling intensity and an approximately ten-day shift in sampling time during the study period, this cannot account for the shift in variability. The interannual variability at 200 m is greater than at 50 m, but smaller than at the surface. However, the temperature at 200 m has large long-term changes, and it spans a range from -0.7 °C (in 1987) to 2.7 °C (in 2004). The most pronounced temperature increase started in the mid/late 1990s. The temperature at 100 m was dominated by ArW ($T<0$ °C) up to the mid/late 1990s and by AW ($T>0$ °C) thereafter.

The total temperature increase during 1970–2009 was estimated from statistically significant linear trends (at the 95% confidence level) in the gridded mean 50–200 m fields for the entire Barents Sea (Fig. 6b). All the boundary areas where AW enters show a statistically significant linear trend at intermediate depths. The temperature rise in and near the NBSO clearly comes from the north and is not due to water advected through the Barents Sea from the BSO. The lack of statistically significant trends at 50–200 m in the central part of the ocean probably reflects the vertical transformation/sinking of the water masses when passing through the Barents Sea, as the Barents Sea is an efficient cooler (Smedsrud et al., 2010). Still, similar trends might be found in deeper layers (below 200 m) in the central and eastern parts. However, the temperature variability below 200 m is affected by variability in dense water formation, and exploring this variability is beyond the scope of this paper. Also evident in Fig. 6b is a strong temperature rise southwest and northwest of Spitsbergen. We investigate in Section 4 whether this signal has been important for the temperature increase in the northern Barents Sea.

3.3. *Driving factors*

The mean state and variability of the driving factors to be investigated in Section 4 are presented below.

3.3.1. *Wind, Ekman transport and pumping (from atmospheric hindcast)*

The 1970–2008-mean surface wind stress field is generally easterly (Fig. 7a), resulting in an Ekman transport toward the north in the entire area (Fig. 7b—arrows). The general wind stress effect is

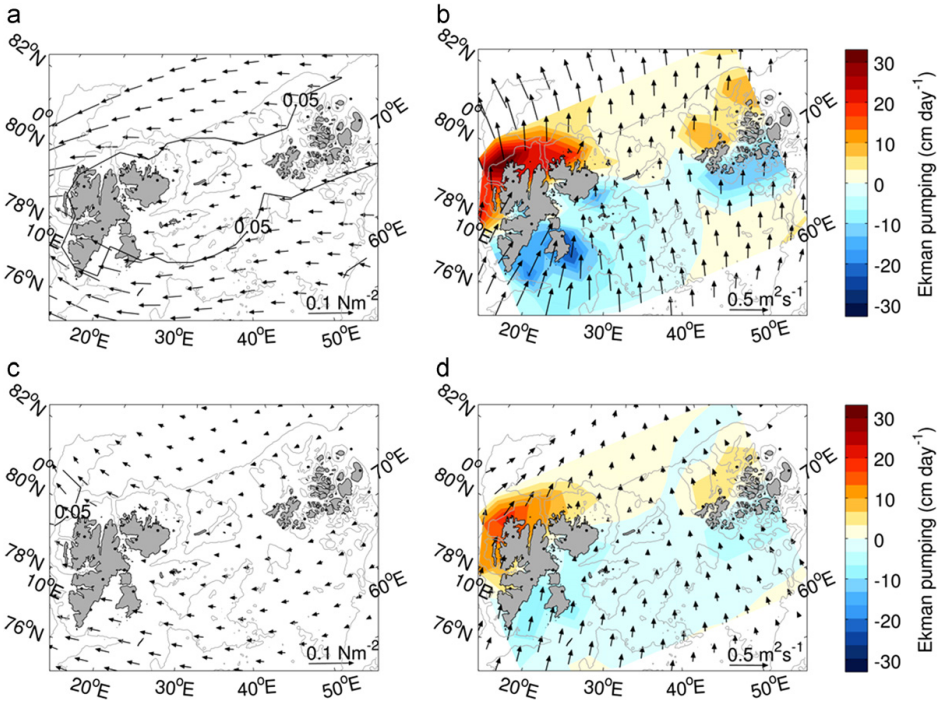

Fig. 7. (a) Mean 1970–2008 total tangential stress on the ocean surface (N m^{-2}) using algorithm in Section 2.1.3 (in effect, the wind stress). (b) Mean 1970–2008 Ekman transport (arrows) and Ekman pumping (cm day^{-1}—filled contours) using algorithm in Section 2.1.3. (c) Mean 1979–2008 total tangential stress on the ocean surface (N m^{-2}) using algorithm with sea ice implemented (see Appendix A). (d) Mean 1979–2008 Ekman transport (arrows) and Ekman pumping (cm day^{-1}—filled contours) using algorithm with sea ice implemented (see Appendix A). See lower right corners for reference arrow.

hence a transport of the upper waters from the northern Barents Sea toward the Arctic Ocean. Ekman pumping (Eq. (1)) occurs (Fig. 7b—filled contours) due to the lateral gradients in the wind stress and the presence of land, and it has large local differences. The mean wind stress and Ekman transport has similar patterns, though are weaker, when sea ice concentration is included directly in the calculations (Fig. 7c and d). The fields are also shifted clockwise due to the turning angle θ_0 (Eq. (A.3)). However, the overall pattern is the same as when ice cover is not included. The shape of the mean Ekman pumping field is not sensitive to the choice of algorithm (compare Fig. 7b and d–filled contours); however, it is slightly weaker overall if sea ice concentration is implemented. (The slight difference in Ekman pumping sign north of Franz Josef Land is attributed to the difference in the period covered (starting in 1979 if sea ice is implemented)).

The 1970-2008-mean Ekman pumping calculated with the approach described in Section 2.1.3 shows that the strongest upwelling (positive Ekman pumping) is north and northwest of Spitsbergen (Fig. 7b–filled contours), where the Ekman Pumping is always positive and has annual mean values ranging from 0 to 50 cm day^{-1}, with an average of 22 cm day^{-1} (not shown). Weaker upwelling is evident further northeast in the Nansen Basin (Fig. 7b–filled contours). The annual mean ranges from −7 to 23 cm day^{-1} in this area (not shown). The mean Ekman pumping is also positive (upwelling) over the outer shelf and shelf-break at the northern boundary of the Barents Sea, which means that, in this area, the subsurface AW will be lifted in the water column. The upper boundary of AW on the Nansen Basin continental shelf slope north of the Barents Sea has been observed to vary between 50 and 200 m, whereas the lower boundary is located beyond the shelf-break (between 800 and 900 m) (Ivanov et al., 2009). Thus, increasing the upper boundary of AW is likely to increase the penetration of AW onto the Barents Sea shelf. The Ekman pumping is close to zero or negative (downwelling) over the Barents Sea (Fig. 7b–filled contours).

Indications of increased cross-shelf exchange due to upwelling caused by Ekman pumping are also evident in the vertical transects (Fig. 3). The high temperature and deep maximum (200–400 m depth) in 2004 compared to 1999 and 2007 indicates a stronger upwelling of AW in the Franz Victoria Trough, and the annual mean Ekman pumping (drawn above the vertical transects in Fig. 3) shows consistently higher values in this region during 2004 compared with the two other years.

3.3.2. *Effects of advection, surface heat loss and sea ice (from observations)*

There is substantial inter- and multiannual variability in AW temperature at the WSC (Fig. 8). The annual unfiltered temperature values varies from 2.7 °C (in 1978) to 5.0 °C (in 1991 and 2006). Warm periods (high temperature over several years) are observed in the early 1980s, the early 1990s and in the mid-2000s. The time series indicates that the AW temperature at the WSC was equally high in the early 1990s as in the mid-2000s; thus, the increase in the observed AW temperature in the northern Barents Sea in the 2000s cannot be explained by the temperature increase in the WSC alone. Over the period 1977–2009, the WSC showed a pronounced temperature increase and a

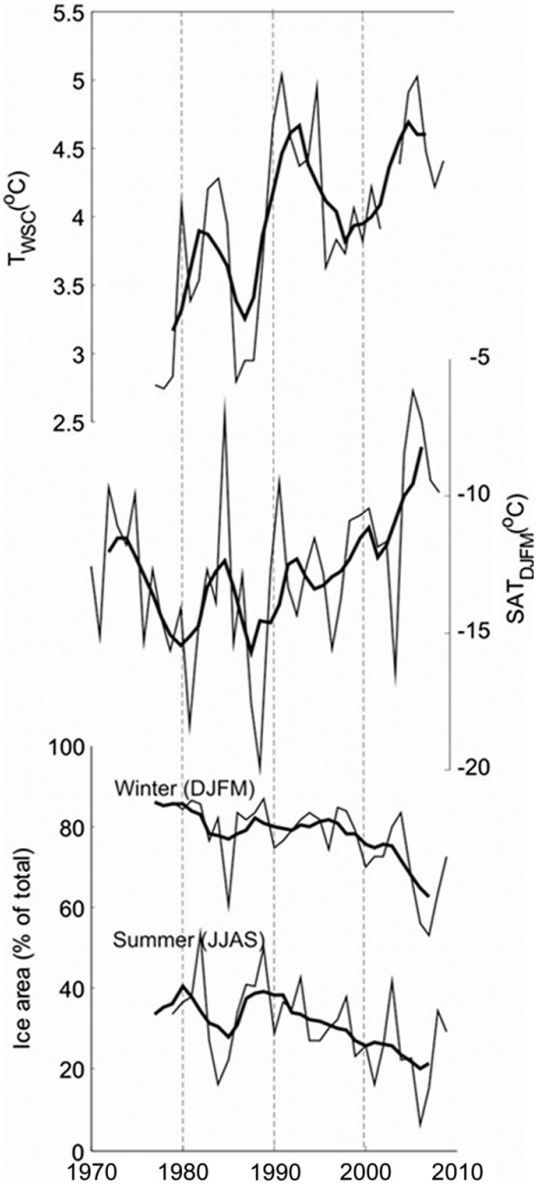

Fig. 8. Time series of temperature at the West Spitsbergen Current at Sørkapp (T_{WSC}; upper panel), winter-mean surface air temperature in Longyearbyen (SAT_{DJFM}; middle panel) and ice area in winter (DJFM) and summer (JJAS) (lower panel). The ice area was calculated for the box 77–82°N, 20–50°E, and is given in percentage of the total area of the box (which is 0.32 million km^2).

statistically significant positive trend (on the 95% confidence level) of 0.44 °C decade^{-1}.

The winter-mean SAT in Longyearbyen varies from −20.0 °C (in 1989) to −6.2 °C (in 2006) (Fig. 8). In contrast to the WSC, there was a substantial winter-mean SAT increase from the 1990s to the 2000s. Over the period 1970–2009, the winter-mean SAT had a statistically significant linear trend (95% confidence level) of 0.78 °C decade^{-1}.

The sea ice area ranges from 87% coverage (0.28 million km^2) in winter and 53% coverage (0.17 million km^2) in summer during the cold years of 1981–1982 to 53% coverage (0.17 million km^2) in winter and 6% coverage (0.02 million km^2) in summer during the warm years of 2006–2007 (Fig. 8). The summer ice area started decreasing in the late 1980s/early 1990s, while the winter ice area shows a pronounced decrease starting in the late 1990s. After the millennium shift, both the winter and summer ice area shows large interannual variability, but the general trend is a reduction in ice cover compared with the previous decades. The linear decreasing trend (statistically significant on the 95% confidence level) is 5.5% (0.018 million km^2) decade^{-1} for winters and 4.8% (0.015 million km^2) decade^{-1} for summers during period 1978–2009.

4. Statistical analysis—results and discussion

To identify the most important driving forces for the observed temperature changes described in Section 3, we use statistical analysis on the spatial temperature fields and the driving factors. The results of the EOF/PC analysis of the temperature and Ekman pumping fields are presented in Section 4.1, and the results of the correlation analysis between the derived PCs and the driving factors are presented and discussed in Section 4.2.

4.1. EOF/PC analysis

4.1.1. Observed temperature fields

In the AW layer (200 m depth), the two leading modes (EOF1-T200 and EOF2-T200), explaining together 64% of the temperature variability, are presented (Fig. 9a and b). For the ArW layer (50 m), only the first mode (EOF1-T50), explaining 29% of the variability, is shown (Fig. 9c) because it was the only mode representing variability associated with ArW. The second mode at 50 m was more closely related to the variability in AW south of the Polar Front and will not be analysed here.

EOF1-T200 explains 40% of the temperature variability in the AW layer. The spatial correlation field between PC1-T200 and the original temperature field (not shown) has large areas with individual correlation coefficients of $r > 0.70$. Thus, in these areas, EOF1-T200 explains more than 49% of the interannual variability. The positive sign of EOF1-T200 over the entire area deeper than 200 m (Fig. 9a) indicates simultaneous temperature increases or decreases in the region. EOF2-T200, however, has a positive sign in the NBSO and a negative sign east of the Great Bank (Fig. 9b). The positive sign pattern has a maximum amplitude near the shelf-break in the Franz Victoria Trough it streches and southwestward into the trench system that is dominated by AW (Fig. 2a). EOF2-T200 thus represents a variability of AW flow that is more confined to the shelf-break and the Franz Victoria Trough compared with EOF1-T200. EOF2-T200 explains 24% of the variability in the AW, but the spatial correlation field between PC2-T200 and the original temperature fields (not shown) indicate that EOF2-T200 explains more than 49% of the temperature variability in the NBSO.

In the ArW layer (at 50 m), EOF1-T50 explains 29% of the temperature variability (Fig. 9c). The spatial correlation field between PC1-T50 and the original temperature fields at 50 m (not shown) exceeds $r > 0.70$ in most of the ArW area. Thus, despite the relatively low explanation percentage for the entire area, EOF1-T50 explains more than 49% of the interannual variability in the ArW. The positive sign of EOF1-T50 over most

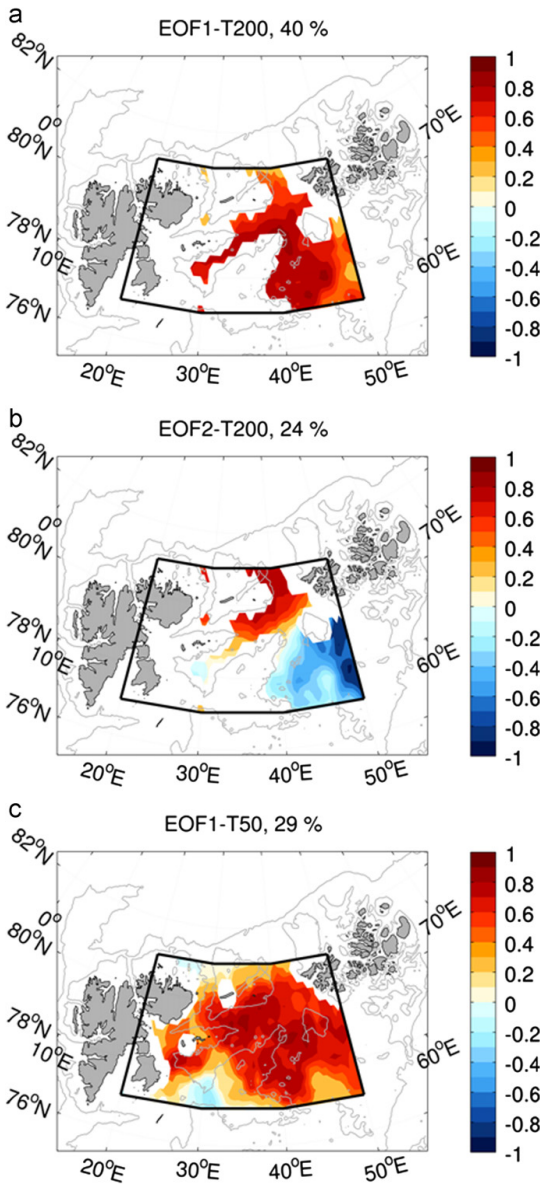

Fig. 9. (a) The first and (b) the second EOF of the gridded temperature fields at 200 m, and (c) the corresponding first EOF at 50 m, all shown in units of standard deviation (°C). The EOF/PC analysis was performed on the area enclosed by the black line.

of the northern Barents Sea indicates a simultaneous temperature increase or decrease in the entire horizontal ArW layer.

4.1.2. Ekman pumping

EOF/PC analysis was performed on both Ekman pumping fields (derived from the approaches described in Section 2.1.3 and Appendix A). Although the mean Ekman transport/pumping fields were relatively consistent in the two approaches (Fig. 7b and d), the variability was not consistent; consequently, the EOF/PC analysis differed between the two approaches. The simplest approach (described in Section 2.1.3), assuming all the momentum in the ice is transferred to the ocean and not implementing the sea ice concentration directly, gave the highest correlations with the PCs from the observed temperature fields. Consequently, this approach will be presented here, but the time series (PCs) of the other approach, implementing sea ice concentration directly (described in Appendix A), are shown and discussed in Fig. 11 and Section 4.2. Calculating the Ekman pumping from the numerical model was not feasible due to the unrealistic vertical distributions and the associated mixing in the model.

The two leading modes from the EOF/PC analysis of the Ekman pumping fields together explain 42% of the variability (Fig. 10a and b). The first mode (EOF1-We) represents a situation with positive Ekman pumping anomalies in the Nansen Basin and in an east-west band just south of the shelf-break (Fig. 10a); thus, it represents variability associated with an open ocean upwelling signal. The wind anomalies causing this Ekman pumping variability are easterly winds north of Franz Josef Land and north of Spitsbergen that increase and decrease northwards, respectively (Fig. 10c). This leads to positive upwelling anomalies north of Franz Josef Land and negative upwelling anomalies north of Spitsbergen. The westerly wind anomaly in the interior northern Barents Sea (Fig. 10c) causes less downwelling here (i.e., a positive Ekman pumping anomaly), as shown in Fig. 10a. The pressure field associated with this wind pattern would be a weak high-pressure anomaly west of Spitsbergen and a low-pressure anomaly between Svalbard and Franz Josef Land.

As discussed in Section 3.3.1, increased upwelling near and just south of the shelf-break increases the penetration of AW onto the shelf, as was observed in 2004. South of the shelf-break, the amplitude of EOF1-We decreases rapidly and turns weakly negative, indicating that the Ekman pumping associated with this mode is limited to the northern Barents Sea. The mode explains 25% of the variability in the Ekman pumping fields; however, the spatial correlation field between PC1-We and the original Ekman pumping fields (not shown) indicates that EOF1-We explains more than 49% of the Ekman pumping variability in the Nansen Basin, south of Svalbard and south of Franz Josef Land.

The second Ekman pumping mode (EOF2-We) represents a situation with anomalously strong Ekman pumping in a band along the shelf-break north of, the NBSO and south-westward in the northern Barents Sea (Fig. 10b). This pattern is associated with cyclonic wind anomalies around Svalbard (Fig. 10d), which pushes water off the coast and causes the positive Ekman pumping anomalies around Svalbard. This wind field must be caused by a strong low-pressure anomaly over Svalbard. The southerly wind anomaly in the northern Barents Sea decreases toward the east. This causes convergent Ekman transport and a negative Ekman pumping anomaly south of Franz Josef Land.

The positive Ekman pumping anomaly on the shelf-break north of Svalbard will (Fig. 10b) bring AW onto the shelf upstream of the NBSO. Cottier et al. (2007) observed a similar upwelling process west of Spitsbergen that caused penetration of AW onto the west Spitsbergen shelf. As it is likely that the AW on the shelf and inner slope north of Svalbard enters the northern Barents Sea, this process may increase the inflow directly. In addition, the higher upwelling between Kvitøya and Hopen can bring the AW from the upper part of the water column to the same depth as the ArW. Because horizontal mixing in the ocean is more efficient than vertical mixing, this can increase the overall mixing between AW and ArW. Thus, the Ekman pumping associated with this signal can impact most of the western part of the northern Barents Sea. EOF2-We explains 17% of the Ekman pumping

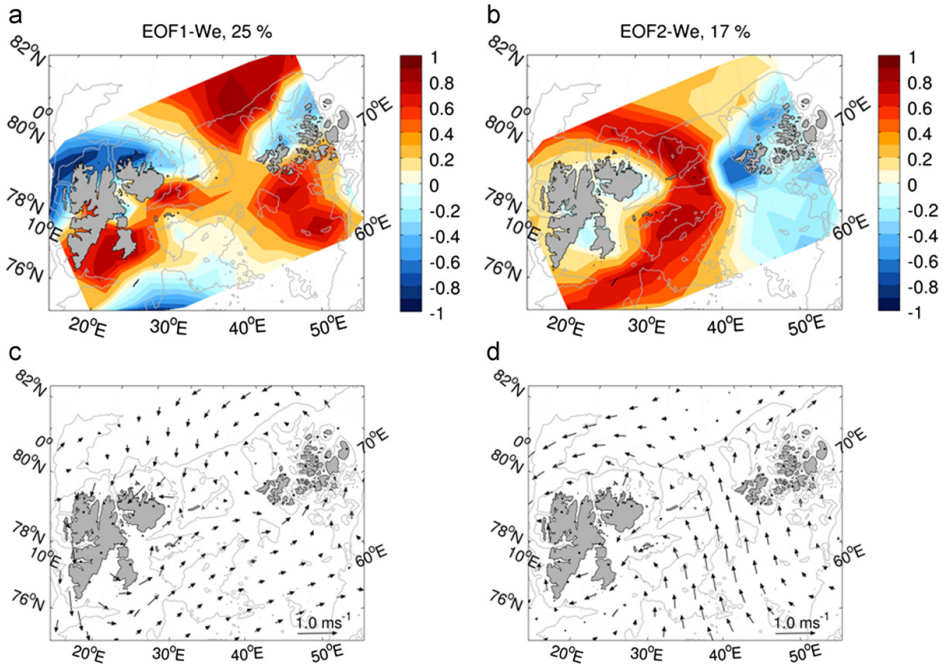

Fig. 10. (a) The first and (b) the second EOF of the annual mean Ekman pumping fields (using approach in Section 2.1.3) shown in units of standard deviations (cm day^{-1}). Wind anomalies (m s^{-1}) causing one standard deviation change in Ekman pumping for (c) PC1-We and (d) PC2-We; see lower right corners for reference arrow.

Table 2
Correlation coefficients between the PCs of the temperature fields in 50 and 200 m and the driving factors. All time series were filtered with a five-year moving average, detrended and standardized before the coefficients were calculated. The analysis has been adjusted for auto-correlation, and the coefficients are significant on the 95% level unless otherwise mentioned.

	PC1-T200	PC2-T200	PC1-T50	T_{WSC}	SAT_{DJFM}	Ice $area_{DJFM}$	Ice $area_{JJAS}$	PC1-We	PC2-We
PC1-T200	1.00	–	–	0.77	–	–	–	–	0.51[a]
PC2-T200	–	1.00	0.48	–	0.61	–	–	0.84	–
PC1-T50	–	0.48	1.00	–	–	–	–	–	–
T_{WSC}	0.77	–	–	1.00	–	–	–	–	0.62
SAT_{DJFM}	–	0.61	–	–	1.00	–	−0.67	0.55	–
Ice $area_{DJFM}$	–	–	–	–	–	–	–	–	–
Ice $area_{JJAS}$	–	–	–	–	−0.67	–	1.00	–	–
PC1-We	–	0.84	–	–	0.55	–	–	1.00	–
PC2-We	0.51[a]	–	–	0.62	–	–	–	–	1.00

[a] Significant on the 90% level.

variability in the whole area. However, the spatial correlation field between PC2-We and the original Ekman pumping field (not shown) indicates that EOF2-We explains more than 49% of the Ekman pumping variability in the western NBSO area.

4.2. Correlation analysis

Focusing on multiannual variability, the correlation coefficients between the PCs of the temperature fields and the driving factors are given in Table 2. Each PC is shown together with its driving factor(s) in Fig. 11.

4.2.1. Driving forces for Atlantic Water temperature variability

The PC of the first AW mode, PC1-T200, is strongly positively correlated with the AW temperature at the WSC (r=0.77, Table 2), showing that variability in the upstream temperature is the dominant source of variability in the AW layer. If the trend is not removed from the time series prior to correlation analysis, the coefficient increases to r=0.87, indicating that this signal may drive both the trend and the multiannual variability of EOF1-T200. Including time lags do not increase the correlation. This may indicate that the real time lag is less than one year, i.e., that the AW temperature at the WSC affects the AW temperature at the northern Barents Sea within the same year. The PC1-T200 also has a moderate correlation with PC2-We (r=0.51; statistically significant on the 90% confidence level), the coastal Ekman pumping around Svalbard, indicating that the increased inflow due to upstream coastal upwelling also influences on the AW temperature in the northern Barents Sea.

A visual inspection of the time series reveals that multiannual variability dominates and that the covariation between PC1-T200

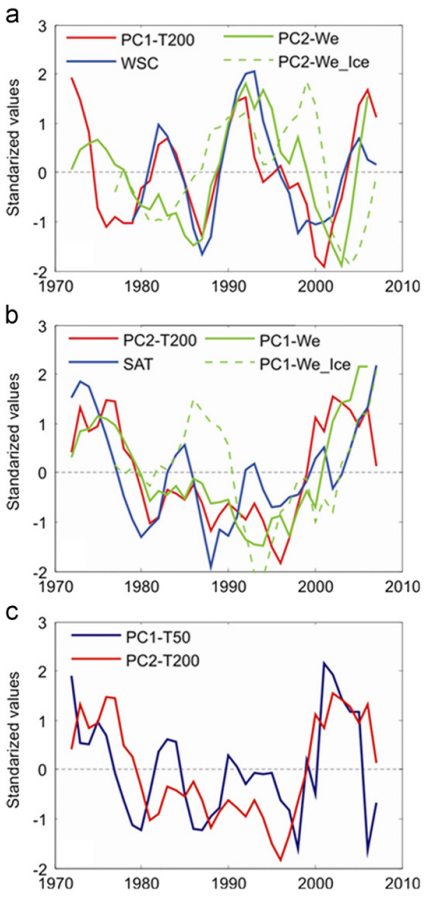

Fig. 11. Standardized detrended and filtered time series of the PCs of the gridded temperature fields and the driving factors identified by the correlation analysis in units of standard deviation. (a) The PC of the first AW mode (PC1-T200), temperature of the West Spitsbergen Current at Sørkapp (WSC), the PC of the second Ekman pumping mode (PC2-We) and the PC of the second Ekman pumping mode using the approach implementing sea ice concentration directly (PC2-We_Ice; see Appendix A). (b) The PC of the second AW mode (PC2-T200), winter-mean surface air temperature in Longyearbyen (SAT) and the PC of the first Ekman pumping mode (PC1-We) and the PC of the first Ekman pumping mode using the approach implementing sea ice concentration directly (PC1-We_Ice; see Appendix A). (c) The PC of the first ArW mode (PC1-T50) and the PC of the second AW mode (PC2-T200).

and the identified driving factors varies over the time period (Fig. 11a). Multiple linear regression shows that the temperature variability in the WSC and coastal upwelling (PC2-We) together explain 64% of the variability in PC1-T200. The WSC has the strongest influence during the first part of the study period, explaining as much as 95% of the variability up until 1992. During the same period, PC2-We explains only 25% of the variability. The influence of PC2-We is stronger toward the last part of the study period. From 1986 onwards, the variability in the WSC and PC2-We has a more equal influence on PC1-T200 than earlier, explaining 59 and 51% of the variability, respectively.

The PC of the second AW mode, PC2-T200, is highly correlated with PC1-We ($r=0.84$, i.e., explaining 71% of the variability in PC2-T200), showing that positive anomalies of open ocean upwelling in the NBSO strongly influences the AW temperature in the northern Barents Sea. Following Proshutinsky and Johnson (1997), upwelling along the Arctic continental shelf-slopes lifts the pycnocline between the ArW and the AW, and consequently, more AW will penetrate onto the shelves (their Fig. 3). This effect will be most pronounced near the shelf-break, consistent with Fig. 9b. Nevertheless, the effect will increase the heat content of the northern Barents Sea, and more heat will be available for mixing with ArW. This finding also corresponds with Abrahamsen et al. (2006), who suggested that the circulation of AW in the northern Barents Sea is controlled by winds between Svalbard and Franz Josef Land. PC2-T200 also has a moderate correlation with the winter-mean SAT in Longyearbyen ($r=0.61$). The AW in the WSC is subjected to both direct surface heat loss to the atmosphere and strong lateral subsurface heat loss (Saloranta and Haugan, 2004; Nilsen et al., 2006; Tverberg and Nøst, 2009). The moderate correlation with winter-mean SAT indicates that the variability of direct surface heat loss impacts on the temperature signal advected clockwise around Svalbard on the multiannual time scale.

PC2-T200 and PC1-We are dominated by multidecadal variability, with rapid shifts occurring in the late 1970s and the late 1990s (Fig. 11b). The co variability of the series is coherent throughout the study period, and both series have overall maxima in the late 2000s. In total, PC1-We and winter-mean SAT explain together 76% of the variability in PC2-T200.

The PCs of the Ekman pumping fields where sea ice concentration was implemented directly in the calculation (i.e., the approach described in Appendix A), PC1-We_Ice and PC2-We_Ice, are shown for comparison in Fig. 11a and b. Although there are some similarities between the PCs with and without ice cover included, there are also substantial differences. The time series with ice cover included has no statistically significant correlation to any of the other time series in this study. The PCs with ice cover included covers a shorter time period (sea ice concentration is available from 1979) than PC1-We and PC2-We. However, performing the correlation analysis on PCs of Ekman pumping fields not including ice cover for the shorter period 1979–2009 did not change the result.

The most likely reason for the poor co-variability between the observed AW temperature and the calculated Ekman pumping including ice cover is the rather crude assumptions, which had to be made when performing the air-ice and ice-ocean stress calculations (Section 2.1.3 and Appendix A). Thus, it is possible that a relationship would have appeared if other assumptions had been made and more sea ice variables were known. Still, we found a strong relationship with the calculated Ekman pumping using a mean air-ocean and air–ice drag coefficient for outer marginal ice zones. In this simplified approach, all the variability in the Ekman pumping comes from the wind stress curl and not from the variability in the ice cover. This situation is also consistent with the lack of relation/correlation between the AW temperature and the sea ice area in summer or winter (Table 2). We interpret the result as that the main forcing factor is likely to be the wind stress curl. It is also likely, or at least possible, that the process from which the wind stress curl acts on the ocean is through Ekman pumping, although firm conclusions on the process cannot be made on the basis of our analysis.

When analysing Ekman pumping, we use annual mean velocities, which, in most of the area, are below 10 cm day^{-1} or 37 m year^{-1} (Figs. 3 and 7). A vertical movement of less than 40 m year^{-1} seems rather insufficient to cause stronger cross-shelf exchanges of AW. The main reason for using annual means is that we do not know the time lag between the shelf-slope and the interior part of the northern Barents Sea. Using a mean advection speed of 4–5 cm s^{-1}, a first approximation gives that the water involved in causing the maximum amplitude in EOF1-T200 (200–500 km south of the shelf-break;

Fig. 9a) crossed the shelf-break 4–6 months earlier (i.e., in late winter or early spring). The Ekman pumping is substantially stronger in winter than in summer, with 2000–2008 winter-mean (November–April) velocities of 21 cm day^{-1} averaged over the area north of the shelf-break from Nordaustlandet and eastward (not shown). This velocity would give a cumulative lift of the water column of 38 m during the winter. The values greatly differ between years, and both 2004 and 2007—years of high observed AW temperature in Fig. 3—were years with high winter-mean Ekman pumping values (25 and 34 cm day^{-1}, respectively). Nevertheless, because we do not know, which period of the year the Ekman pumping is most important, we find it appropriate to consider annual means. Other mechanisms, e.g., lateral and vertical mixing of the AW slope-current; heat loss to the atmosphere and to sea ice melting upstream of the submergence of the AW slope-current; and mixing with cascading cold density plumes might also have an impact on the thickness and vertical distribution of the AW slope-current. In particular, variability in the submergence of AW north of Spitsbergen may play an important role.

Our results show that on multiannual time scales, the AW temperature in the northern Barents Sea depends on the upstream temperature (in the WSC), on cross-shelf exchange caused by the wind stress curl in the open ocean, (weakly) on the the wind stress curl in the coastal areas and (weakly) on upstream direct surface heat loss. The most likely process associated with the wind stress curl is Ekman pumping. We find no relationship between the subsurface AW and sea ice area during summer or winter.

4.2.2. Impacts on Arctic Water

The temperature variability in ArW, represented by PC1-T50, is not related to any of the investigated driving factors (Table 2), but it has a moderate significant correlation of $r = 0.48$ with the AW temperature itself (PC2-T200). This result indicates that vertical mixing transfers heat from the AW upwards to the ArW. The effect will likely be strongest in the NBSO, where EOF2-T200 and EOF1-We have maximum amplitude (Figs. 9b and 10a). This finding is consistent (1) with Fig. 2b showing a higher variability of ArW in the NBSO area, (2) with Fig. 3 showing a thinner, warmer and more saline ArW layer in the northern part of the transect and (3) with Sundfjord et al. (2007) showing that wind stress, tidal mixing and tidal-generated internal waves cause significant turbulent mixing between ArW and AW in this area.

The temporal variability of PC1-T50 and PC2-T200 (Fig. 11c) indicates that the rapid increase in ArW temperature that occurred in the late 1990s (Fig. 6a) was linked to the raised subsurface AW interface. Thus, it is likely that the AW reached high enough in the water column during the late 1990s/early 2000s to substantially impact the ArW at 50 m.

5. Discussion and summary

The first objective of this paper was to give a basic description of the AW inflow to the Barents Sea from the north (between Svalbard and Franz Josef Land) and its impacts on the ArW. We find that most of the AW in the northern Barents Sea enters the area from the north. Since the AW that enters from the north is below the ArW, this AW is subjected to a relatively slow heat loss rate (through mixing) compared with being in direct contact with the atmosphere (through direct surface heat loss), as AW in the southern Barents Sea is. The AW entering the Barents Sea from the north therefore maintains a temperature above 0 °C far into the northern Barents Sea trench system. The hydrographic observations show that the AW temperature in the northern Barents Sea increased substantially during 1970–2009 and that the AW temperature increase accelerated in the late 1990s.

ArW occupies the upper 20–100 m of the northern Barents Sea, with temperature down to the freezing point. The ArW layer is thickest, coldest and freshest in the Olga Basin just north of the Polar Front, and gradually thins toward the Franz Victoria Trough. The vertical extent of the ArW layer varies on interannual time scales due to the variations in mixing with the AW. We also find that the temporal variability in the ArW temperature is partly influenced by the variations in the AW. Before the late 1990s/early 2000s, the ArW temperature was extremely stable and low; after this period, the temperature and the interannual variability increased. This effect was caused by increased penetration of AW onto the northern Barents Sea shelf. Note that we ignored the factors producing and/or advecting ArW into the region. We also chose a method (EOF/PC analysis) that analyses the variance in the fields. As the temperature variability in the ArW is weak compared with the AW, this is not the most suitable method for the general identification of structures in the ArW. Consequently, we can only evaluate the impact of AW on ArW.

The second objective of this paper was to identify the factors driving the multiannual temperature variability of the AW entering the Barents Sea from the north. Our conclusion is that the most dominant driving factor is upstream temperature variations in the WSC advected with the AW, and this forcing causes a simultaneous temperature response over most of the northern Barents Sea AW layer. The signal has multiannual variability and a strong trend, but it cannot account for the observed accelerating temperature increase in the northern Barents AW in the late 1990s. Also of importance for the multiannual variability in the AW temperature is the wind stress curl along the coast north of Svalbard. The most likely process is that the wind stress curl causes coastal upwelling, which brings AW onto the shelf north of Svalbard and increases the amount of AW entering the Barents Sea through the NBSO.

The second most important driving factor of the AW temperature is the open ocean wind stress curl in the Nansen Basin and the NBSO. The probable mechanism is that the wind stress curl causes Ekman pumping, which lifts the AW slope-current in the Nansen Basin and increases the cross-shelf exchange and the penetration of AW onto the shelf. This process will in turn cause higher AW temperature on the northern Barents Sea shelf and the shelf-break facing the Nansen Basin. This signal has multidecadal variability with rapid shifts, including an abrupt increase in the late 1990s. Thus, the enhanced warming of the northern Barents Sea in the late 1990s was caused by an increased open-ocean wind stress curl/Ekman pumping over the shelf-break. We also find that upstream direct surface heat loss from the WSC to the atmosphere may have an effect with similar temporal variability. Variability in the sea ice cover does not appear to influence on the AW temperature.

The accelerating AW temperature increase in the northern Barents Sea during the late 1990s and the early 2000s may have been linked to changing large-scale atmospheric circulation in the Arctic. According to Proshutinsky and Johnson (1997), upwelling along the Arctic continental shelf-slopes and the penetration of AW onto the Arctic shelves are associated with the large-scale atmospheric circulation in the Arctic Ocean. During anticyclonic atmospheric circulation, the sea surface height increases in the central Arctic Ocean and decreases on the surrounding shelves. This pushes the pycnocline down in the centre of the basin and lifts it up on the shelf-slopes. Thus, AW advected along the shelf-slopes is lifted, and the penetration onto the shelves increases. The period of increased upwelling in the late 1990s and early 2000s coincides with the prevailing anticyclonic atmospheric circulation in the Arctic from 1997 to 2008 (A. Proshutinsky, personal comm., 2010). During the 2000s, an abnormal dipole pattern of the Arctic atmospheric circulation also occurred (Zhang et al., 2008).

The inflow of warm AW through the BSO has a strong impact on the Barents Sea climate variability (e.g., Loeng, 1991; Sandø et al., 2010). Regional downscaled climate models indicate that future heating due to anthropogenic signals will dominate in the Barents Sea south of the Polar Front (Ellingsen et al., 2009). The location of the front in the western Barents Sea is strongly linked to topography. Strong changes in location have not been observed earlier and are not predicted to happen in the future (Loeng, 1991; Ellingsen et al., 2009). Still, our results document increasing temperature and a decreasing vertical extent of the ArW from below, and it links these changes to the inflow of AW through the NBSO. Because this AW inflow is cooled through vertical mixing rather than direct surface heat loss, which is the case in the southern Barents Sea, it has much stronger impacts on the ArW. Thus, major changes in the ArW and the Polar Front in the future will most likely be caused by the AW coming from the north and below, not from the AW entering in the upper waters in the BSO. A detailed study of the formation and modification processes of ArW in the Barents Sea is needed before conclusions can be made on this topic. Nevertheless, our results have shown that future generations of regional downscaled climate models should have a good representation of the subsurface flow of AW coming from the NBSO and the factors controlling its variability.

The ocean general circulation model results from this and other studies indicate that a part of the AW following the Nansen Basin shelf slope eastward takes a detour in the northern Barents Sea before re-entering the Nansen Basin through the Franz Victoria Trough. During this detour, the AW is substantially cooled and freshened through mixing with the ArW, and the outflow through the Franz Victoria Trough modifies the AW slope-current downstream of the NBSO. This modification of the slope-current is consistent with Schauer et al. (1997). Thus, the modelled circulation pattern indicates that not only the large transit of AW through the Barents and Kara seas from the BSO to the St. Anna Trough is transformed in the Barents Sea; also the AW entering the Arctic Ocean through Fram Strait, specifically the Nansen Basin AW slope-current, is modified by water mass transformations in the Barents Sea due to the detour that parts of the AW take in the northern Barents Sea. Furthermore, the latter transformations impact on the AW slope-current downstream of the NBSO, and these changes arise from mixing with the ArW.

Acknowledgements

This is publication no. 386 from the Bjerknes Centre for Climate Research. The work has been funded by the Bjerknes Centre for Climate Research, the Institute of Marine Research in Norway, the International Polar Year projects Bipolar Atlantic Thermohaline Circulation (BIAC, IPY Cluster # 23) and the Norwegian Component of the Ecosystem Studies of Subarctic and Arctic Regions (NESSAR, part of IPY Cluster # 155), both supported by the Norwegian Research Council. We thank the Norwegian Meteorological Institute for the atmospheric hindcast archive and the weather observations in Longyearbyen, the National Snow and Ice Data Centre for the sea ice concentration data, M. Skogen for preparing the atmospheric hindcast fields, and P. Budgell for the ROMS general circulation model results. We are also grateful to K. Gjertsen for help with preparing the figures and T. Furevik, V. Tverberg, and three anonymous referees for constructive comments.

Appendix A. Ekman pumping analysis with sea ice concentration implemented

An alternative Ekman pumping analysis was carried out with the aim of implementing the effect of the drifting sea ice cover in the northern Barents Sea. The principal components of this EOF analysis (PC1-We_Ice and PC2-We_Ice) are shown in Fig. 11a and b. A detailed description of the method is given below.

For each grid cell of the surface wind field $\boldsymbol{U}_a$ at 10 m above sea level (from the atmospheric hindcast fields, Section 2.1.3), the total tangential stress on the ocean surface was calculated as

$$\boldsymbol{\tau} = (\tau_x, \tau_y) = \rho_a C_a U_a \boldsymbol{U}_a \quad \text{for} \quad A = 0 \tag{A.1a}$$

and

$$\boldsymbol{\tau} = (\tau_x, \tau_y) = \rho_w C_w U_i \boldsymbol{U}_i \quad \text{for} \quad A > 0 \tag{A.1b}$$

where $\rho_a = 1.25\ \mathrm{kg\ m^{-3}}$ is the mean air density, $C_a = C_a(A) = 1.5 \times 10^{-3} + 2.233 \times 10^{-3} A - 2.333 \times 10^{-3} A^2$ is an empirically based parameterisation of the air-ocean and air–ice drag coefficient for areas that are a mixture of open water and sea ice (Andreas et al., 2010), A is the fractional sea ice concentration field (from remote sensing data from the National Snow and Ice Data Centre, Section 2.1.3) ranging from 0 for open water to 1 for complete ice cover, and $\rho_w = 1025\ \mathrm{kg\ m^{-3}}$ is the mean ocean mixed layer density.

$$C_w = (C_e AD/2L)[1-(AD/L(1-A))^{1/2}]^2 + (C_r A H_r/\pi D_r)[1-(H_r/D_r)^{1/2}]^2 + C_s A(1-(mH_r/D_r)) \tag{A.2}$$

is the total ice-ocean drag coefficient parameterisation by Lu et al. (2011), derived according to the quadratic drag law. C_e and C_r are form drag coefficients of a single floe edge and a single ridge keel, respectively, C_s is the skin friction drag coefficient of the ice bottom, D/L is the ice floe draft/length ratio, H_r/D_r is the ice floe ridging intensity (H_r is the ridge keel depth and D_r is the distance between ridge keels) and $m = 10$ is assumed to be constant and is related to the shadowing effect on the ice bottom between adjacent ridges (Eq. (12) of Lu et al., 2011). Eq. (A.2) is valid only for $H_r/D_r \le 1/m$ ($m = 10$) and $A < 1/(1 + D/L)$. The first right-hand term of (A.2) becomes zero for $A \ge 1/(1 + D/L)$.

In estimating C_w, we followed Lu et al. (2011) and set $C_e = 1.0$ (Horner, 1965), $C_r = 0.5$ (found by Pite et al. (1995) for ridge keel slope angles of $\sim 10^\circ$), $C_s = 2.0 \times 10^{-3}$ (measured under a relatively smooth ice bottom in the Beaufort Sea by Hunkins (1975)) and $H_r/D_r = 1/100$ (moderate ridging intensity close to that measured in the Barents Sea by Overgaard et al. (1983)). The draft over length ratio varies from $D/L = 1/10{,}000$ for large floes in the central ice zone to $D/L = 1/10$ for pancake ice or floes in the marginal ice zone. Sensitivity studies by Lu et al. (2011) showed that the form drag of the floe edge (the first right-hand term of Eq. (A.2)) is always the dominant term for large draft over length ratios ($D/L \ge 1/100$). However, for small D/L, C_w mostly depends on the form drag of the floe keel or the skin friction (second and third right-hand terms of Eq. (A.2), respectively). Thus, when parameterising C_w for ice fields with a highly varying D/L, such as from a marginal ice zone to a central ice pack as in the northern Barents Sea, it is important to treat D/L as a variable. To our knowledge, an empirical relationship between D/L and A has not been published. However, we deduced such a relationship by combining the empirical formulas $H = D + F = 9.46F + 0.15$ (for first-year ice based on the isostatic equilibrium equation by Alexandrov et al. (2010)) and $L = 31F/(1-A)$ (Mai, 1995; and applied by Lüpkes and Birnbaum, 2005), where H is the total ice thickness and F is the freeboard. Setting $D = 1$ and solving for L gave $L = 3.114657/(1-A)$.

Finally, the ice velocity is

$$\boldsymbol{U}_i = N_a[\cos\theta_0, \sin\theta_0]\boldsymbol{U}_a + \boldsymbol{U}_{wg} \tag{A.3}$$

(Leppäranta, 2005), where $N_a = (\rho_a C_a/\rho_w C_w)^{1/2}$ is the wind factor (the Nansen number), $\theta_0 = -25^\circ$ is the turning angle and $\boldsymbol{U}_{wg}$ is the geostrophic ocean current. We assumed $\boldsymbol{U}_{wg} = 0$ 'slippery ice', an assumption that Perrie and Hu (1997) found adequate for similar conditions. Eq. (A.3) also assumes the ice velocity is

negligible compared with the wind velocity, an assumption that is valid in most cases. For each grid cell of the sea ice concentration field A, the nearest surface wind grid cell was found through nearest neighbour interpolation and was applied in Eq. (A.3).

References

Aagaard, K., Foldvik, A., Gammelsrød, T., Vinje, T., 1983. One-year records of current and bottom pressure in the strait between Nordaustlandet and Kvitøya, Svalbard, 1980–81. Polar Res. 1n.s., 107–113.

Aagard, K., Woodgate, R.A., 2001. Some thoughts on the freezing and melting of sea ice and their effects on the ocean. Ocean Model. 3, 127–135.

Abrahamsen, E., Østerhus, S., Gammelsrød, T., 2006. Ice draft and current measurements from the north-western Barents Sea, 1993–96. Polar Res. 25, 25–37.

Aksenov, Y., Bacon, S., Coward, A.C., Nurser, A.J.G., 2010. The North Atlantic inflow to the Arctic Ocean: high-resolution model study. J. Mar. Syst. 79, 1–22.

Alexandrov, V., Sandven, S., Wahlin, J., Johannessen, O.M., 2010. The relation between sea ice thickness and freeboard in the Arctic. Cryosphere 4, 373–380.

Andreas, E.L., Horst, T.W., Grachev, A.A., Persson, P.O.G., Fairall, C.W., Guest, P.S., Jordan, R.E., 2010. Parametrizing turbulent exchange over summer sea ice and the marginal ice zone. Q. J. R. Meteorol. Soc. 136, 927–943.

Årthun, M., Ingvaldsen, R.B., Smedsrud, L.H., Schrum, C., 2011. Dense water formation and circulation in the Barents Sea. Deep-Sea Res. I 58, 801–817.

Bauer, S., Hitchcock, G.L., Olson, D.B., 1991. Influence of monsoonally-forced Ekman dynamics upon surface layer depth and plankton biomass distribution in the Arabian Sea. Deep-Sea Res. A 38, 531–533.

Bentsen, M., Drange, H., 2000. Parameterizing Surface Fluxes in Ocean Models using the NCEP/NCAR Reanalysis Data. RegClim General Technical Report No. 4. Norwegian Institute for Air Research, Kjeller, Norway, pp. 44–57.

Bentsen, M., Evensen, G., Jenkins, A.D., 1999. Coordinate transformation on a sphere using conformal mapping. Mon. Weather Rev. 127, 2733–2740.

Blindheim, J., Borovkov, V., Hansen, B., Marmberg, S.-Aa, Turrell, W.R., Østerhus, S., 2000. Upper layer cooling and freshening in the Norwegian Sea in relation to atmospheric forcing. Deep-Sea Res. I 47, 655–680.

Budgell, W.P., 2005. Numerical simulation of ice-ocean variability in the Barents Sea region. Towards dynamical downscaling. Ocean Dyn. 55, 370–387.

Cavalieri, D., Parkinson, C., Gloersen, P., Zwally, H.J., 1996. Sea-ice Concentrations from Nimbus-7 SMMR and DMSP SSM/I Passive Microwave Data, 1978–2007. National Snow and Ice Data Center, Boulder, Colorado USA. Digital Media (updated 2008).

Comiso, J.C., Parkinson, C.L., Gersten, R., Stock, L., 2008. Accelerated decline in the Arctic sea ice cover. Geophys. Res. Lett. 35, L01703. doi:10.1029/2007GL031972.

Cottier, F.R., Nilsen, F., Inall, M.E., Gerland, S., Tverberg, V., Svendsen, H., 2007. Wintertime warming of an Arctic shelf in response to large-scale atmospheric circulation. Geophys. Res. Lett. 34, L10607. doi:10.1029/2007GL029948.

Eide, L.I., Reistad, M., Guddal, J., 1985. A Database of Estimated Wind and Wave Parameters for the North Sea and Barents Sea, Every 6th hour 1955–81. Technical Report. Norwegian Meteorological Institute, Oslo/Bergen, Norway, p. 38 (in Norwegian).

Ellingsen, I., Slagstad, D., Sundfjord, A., 2009. Modification of water masses in the Barents Sea and its coupling to ice dynamics: a model study. Ocean Dyn. 59, 1095–1108.

Emery, W.J., Thomson, R.E., 2004. Data Analysis Methods in Physical Oceanography, 2nd ed. Elsevier, Amsterdam.

Furevik, T., 2001. Annual and interannual variability of the Atlantic Water temperatures in the Norwegian and the Barents Seas: 1980–1996. Deep-Sea Res. I 48, 383–404.

Gill, A.E., 1982. Atmosphere–Ocean Dynamics. Academic Press, New York.

Guest, P.S., Glendening, J.W., Davidson, K.L., 1995. An observational numerical study of wind stress variations within marginal ice zones. J. Geophys. Res. 100, 10887–10904.

Häkkinen, S., Mellor, G.L., 1992. Modelling the seasonal variability of a coupled arctic ice-ocean system. J. Geophys. Res. 97, 20285–20304.

Hanzlick, D., Aagard, K., 1980. Freshwater and Atlantic water in the Kara Sea. J. Geophys. Res. 85, 4937–4942.

Horner, S., 1965. Fluid Dynamic Drag, Practical Information on Aerodynamic Drag and Hydrodynamic Resistance. Hoerner Fluid Dyn., Midland Park, N. J.

Hunke, E., Dukowicz, J., 1997. An elastic–viscous–plastic model for sea ice dynamics. J. Phys. Oceangr. 27, 1849–1867.

Hunke, E., 2001. Viscous–plastic sea ice dynamics with the EVP model: linearization issues. J. Comput. Phys. 170, 18–38.

Hunkins, K., 1975. Geostrophic drag coefficients for resistance between pack ice and ocean. AIDJEX Bull. 28, 61–67.

ICES, 2011. Barents Sea Capelin. Report of the Arctic Fisheries Working Group (AFWG). Hamburg, Germany. ICES CM 2011/ACOM:05, 28 April–4 May 2011, pp. 500–503.

International Hydrographic Organization, 1953. Limits of Oceans and Seas. Special Publication No. 23. 〈http:\\www.iho-ohi.net/iho-pubs/IHO_Download.htm#S-23〉.

Ivanov, V.V., Polyakov, I.V., Dmitrenko, I.A., Hansen, E., Repina, I.A., Kirillov, S.A., Mauritzen, C., Simmons, H., Timokhov, L.A., 2009. Seasonal variability in Atlantic Water off Spitsbergen. Deep-Sea Res. I 56, 1–14.

Ivanov, V.V., Shapiro, G.I., Huthnance, J.M., Aleynik, D.L., Golovin, P.N., 2004. Cascades of dense water around the world ocean. Prog. Oceanogr. 60, 47–98.

Jakobsson, M., Grantz, A., Kristoffersen, Y., Macnab, R., 2004. Bathymetry and physiography of the Arctic Ocean and its constituent seas. in: Stein, R., Macdonald, R.W. (Eds.), The Arctic Ocean Organic Carbon Cycle: Present and Past. , Springer, Berlin-Heidelberg-New York, pp. 1–6.

Johansen, S.L., 2008. Climatic Mean and Interannual Variation of Northern Barents Sea Water Mass Distribution and Circulation—A Combined Study of ROMS, Current and Hydrography Observations. M.S. Thesis. Geophysical Institute, University of Bergen, Norway, p. 47.

Kvingedal, B., 2005. Sea-ice extent and variability in the Nordic Seas, 1967–2002. in: Drange, H., Dokken, T., Furevik, T., Gerdes, R., Berger, W. (Eds.), The Nordic Seas: An integrated perspective. Geophysical Monograph Series, vol. 158. American Geophysical Union, pp. 39–49.

Kwok, R., Maslowski, W., Laxon, S., 2005. On large outflows of Arctic sea-ice into the Barents Sea. Geophys. Res. Lett. 32, L22503. doi:10.1029/2005GL024485.

Large, W.G., McWilliams, J.C., Doney, S.C., 1994. Oceanic vertical mixing: a review and a model with a nonlocal boundary layer parameterization. Rev. Geophys. 32, 10937–10954.

Leppäranta, M., 2005. The Drift of Sea Ice. Springer, Berlin.

Loeng, H., 1991. Features of the physical oceanographic conditions in the Barents Sea. Polar Res. 10, 5–18.

Løyning, T., 2001. Hydrography in the north-western Barents Sea, July–August 1996. Polar Res. 20, 1–12.

Lu, P., Li, Z., Cheng, B., Leppäranta, M., 2011. A parameterization of the ice-ocean drag coefficient. J. Geophys. Res. 116, C07019. doi:10.1029/2010JC006878.

Lüpkes, C., Birnbaum, G., 2005. Surface drag in the Arctic marginal sea-ice zone: a comparison of different parameterization concepts. Boundary-Layer Meteorol. 117, 179–211.

Mai, S., 1995. Beziehungen zwischen geometrischer und aerodynamischer Oberflächenrauhigkeit arktischer Meereisflächen. M.S. Thesis. University of Bremen, Germany, p. 75 (in German).

Maslanik, J., Stroeve, J., 1999. Near-Real-Time DMSP SSM/I-SSMIS Daily Polar Gridded Sea-ice Concentrations, 2008–2009. National Snow and Ice Data Center, Boulder, Colorado USA. Digital Media (updated daily).

Maslowski, W., Marble, D., Walczowski, W., Schauer, U., Clement, J., Semtner, A., 2004. On climatological mass, heat and salt transports through the Barents Sea and Fram Strait from a pan-Arctic coupled ice-ocean model simulation. J. Geophys. Res. 109, C03032. doi:10.1029/2001JC001039.

Matishov, G.G., Matishov, D.G., Moiseev, D.V., 2009. Inflow of Atlantic-origin waters to the Barents Sea along glacial troughs. Oceanologica 51, 321–340.

Meier, W., Fetterer, F., Knowles, K., Savoie, M., Brodzik, M.J., 2006. Sea-ice Concentrations from Nimbus-7 SMMR and DMSP SSM/I Passive Microwave Data, 1978–2007. National Snow and Ice Data Center, Boulder, Colorado USA. Digital Media (updated quarterly).

Mellor, G.L., Kantha, L., 1989. An ice-ocean coupled model. J. Geophys. Res. 94, 10937–10954.

Mellor, G.L., Yamada, T., 1982. Development of a turbulence closure-model for geophysical fluid problems. Rev. Geophys. 20, 851–875.

Midttun, L., 1985. Formation of dense bottom water in the Barents Sea. Deep-Sea Res. A 32, 1233–1241.

Mosby, H., 1938. Svalbard Waters. Geofys. Publ. 12, 1–86.

Nilsen, F., Gjevik, B., Schauer, U., 2006. Cooling of the West Spitsbergen current: isopycnal diffusion by topographic vorticity waves. J. Geophys. Res. 111, C08012. doi:10.1029/2005JC002991.

Novitskiy, V.P., 1961. Permanent currents of the northern Barents Sea. Tr. Gos. Okeanogr. Inst. 64, 1–32. (English Translation).

Overgaard, S., Wadhams, P., Leppäranta, M., 1983. Ice properties in the Greenland and Barents Seas during the summer. J. Glaciol. 29, 142–164.

Overland, J.E., Wang, M.Y., 2005. The third Arctic climate pattern: 1930s and early 2000s. Geophys. Res. Lett. 32, L23808. doi:10.1029/2005GL24254.

Overland, J.E., Wang, M., Salo, S., 2008. The recent Arctic warm period. Tellus 60A, 589–597.

Padman, L., Erofeeva, S., 2004. A barotropic inverse tidal model for the Arctic Ocean. Geophys. Res. Lett., 31. doi:10.1029/2003GL019003.

Perrie, W., Hu, Y.C., 1997. Air–ice-ocean momentum exchange. Part II: ice drift. J. Phys. Oceanogr. 27, 1976–1996.

Pfirman, S., Bauch, D., Gammelsrød, T., 1994. The northern Barents Sea: water mass distribution and modification. in: Johannesen, O.M., Muench, R., Overland, J. (Eds.), The Polar Oceans and their Role in Shaping the Global Environment. Geophysical Monograph Series, vol. 85, American Geophysical Union, pp. 77–94.

Pite, H.D., Topham, D.R., Hardenberg, B.J., 1995. Laboratory measurements of the drag force on a family of two-dimensional ice keel models in a two-layer flow. J. Phys. Oceanogr. 25, 3008–3031.

Platov, G.A., 2011. Numerical modeling of the Arctic Ocean deepwater formation: part II. Results of regional and global experiments. Izv. Atmos. Oceanic Phys., 47. doi:10.1134/S0001433811020083.

Postlethwaite, C.F., Morales Maqueda, M.A., Fouest, V.l., Tattersall, G.R., Holt, J., Willmott, A.J., 2011. The effects of tides on dense water formation in Arctic shelf seas. Ocean Sci., 7. doi:10.5194/os-7-203-2011.

Proshutinsky, A.Y., Johnson, M.A., 1997. Two circulation regimes of the wind-driven Arctic Ocean. J. Geophys. Res. 102, 12493–12514.

Pyper, B.J., Peterman, R.M., 1998. Comparison of methods to account for autocorrelation in correlation analyses of fish data. Can. J. Fish. Aquat. Sci. 55, 2127–2140.

Reistad, M., Iden, K.A., 1998. Updating, Correction and Evaluation of a Hindcast Data Base of Air Pressure, Winds and Waves for the North Sea and Barents

Sea. Technical Report 9. Norwegian Meteorological Institute, Oslo, Norway, p. 42.
Rudels, B., 1986. The Θ–S relations in the northern seas: implications for the deep circulation. Polar Res. 4, 133–159.
Rudels, B., Friedrich, H.J., 2000. The transformation of Atlantic Water in the Arctic Ocean and their significance for the freshwater budget. in: Lewis, E.L., Jones, E.P., Lemke, P., Prowse, T.D., Wadhams, P. (Eds.), The Freshwater Budget of the Arctic Ocean. , Kluwer Academic Publishers, pp. 503–532.
Rudels, B., Jones, B., Anderson, L., Kattner, G., 1994. On the Intermediate Depth Waters of the Arctic Ocean. in: Johannessen, O.M., Muench, R., Overland, J. (Eds.), The polar Oceans and their Role in Shaping the Global Enviroment. Geophysical Monograph Series, vol. 85. , American Geophysical Union, pp. 33–46.
Rudels, B., Jones, E.P., Schauer, U., Eriksson, P., 2004. Atlantic sources of the Arctic Ocean surface and halocline waters. Polar Res. 23, 181–208.
Saloranta, T.M., Haugan, P.M., 2001. Interannual variability in the hydrography of Atlantic Water northwest of Svalbard. J. Geophys. Res. 106, 13931–13943.
Saloranta, T.M., Haugan, P.M., 2004. Northward cooling and freshening of the warm core of the West Spitsbergen Current. Polar Res. 23, 79–88.
Sandø, A.B., Nilsen, J.E.Ø., Gao, Y., Lohmann, K., 2010. Importance of heat transport and local air-sea heat fluxes for Barents Sea climate variability. J. Geophys. Res. 115, C07013. doi:10.1029/2009JC005884.
Schauer, U., Muench, R.D., Rudels, B., Timokhov, L., 1997. Impact of eastern Arctic shelf waters on the Nansen Basin intermediate layers. J. Geophys. Res. 102, 3371–3382.
Schlitzer, R., 2009. Ocean Data View. 〈http://odv.awi.de〉.
Skagseth, Ø., Furevik, T., Ingvaldsen, R., Loeng, H., Mork, K.A., Orvik, K.A., Ozhigin, V., 2008. Volume and heat transports to the Arctic Ocean via the Norwegian and Barents Seas. in: Dickson, R., Meincke, J., Rhines, P. (Eds.), Arctic–Subarctic Ocean Fluxes. Springer, Netherlands, pp. 45–64.
Smedsrud, L.H., Ingvaldsen, R., Nilsen, J.E.Ø., Skagseth, Ø., 2010. Heat in the Barents Sea: transport, storage, and surface fluxes. Ocean Sci. 6, 219–234.
Sorteberg, A., Kvingedal, B., 2006. Atmospheric forcing on the Barents Sea winter ice extent. J. Climate 19, 4772–4784.
Steele, M., Morison, J., Curtin, T., 1995. Halocline water formation in the Barents Sea. J. Geophys. Res. 100, 881–894.
Sundfjord, A., Ellingsen, I., Slagstad, D., Svendsen, H., 2008. Vertical mixing in the marginal ice zone of the northern Barents Sea—results from numerical model experiments. Deep-Sea Res. II 55, 2154–2168.
Sundfjord, A., Fer, I., Kasajima, Y., Svendsen, H., 2007. Observations of turbulent mixing and hydrography in the marginal ice zone of the Barents Sea. J. Geophys. Res. 112, C05008. doi:10.1029/2006JC003524.
deSzoeke, R.A., 1980. On the effects of horizontal variability of wind stress on the dynamics of the ocean mixed layer. J. Phys. Oceanogr. 10, 1439–1454.
Tantsiura, A.I., 1973. On seasonal Changes in Currents in the Barents Sea. Transactions of the Polar Scientific Research Institute of Marine Fisheries and Oceanography—N.M. Knipovic (PINRO) (English translation by the Norwegian Polar Research Institute, Oslo, Norway).
Taylor, J., 1976. CONMAP: A Computer Program for Contouring Oceanographic Data. Marine Environmental Data Service, Canada.
Tverberg, V., Nøst, O.A., 2009. Eddy overturning across a shelf edge front: Kongsfjorden, West Spitsbergen. J. Geophys. Res. 114, C04024. doi:10.1029/2008JC005106.
Wadhams, P., 2000. Ice in the Ocean. Gordon and Breach, Amsterdam.
Warner, J.C., Sherwood, C.R., Arango, H.G., Signell, R.P., 2005. Performance of four turbulence closure methods implemented using a generic length scale method. Ocean Model. 8, 81–113.
Zhang, X.D., Sorteberg, A., Zhang, J., Gerdes, R., Comiso, J.C., 2008. Recent radical shifts of atmospheric circulations and rapid changes in Arctic climate system. Geophys. Res. Lett. 35, L22701. doi:10.1029/2008GL035607.

Additional sources

SAT observations in Longyearbyen from: 〈http://eklima.met.no〉.
Sea ice concentration data from: 〈http://nsidc.org〉.
Bathymetry data from: 〈http://www.gebco.net〉.

AGU PUBLICATIONS

Geophysical Research Letters

RESEARCH LETTER
10.1002/2016GL068421

Key Points:
- Arctic layer salinity largely determines stratification and vertical mixing
- The described mechanism has a strong analogy in the interior Arctic Ocean
- The water column structure has been quite stable over the last 40 years

Supporting Information:
- Supporting Information S1

Correspondence to:
S. Lind,
sigridl@imr.no

Citation:
Lind, S., R. B. Ingvaldsen, and T. Furevik (2016), Arctic layer salinity controls heat loss from deep Atlantic layer in seasonally ice-covered areas of the Barents Sea, *Geophys. Res. Lett.*, *43*, doi:10.1002/2016GL068421.

Received 19 JUN 2015
Accepted 9 MAY 2016
Accepted article online 13 MAY 2016

Arctic layer salinity controls heat loss from deep Atlantic layer in seasonally ice-covered areas of the Barents Sea

Sigrid Lind[1,2,3], Randi B. Ingvaldsen[1], and Tore Furevik[2,3]

[1]Institute of Marine Research, Tromsø, Norway, [2]Geophysical Institute, University of Bergen, Bergen, Norway, [3]Bjerknes Centre for Climate Research, Bergen, Norway

Abstract In the seasonally ice-covered northern Barents Sea an intermediate layer of cold and relatively fresh Arctic Water at ~25–110 m depth isolates the sea surface and ice cover from a layer of warm and saline Atlantic Water below, a situation that resembles the cold halocline layer in the Eurasian Basin. The upward heat flux from the Atlantic layer is of major concern. What causes variations in the heat flux and how is the Arctic layer maintained? Using observations, we found that interannual variability in Arctic layer salinity determines the heat flux from the Atlantic layer through its control of stratification and vertical mixing. A relatively fresh Arctic layer effectively suppresses the upward heat flux, while a more saline Arctic layer enhances the heat flux. The corresponding upward salt flux causes a positive feedback. The Arctic layer salinity and the water column structures have been remarkably stable during 1970–2011.

1. Introduction

The northern Barents Sea has had the largest reductions in winter sea ice cover in the Arctic Ocean [*Parkinson and Cavalieri*, 2008; *Screen and Simmonds*, 2010]. These changes were accompanied by increasing temperatures in the entire water column [*Lind and Ingvaldsen*, 2012; *Smedsrud et al*., 2013] as well as in the lower troposphere [*Screen and Simmonds*, 2010; *Cohen et al*., 2014]. The latter has been linked to cold winter extremes in midlatitudes [*Petoukhov and Semenov*, 2010; *Cohen et al*., 2014]. There have also been substantial changes in the northern Barents Sea ecosystem in the last decade, impacting the food chain from plankton production [*Dalpadado et al*., 2014], via fish distribution [*Fossheim et al*., 2015], to marine mammals [*Bogstad et al*., 2015].

The northern Barents Sea has a seasonal ice cover, a surface mixed layer of meltwater in summer and autumn ("the surface layer"), an intermediate, cold, and relatively fresh layer of Arctic Water ("the Arctic layer"), and in most of the region a deep, warm, and saline layer of Atlantic Water ("the Atlantic layer"). In some areas dense water formed by cooling and brine release is present near the bottom [e.g., *Midttun*, 1985; *Årthun et al*., 2011]. The Arctic layer in the northern Barents Sea resembles the cold halocline layer of the Arctic Ocean, and particularly of the Eurasian Basin, in that it has a vertical salinity gradient, a negligible vertical temperature gradient, and that it isolates the surface mixed layer and sea ice cover from the deep Atlantic layer. The cold halocline layer of the Arctic Ocean has been widely discussed and investigated [e.g., *Steele et al*., 1995; *Rudels et al*., 1996; *Steele and Boyd*, 1998; *Bourgain and Gascard*, 2011; *Polyakov et al*., 2013], and particular attention has been given to how it is maintained and what its effect is on the upward heat fluxes from the Atlantic layer, since this is of major importance for understanding changes in the Arctic sea ice cover.

The Arctic layer in the northern Barents Sea is the remnants of the winter mixed layer formed by cooling and brine release in winter [e.g., *Rudels et al*., 1996]. The temperature minimum at ~50–75 m depth with typical characteristics of $S \sim 34.45$–34.5 and $\Theta \sim -1.8$°C [*Loeng*, 1991] marks the vertical extent of the local winter convection [*Rudels et al*., 2004]. Air-ice-ocean interaction in the marginal ice zone could modify Atlantic Water present at the surface such that it forms Arctic Water at intermediate depths with properties equivalent to lower halocline water in the Arctic Ocean [*Steele et al*., 1995]. The winter mixed layer is supplied with freshwater through net precipitation, ice import, river runoff, and "the separator effect" (cf. salt separation in connection with ice production over shallow areas) [*Rudels et al*., 2004]. Sea ice import from the Nansen Basin and Kara Sea is probably the most important freshwater source for the northern Barents Sea [*Kwok et al*., 2005; *Ellingsen et al*., 2009]. There are basically no observation-based estimates of Arctic Water advection within or across the boundaries of the Barents Sea.

The Atlantic layer in the northern Barents Sea ($S \sim 34.8$–35.0 and $\Theta \sim 0$–$4°C$) has a temperature maximum at ~150–200 m depth and occasionally several deeper temperature maxima. It is supplied by a subsurface inflow of Atlantic Water to the Barents Sea from the north—a branch of the eastern boundary current entering the Arctic Ocean through the Fram Strait [e.g., *Mosby*, 1938; *Lind and Ingvaldsen*, 2012]— and from the south—the continuation of the branch entering the Arctic Ocean through the Barents Sea [*Loeng*, 1991]. The strengths and variations in temperature and salinity of the Atlantic Water inflows are unknown. The Atlantic layer is further modified on its way through the northern Barents Sea by mixing with the Arctic Water above [e.g., *Pfirman et al*., 1994]. Observations from the period 1970–2009 showed a positive trend in the Atlantic Water temperature, with a more rapid warming after the late 1990s that also affected the Arctic Water [*Lind and Ingvaldsen*, 2012].

Observations and simulations have shown that velocity shear and turbulent mixing are rather weak away from coastal boundaries in the northern Barents Sea [*Sundfjord et al*., 2007, 2008]. This corresponds well with observed velocity shear below the surface mixed layer in the interior Arctic Ocean [*Fer*, 2009; *Rainville et al*., 2011]. The small vertical turbulent transport of heat allows maintenance of the cold halocline layer [*Fer*, 2009]. The weak turbulent mixing and the vertical structure in the northern Barents Sea, where temperature and salinity increase with depth, are conditions favorable for double-diffusive convection. Such convection has been observed in the region [*Sundfjord et al*., 2007] and may cause significant vertical fluxes of heat and salt. However, *Polyakov et al*. [2013] observed stronger mixing and winter intensification in the Eurasian Basin. They suggested that the winter intensification is a combination of brine-driven convection, large velocity shears caused by storms, and reduced stratification in the upper layers.

The full interplay between the surface-, Arctic-, and Atlantic layers in the northern Barents Sea, as well as the equivalent cold halocline layer in the Eurasian Basin, is poorly understood. In particular, it is not known to what extent the variability in the characteristics of the Arctic layer (i.e., salinity, temperature, and thickness) influences turbulent mixing and heat flux from the Atlantic layer below. In these cold waters, density is mainly controlled by salinity. Thus, the salinity difference between the Arctic and Atlantic waters in the northern Barents Sea maintains a stratification that impedes turbulent mixing. The working hypothesis for this paper is that the Arctic layer salinity determines the interannual variability in stratification in the part of the water column separating the Arctic and Atlantic layers and that this in turn largely determines the bulk turbulent mixing between the two water masses. This implies that the Arctic Water salinity affects the heat flux from the Atlantic layer and thus controls the isolating effect of the Arctic layer.

We use an extensive set of temperature and salinity fields interpolated from late summer/autumn in situ data collected over a period of 42 years (1970–2011). Having defined a schematic two-layer vertical model, we identify the annual depths and characteristics of the Arctic and Atlantic cores and estimate the annual buoyancy frequency of the part of the ocean column bounded by the cores. The effect of the buoyancy frequency variability on the turbulent mixing and corresponding changes in mean properties of the two layers are investigated. The data and methodologies are presented in section 2, and results are given in section 3. Implications of the findings are discussed in section 4 before the paper is summarized and concluded in section 5.

2. Data and Method

2.1. Data Set

Temperature and salinity fields of the Barents Sea were interpolated from a set of 70,000 conductivity-temperature-depth (CTD) profiles and water bottle stations. The data are from August and September every year from 1970 to 2011 and were sampled by the Institute of Marine Research and Knipovich Polar Research Institute of Marine Fisheries and Oceanography in joint Norwegian-Russian surveys designed to cover the entire Barents Sea. The data were interpolated horizontally on finite element grids at 51 vertical z-levels and regridded on a 25×25 km area-conserving grid. (For further details on the interpolation, see Text S1 in the supporting information.) The gridded data were averaged over a subset covering 85,000 km^2 for each year and each vertical level (hereby denoted "the study area," in total, 135 grid cells; Figure 1a). Of the total set of 70,000 CTD profiles, the study area covered approximately 1800 in total (i.e., 13.3 CTD profiles per grid cell on average). The averaging produced one mean vertical temperature-salinity (TS) profile with a vertical resolution of 5 m for each year from 1970 to 2011 (Figure 1b). These TS profiles provided the mean interannual TS variability during the four decades for a bulk part of the northern Barents Sea.

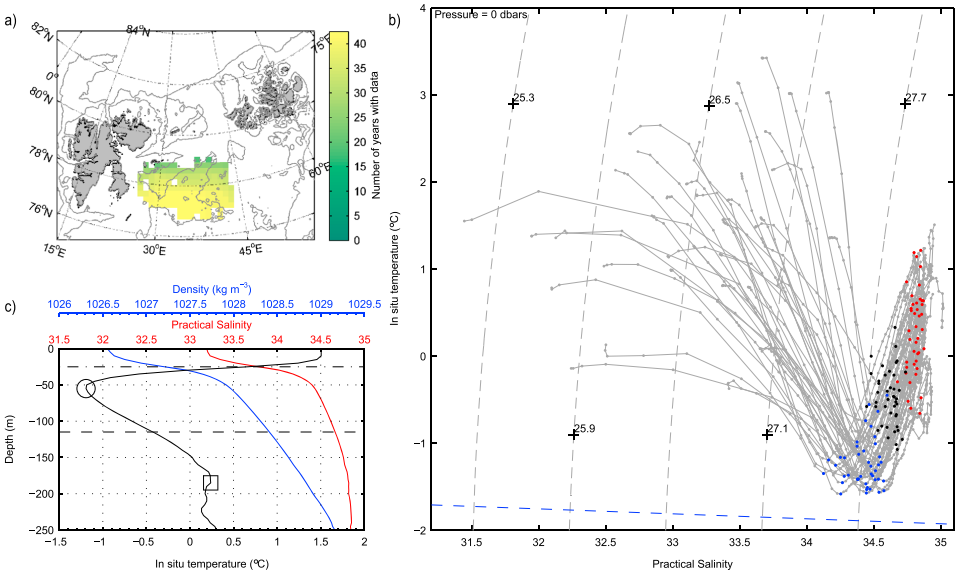

Figure 1. (a) Map of the northern Barents Sea showing the study area with the number of years with data coverage in each grid cell. (b) TS diagram of each annual TS profile averaged over the study area (annotations are the Arctic core (blue dot), the Atlantic core (red dot), and the midpoint in TS space between the cores (black dot)). (c) The 1970–2011 mean TS profile (annotations are the Arctic core (open black circle), the Atlantic core (open black square), the pycnocline (dash-dotted line), and the Arctic/Atlantic interface (dashed line)).

The extent of the study area, its diverseness in topography, and the very good data coverage ensured that the results were representative for the northern Barents Sea. There is considerable local hydrographic variability in space and time as well as substantial regional differences within the study area. These regional differences were averaged out in the annual mean TS profiles. For additional details on the study area, including an evaluation of the sensitivity to depths where data are discarded, see Text S2 and Figure S1.

2.2. Method

2.2.1. Defining the Layers

The temporal mean of the 42 annual TS profiles showed three evident layers (Figure 1c): (1) a relatively fresh, warm, homogenous surface layer; (2) a cold, moderately fresh Arctic layer (the bulk part is <-0.5°C) with a negligible vertical temperature gradient and a temperature minimum at 55 m ("the Arctic core"); and (3) a warm, saline Atlantic layer (the bulk part is >-0.2°C) with a temperature maximum at 185 m ("the Atlantic core"). The depth span of the part of the Arctic layer having a constant or negligible vertical temperature gradient (i.e., $<0.01°\,m^{-1}$) varied in time and space from only a few meters to several tens of meters, and it is averaged out in the temporal-spatial mean profile. Some annual profiles had relatively low temperatures below the Arctic layer, but there was always a temperature maximum below showing presence of (modified) Atlantic Water. There were evidence of mixing between the layers (i.e., linear transitions in temperature and salinity). The TS transitions were very sharp from the surface layer to the Arctic layer (i.e., the pycnocline) and more gradual from the Arctic core to the Atlantic core (i.e., the mixing line between the cores).

In order to define the layers in each annual TS profile, an algorithm was developed (the full description is given in Text S3). The Arctic and Atlantic cores were identified by the temperature minimum and the deeper temperature maximum. The pycnocline was identified by the maximum in salinity gradient above the Arctic core and the Arctic/Atlantic interface by the midpoint in temperature between the cores. The Arctic layer was defined as the vertical layers from the pycnocline to the Arctic/Atlantic interface. Annual mean TS values were calculated for each layer (see Text S3 and Figure S2 for details).

2.2.2. Estimation of Buoyancy Frequency

The buoyancy frequency or Brunt-Väisälä frequency N is a fundamental measure for stratified fluids because it quantifies the opposing force a fluid particle feels when being perturbed vertically. It is defined by

$$N^2 = -\frac{g}{\rho_0}\frac{\mathrm{d}\rho_0(z)}{\mathrm{d}z} \tag{1a}$$

where g is the acceleration due to gravity, ρ_0 is the unperturbed density, and z is the vertical coordinate [e.g., *Gill*, 1982]. We estimated the annual buoyancy frequency between the Arctic and Atlantic cores by inserting

$$\frac{\mathrm{d}\rho_0(z)}{\mathrm{d}z} \approx \frac{\Delta\rho_0}{\Delta z} = \frac{\rho_{\mathrm{Arctic\_core}} - \rho_{\mathrm{Atlantic\_core}}}{z_{\mathrm{Arctic\_core}} - z_{\mathrm{Atlantic\_core}}} \tag{1b}$$

into (1a), where ρ is the potential density and z is the vertical depth of each core, $g = 9.81\ \mathrm{m\,s^{-2}}$, and mean potential density, $\rho_0 = 1028\ \mathrm{kg\,m^{-3}}$. The Richardson number ($Ri = N^2/(\mathrm{d}u/\mathrm{d}z)^2$) is a measure of the relative strengths of buoyancy and velocity shear, and $Ri < 0.25$ is a necessary condition for turbulence to occur [*Gill*, 1982]. This implies that moving a water parcel 10 m vertically for the median value of N estimated here ($4.1 \cdot 10^{-3}\ \mathrm{s^{-1}}$) demands a velocity shear $>0.08\ \mathrm{m\,s^{-1}}$. This is a large velocity shear compared to the measured velocities in the area, which are on the order of 0.01–0.1 $\mathrm{m\,s^{-1}}$ [*Sundfjord et al.*, 2007]. However, the data set used here is averaged over a large area and many subsequent observations, and local effects (e.g., due to topography) and higher-frequency variability (e.g., combined effects of winds and tides) will be more likely to induce turbulence occasionally for weak rather than for strong stratification even if the mean $Ri > 0.25$.

2.2.3. A Two-Layer Model

The observations represent the late summer situation, and the observed vertical structure is a result of Arctic Water that formed during the preceding winter by cooling and brine release, advection of Atlantic Water below, and mixing between the two water masses. To investigate mixing between the layers and to be able to distinguish between cause and effect, a simple two-layer vertical model was defined. The model consisted of two homogenous layers: a winter mixed layer of Arctic Water with temperature and salinity as observed in the Arctic core in autumn, above a layer of Atlantic Water with temperature and salinity as in the Atlantic core. This situation would correspond to the end of the winter season. The observed situation in late summer, with a constant gradient between the cores (Figure 1c), would be a result of mixing between the two layers. The core properties were considered to contain the original properties from winter. The associated buoyancy frequency, based on calculations between the cores, gave a measure of the potential for mixing between the layers.

2.2.4. Statistical Analysis

Correlation coefficients between the time series were estimated (Table S1 in the supporting information). To adjust for autocorrelation, the effective number of degrees of freedom n^* was calculated for each cumulative correlation in accordance with *Pyper and Peterman* [1998]:

$$\frac{1}{n^*} = \frac{1}{n} + \frac{2}{n}\sum_{j=1}^{n/5} r_{xx}(j)\,r_{yy}(j) \tag{2}$$

where n is the sample size (up to and including year n) and $r_{xx}(j)$ and $r_{yy}(j)$ are the autocorrelations of the time series X and Y (up to and including year n) at lag j. A maximum of $n/5$ lags were included in the calculation of n^*. The statistical significance of the linear correlation coefficients was calculated using the derived effective number of degrees of freedom, and the significance criterion was 99%. Linear trends were removed prior to the correlation analysis. No temporal smoothing was applied. Sliding 15 years correlation coefficients were estimated with and without 1 year time lags to examine varying strengths of the relationships over time and causal relations.

3. Results

Hovmöller diagrams of temperature and salinity with indicated core and interface depths showed the temporal development of the layers over the 42 years (Figure 2) (see Text S3 and Figure S2 for more details). The surface layer had the highest temperatures, the largest temperature variations, and a positive trend of 0.26°C $\mathrm{decade^{-1}}$, whereas the Arctic layer generally had low (<0°C) and relatively stable temperatures (Figures 2a and S2a). The Atlantic layer temperature had large interannual variability, multiannual periods

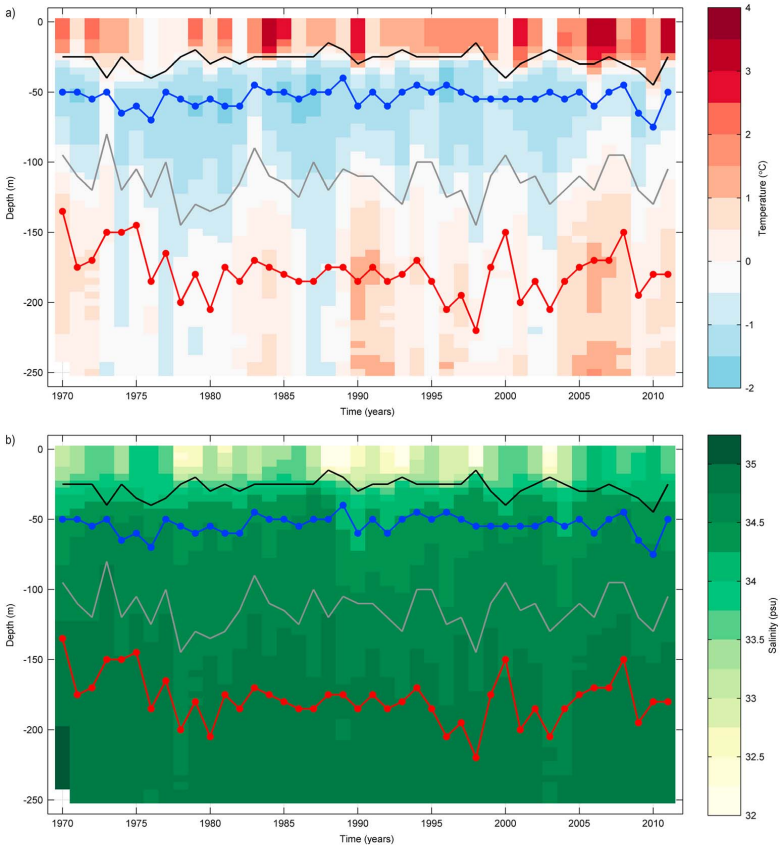

Figure 2. Hovmöller diagram of (a) temperature and (b) salinity. Annotations are the Arctic core (blue line), the Atlantic core (red line), the pycnocline (black line), and the Arctic/Atlantic interface (gray line).

with sustained high or low values, and a positive trend of 0.15°C decade^{-1}. The variations in salinity were largest in the surface layer, moderate in the Arctic layer, and very small in the Atlantic layer (Figures 2b and S2b). There were no obvious trends in salinities or layer thicknesses over the complete time period being studied. The Arctic layer thickness varied mainly due to changes in the depth of the Arctic/Atlantic interface and ranged from 40 to 120 m (Figures 2 and S2c). There is a near-perfect anticorrelation ($r = -0.94$) between the Arctic and Atlantic layer thicknesses since the pycnocline depth is varying very little compared with the Arctic/Atlantic interface (Figures 2 and S2c).

The Arctic core was colder than −0.5°C and generally near 55 m depth, whereas the Atlantic core had larger interannual variability in both temperature and depth (~150–200 m, Figure 2). The depth of the Atlantic core was, however, noticeably stable at ~170 m from the early 1980s to mid-1990s. Density variations in both of the cores were driven by their respective salinity variations and were much larger in the Arctic core due to its higher variability in salinity (Figure S3a). Buoyancy frequency variations were in turn mainly driven by density variations (i.e., salinity variations) in the Arctic core (Figure S3b).

The Arctic core salinity, the buoyancy frequency, and the Atlantic layer mean temperature all had strong interannual variability and sustained periods of larger and smaller values compared with the 1970–2011 mean (Figures 3a–3c). Standardized time series showed that the three time series covaried with a strength

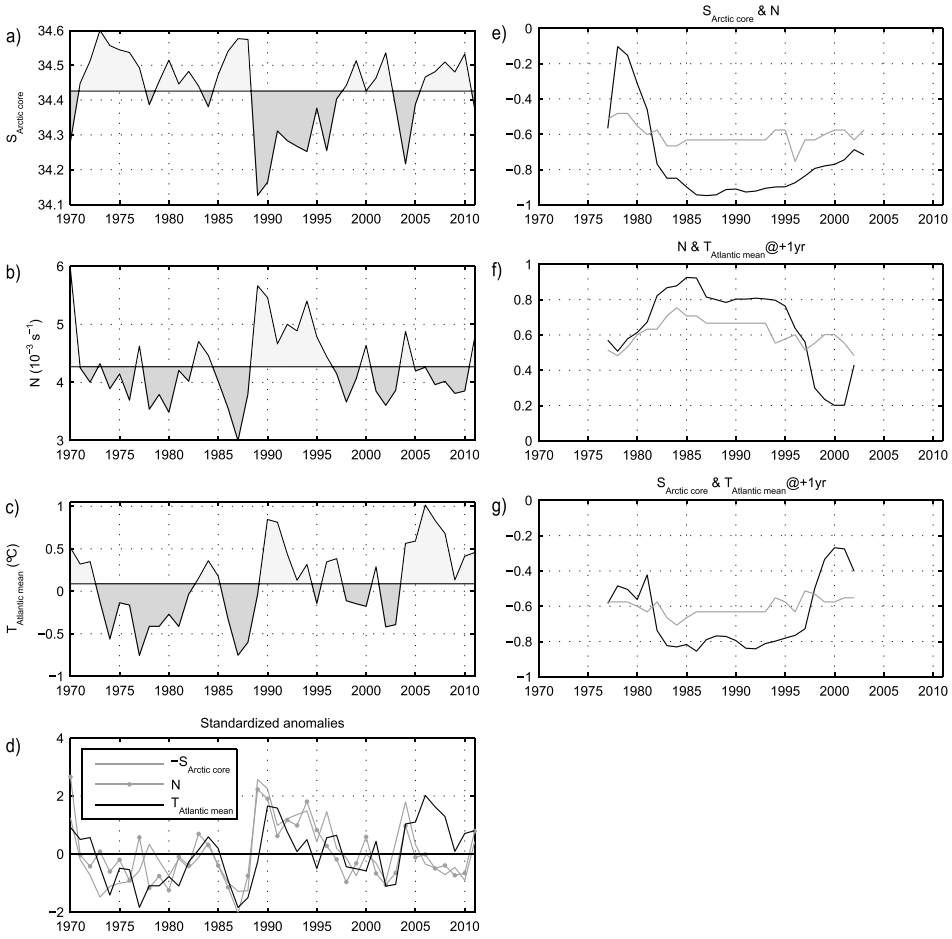

Figure 3. Time series of (a) Arctic core salinity ($S_{Arctic\ core}$), (b) buoyancy frequency (N), (c) Atlantic layer mean temperature ($T_{Atlantic\ mean}$), and (d) standardized anomalies of $-S_{Arctic\ core}$, N, and $T_{Atlantic\ mean}$. In Figures 3a–3c, the baseline is the 1970–2011 mean. Fifteen years sliding correlation coefficients (black lines) with the 95% significance level indicated (gray lines)between (e) $S_{Arctic\ core}$ and N, (f) N and $T_{Atlantic\ mean}$ with a 1 year time lag ($T_{Atlantic\ mean}$@+1yr), and (g) $S_{Arctic\ core}$ and $T_{Atlantic\ mean}$@+1yr.

that varied over time (Figure 3d). In particular, the Atlantic layer mean temperature was "off-track" with the two others in the late 2000s. The statistical analysis showed that the Arctic core salinity had a strong negative correlation with the buoyancy frequency ($r = -0.81$, Table S1 in the supporting information), which in turn had a moderate positive correlation with the Atlantic layer mean temperature ($r = 0.51$). Both of these relationships were strengthened from the early 1980s to the late 1990s, and the latter relationship was substantially stronger when the Atlantic layer mean temperature lagged 1 year (Figures 3e and 3f). The Arctic core salinity also had a significant negative correlation with the Atlantic layer mean temperature over the same period when the Atlantic layer mean temperature lagged 1 year (Figure 3g). The statistical analysis showed that the core properties of the two layers were independent of each other and that the surface layer mean salinity had a moderate positive correlation with the mean salinity of the two deeper layers ($r = 0.56$ and 0.52, respectively).

4. Discussion

4.1. The Cold, Fresh Arctic Layer

The northern Barents Sea hydrography resembles the Eurasian Basin of the Arctic Ocean as it consists of a three-layer structure with a seasonally varying surface layer, a cold, fresh Arctic layer (resembling the cold halocline in the Arctic Ocean), and a warm, saline Atlantic layer. Regarding the Arctic Ocean, there has been some debate on the persistence of the cold halocline layer. While some studies have concluded that the Eurasian Basin cold halocline layer does not appear to be a permanent feature [*Steele and Boyd*, 1998; *Björk et al*., 2002], others have shown that when the layer was defined both in terms of its salinity gradient and its thickness, it was a stable feature for the same area and time period [*Bourgain and Gascard*, 2011]. Some studies have reported direct effects of Atlantic Water on sea ice reduction in the Arctic [*Årthun et al*., 2012; *Polyakov et al*., 2012a, 2012b; *Onarheim et al*., 2014]. However, the documented effect has so far been limited to inflow regions where there is direct contact between Atlantic Water and sea ice, and not where Atlantic Water has been separated from sea ice by an Arctic layer or a cold halocline layer. A major question is how and to what extent the heat from the Atlantic layer can be transferred through the Arctic layer or the cold halocline layer to the surface. Other major questions are what causes variations in the heat transfer and how the Arctic layer or cold halocline layer is maintained.

In this study we investigate the effects of varying stratification in the part of the ocean column bounded by the Arctic and Atlantic cores. As far as we know, this method has never before been applied to a correspondingly extensive observation-based data set. Here the Arctic layer is investigated for a relatively small area compared with the entire Arctic Ocean, but by using observational data with high spatial and temporal resolution over a long time period (42 years), it is possible to investigate relationships between the Arctic and Atlantic layers on an interannual scale with high degree of confidence.

4.2. Heat Loss From the Atlantic Layer

Forming a relatively homogenous horizontal layer bounded by the Arctic layer above and the bottom below, the Atlantic layer in the northern Barents Sea will mainly lose heat (and salt) by vertical mixing and mainly gain heat and salt from advection of "new" Atlantic Water into the area. Advection is always active, and variations in it must be considered when discussing observed changes.

Salinity in the Arctic layer is the main factor contributing to the interannual variability of buoyancy frequency in the ocean column between the Arctic and Atlantic cores ($r = -0.81$, Table S1). This indicates that the Arctic core salinity determines 66% of the interannual variability in the buoyancy frequency when considering the entire time span. The Arctic core salinity is the only factor having substantial impact on the stratification (Figure S3), because salinity variations determine density variations at low temperatures and because Atlantic Water shows very little interannual variability in salinity compared with Arctic Water.

Buoyancy frequency, in turn, is seen to affect the Atlantic layer mean temperature ($r = 0.51$). The correlation increases to $r = 0.63$ when the Atlantic layer mean temperature lags 1 year, which should be expected since mixing between the water masses is a very slow process and the mixing is probably most intense during winter, causing a delayed response. If only vertical mixing was active, that is, if there were no advection of new Atlantic Water, the fluxes of heat and salt from the Atlantic layer would correspond. Changes in Atlantic core temperature and salinity from 1 year to the next did show some coherence (not shown), but the signal in salinity was indistinct due to very weak variability. Mixing coefficient estimates based on the changes in temperature of the cores from 1 year to the next ranged from -2.3 to $1.3 \cdot 10^{-4}\ m^2\ s^{-1}$. All processes that alter the temperatures will influence these estimates, including horizontal mixing and advection in the two layers and exchanges with the atmosphere during winter. The years with the unphysical negative values could thus be due to strong advection of new warm Atlantic Water in the Atlantic layer, causing this advected signal to dominate over cooling from vertical mixing with the Arctic layer. There are, however, no observations that can support or contradict this hypothesis. The layered structure has been remarkably stable over the four decades, implying some overall balance between the effects of mixing and advection.

Despite being generally a slow process, the results show that vertical mixing is important for the hydrography of the northern Barents Sea. Given that the Atlantic layer mean temperature generally is lower after a year of weak stratification, the variations of the Arctic layer salinity and the Atlantic layer temperature are clearly indicative of mixing between the two layers being the main source of heat loss for the Atlantic layer.

The results also demonstrate that Arctic layer salinity is the main driver of variability in stratification and vertical mixing, and it is therefore the main driver for heat loss from the Atlantic layer.

In addition to heat loss, variations in lateral heat advection will cause changes in the Atlantic layer temperature. The relation between Arctic layer salinity and Atlantic layer temperature varies with time and was stronger in the period between the early 1980s and the late 1990s than before and after that interval (Figures 3d and 3g). The relation weakened after 2005, with a positive anomaly in the Atlantic layer temperature despite weak stratification. This was likely caused by increased lateral heat advection, in line with *Årthun et al.* [2012] and *Lind and Ingvaldsen* [2012], but other explanations such as weaker winds and less mixing cannot be ruled out. During this period, the Atlantic layer mean temperature was higher than the long-term average despite weak stratification and hypothesized strong mixing/high heat loss. If the stratification had been stronger, more of the advected heat would probably have been kept in the Atlantic layer and the temperatures would hence have been even higher.

The vertical mixing appears as a clear signal on the Arctic layer mean temperature and salinity, which are both positively correlated with Atlantic layer mean temperature and salinity ($r = 0.52$ and 0.54, respectively; see Table S1). The correlations become insignificant when the Arctic layer lags 1 year, indicating that the Arctic layer characteristics are largely determined by exchanges with the atmosphere in winter. As the Arctic layer becomes warmer and more saline from mixing with the Atlantic layer, it also becomes thinner ($r = -0.53$ between Arctic layer thickness and Arctic layer mean temperature). This agrees with the spatial relation between temperature, salinity, and thickness in the vertical section of temperature and salinity in Figure 3 of *Lind and Ingvaldsen* [2012] which is also inverse proportional: The Arctic layer is colder, fresher, and thicker in Olga Basin and gradually becomes warmer, saltier, and thinner toward northwest in the trench system, i.e., near the Atlantic inflow in Franz-Victoria Trough where the upward heat and salt fluxes probably are larger.

4.3. Maintenance of the Arctic Layer

Our results show that high salinity in the Arctic core will increase the turbulent mixing between the Arctic and Atlantic layers, which will make the Arctic layer even more saline due to the high salinity of Atlantic Water ($r = 0.54$). This will decrease the stratification and make the ocean column more prone to turbulent mixing (a positive feedback). Consequently, the Arctic layer needs a regular supply of freshwater to be sustained; otherwise, it will be slowly eroded from below.

An important source of freshwater in this region is downward mixing of surface meltwater in fall and early winter. Ice import from the Nansen Basin and Kara Sea can be substantial and explain part of the year-to-year variability in the Barents Sea ice cover [e.g., *Hilmer et al.*, 1998], and it is one of the two major freshwater sources for the Barents Sea [*Kwok et al.*, 2005]. Observations indicate huge interannual variability in ice import (from $-280\ km^3$ to $340\ km^3$) that averages to only $40\ km^3$ [*Kwok et al.*, 2005]. A simulation also indicated very large interannual variability (from 143 to $1236\ km^3\ yr^{-1}$), and this caused substantial variability in annual ice melt and freshwater content that affected the stratification, vertical mixing rates, and heat loss from the Atlantic Water [*Ellingsen et al.*, 2009]. This finding is in line with *Aagaard and Woodgate* [2001] who also found that ice import, melting, and freshwater injection into the interior ocean are important processes in the northern Barents Sea.

Our results are in line with the former investigations and also demonstrate that the freshwater input is critical for maintaining the Arctic layer and keeping its isolating effect. Over the 42 years, the Arctic layer salinity and water column structures (i.e., core depths, interface depths, and buoyancy frequency) in the study area were remarkably stable in spite of the large changes in the Barents Sea and the Arctic climate in general. This may indicate some delay or stabilizing factor, perhaps due to accumulated freshwater in the Arctic layer in combination with the positive salinity feedback. However, it is beyond the scope of this paper to investigate this. Still, sustained major reductions in freshwater input to the Arctic layer will at some point start a slow erosion of the Arctic layer from below which eventually changes the northern Barents Sea into a warmer, vertically homogeneous domain like the southern Barents Sea. Thus, future ice reductions in the Arctic Ocean, if associated ice import decreases substantially, will most likely change the water column structure in the northern Barents Sea entirely. This will likely have a substantial impact on the Arctic Ocean, as the northern Barents Sea has been found to give a considerable contribution to maintenance of the cold halocline layer in the Arctic Ocean [e.g., *Steele et al.*, 1995] as well as to water mass transformations affecting the deeper parts of the Arctic Ocean [e.g., *Rudels et al.*, 1994; *Aagaard and Woodgate*, 2001].

5. Conclusions

The objective of this paper is to investigate the effect of the Arctic layer salinity on turbulent mixing between the intermediate, cold Arctic layer and the deep, warm Atlantic layer in the northern Barents Sea using observational data with high spatial and temporal resolution over a period of 42 years. We find that salinity variations of the Arctic layer determine 66% of the interannual variability in stratification, which in turn seem to largely determine heat loss in the Atlantic layer. The relative strengths of the effect of mixing and advection varied over the study period: The mixing effect was particularly evident from the early 1980s to late 1990s, whereas advection probably dominated between 2005 and 2010, a period of stronger advection of Atlantic Water coming from the north [cf. *Lind and Ingvaldsen*, 2012].

This mixing process constitutes a positive feedback because stratification decreases when mixing occurs. This implies that the Arctic layer is depending on freshwater supply to remain relatively fresh compared with the Atlantic layer, which keeps the heat and salt fluxes from the Atlantic layer at a minimum. Compared with the large changes in the northern Barents Sea in general (e.g., in the sea ice field), the water column structure and the Arctic layer salinity have been noticeably stable over the investigated 42 years. There is a clear analogy between the Arctic layer in the Barents Sea and the cold halocline layer in the Eurasian Basin. Processes that keep the Arctic layer relatively fresh are important for limiting the heat loss from the Atlantic layer and maintaining conditions favorable for ice production.

Acknowledgments

The data sampled by the Institute of Marine Research are available in World Ocean Data Base 2013 (https://www.nodc.noaa.gov/OC5/WOD13/). The data sampled by Knipovich Polar Research Institute of Marine Fisheries and Oceanography are not publicly available due to Russian data restriction policy. The work of S.L. and R.I. was supported by the Research Council of Norway (RCN 228896) and the Institute of Marine Research, Norway. The work of T.F. was supported by the University of Bergen. We thank Arild Sundfjord, Vigdis Tverberg, and two anonymous reviewers for their valuable discussions and comments.

References

Aagaard, K., and R. A. Woodgate (2001), Some thoughts on the freezing and melting of sea ice and their effects on the ocean, *Ocean Model.*, *3*(1–2), 127–135, doi:10.1016/S1463-5003(01)00005-1.

Årthun, M., R. B. Ingvaldsen, L. H. Smedsrud, and C. Schrum (2011), Dense water formation and circulation in the Barents Sea, *Deep Sea Res., Part I*, *58*, 801–817, doi:10.1016/j.dsr.2011.06.001.

Årthun, M., T. Eldevik, L. H. Smedsrud, Ø. Skagseth, and R. B. Ingvaldsen (2012), Quantifying the influence of Atlantic heat on Barents Sea ice variability and retreat, *J. Clim.*, *25*, 4736–4743, doi:10.1175/JCLI-D-11-00466.1.

Björk, G., J. Söderkvist, P. Winsor, A. Nikolopoulos, and M. Steele (2002), Return of the cold halocline layer to the Amundsen Basin of the Arctic Ocean: Implications for the sea ice mass balance, *Geophys. Res. Lett.*, *29*(11), 1513, doi:10.1029/2001GL014157.

Bogstad, B., H. Gjøsæter, T. Haug, and U. Lindstrøm (2015), A review of the battle for food in the Barents Sea: Cod vs. marine mammals, *Front. Ecol. Evol.*, *3*(29), doi:10.3389/fevo.2015.00029.

Bourgain, P., and J. C. Gascard (2011), The Arctic Ocean halocline and its interannual variability from 1997 to 2008, *Deep Sea Res., Part I*, *58*(7), 745–756, doi:10.1016/j.dsr.2011.05.001.

Cohen, J., et al. (2014), Recent Arctic amplification and extreme mid-latitude weather, *Nat. Geosci.*, *7*, 627–637, doi:10.1038/ngeo2234.

Dalpadado, P., K. R. Arrigo, S. S. Hjøllo, F. Rey, R. B. Ingvaldsen, E. Sperfeld, G. L. van Dijken, L. C. Stige, A. Olsen, and G. Ottersen (2014), Productivity in the Barents Sea—Response to recent climate variability, *PLoS One*, *9*(5), doi:10.1371/journal.pone.0095273.

Ellingsen, I., D. Slagstad, and A. Sundfjord (2009), Modification of water masses in the Barents Sea and its coupling to ice dynamics: A model study, *Ocean Dyn.*, *59*(6), 1095–1108, doi:10.1007/s10236-009-0230-5.

Fer, I. (2009), Weak vertical diffusion allows maintenance of cold halocline in the central Arctic, *Atmos. Ocean. Sci. Lett.*, *2*(3), 148–152.

Fossheim, M., R. Primicerio, E. Johannesen, R. B. Ingvaldsen, M. M. Aschan, and A. V. Dolgov (2015), Recent warming leads to a rapid borealization of fish communities in the Arctic, *Nat. Clim. Change*, doi:10.1038/nclimate2647.

Gill, A. E. (1982), *Atmosphere-Ocean Dynamics*, Academic Press, New York.

Hilmer, M., M. Harder, and P. Lemke (1998), Sea ice transport: A highly variable link between Arctic and North Atlantic, *Geophys. Res. Lett.*, *25*, 3359–3362, doi:10.1029/98GL52360.

Kwok, R., W. Maslowski, and S. W. Laxon (2005), On large outflows of Arctic sea ice into the Barents Sea, *Geophys. Res. Lett.*, *32*, L22503, doi:10.1029/2005GL024485.

Lind, S., and R. B. Ingvaldsen (2012), Variability and impacts of Atlantic Water entering the Barents Sea from the north, *Deep Sea Res., Part I*, *62*, 70–88, doi:10.1016/j.dsr.2011.12.007.

Loeng, H. (1991), Features of the physical oceanographic conditions in the Barents Sea, *Polar Res.*, *10*(1), 5–18, doi:10.3402/polar.v10i1.6723.

Midttun, L. (1985), Formation of dense bottom water in the Barents Sea, *Deep Sea Res., Part A*, *32*(10), 1233–1241, doi:10.1016/0198-0149(85)90006-8.

Mosby, H. (1938), Svalbard waters, *Geofys. Publ.*, *12*(4), 1–86.

Onarheim, I. H., L. H. Smedsrud, R. B. Ingvaldsen, and F. Nilsen (2014), Loss of sea ice during winter north of Svalbard, *Tellus A*, *66*, doi:10.3402/tellusa.v66.23933.

Parkinson, C. L., and D. J. Cavalieri (2008), Arctic sea ice variability and trends, 1979–2006, *J. Geophys. Res.*, *113*, C07003, doi:10.1029/2007JC004558.

Petoukhov, V., and V. A. Semenov (2010), A link between reduced Barents-Kara sea ice and cold winter extremes over northern continents, *J. Geophys. Res.*, *115*, D21111, doi:10.1029/2009JD013568.

Pfirman, S. L., D. Bauch, and T. Gammelsrød (1994), The northern Barents Sea: Water mass distribution and modification, in *The Polar Oceans and Their Role in Shaping the Global Environment*, *Geophys. Monogr. Ser.*, vol. 85, edited by O. M. Johannesen et al., pp. 77–94, AGU, Washington, D. C., doi:10.1029/GM085p0077.

Polyakov, I. V., A. V. Pnyushkov, and L. A. Timokhov (2012a), Warming of the Intermediate Atlantic Water of the Arctic Ocean in the 2000s, *J. Clim.*, *25*(23), 8362–8370, doi:10.1175/JCLI-D-12-00266.1.

Polyakov, I. V., J. E. Walsh, and R. Kwok (2012b), Recent changes of Arctic multiyear sea ice coverage and the likely causes, *Bull. Am. Meteorol. Soc.*, *93*(2), 145–151, doi:10.1175/BAMS-D-11-00070.1.

Polyakov, I. V., A. V. Pnyushkov, R. Rember, L. Padman, E. C. Carmack, and J. M. Jackson (2013), Winter convection transports Atlantic Water heat to the surface layer in the eastern Arctic Ocean, *J. Phys. Oceanogr.*, *43*(10), 2142–2155, doi:10.1175/JPO-D-12-0169.1.

Pyper, B. J., and R. M. Peterman (1998), Comparison of methods to account for autocorrelation in correlation analyses of fish data, *Can. J. Fish. Aquat. Sci.*, *55*(9), 2127–2140, doi:10.1139/f98-104.

Rainville, L., C. M. Lee, and R. A. Woodgate (2011), Impact of wind-driven mixing in the Arctic Ocean, *Oceanography*, *24*(3), 136–145, doi:10.5670/oceanog.2011.65.

Rudels, B., E. P. Jones, L. G. Anderson, and G. Kattner (1994), On the intermediate depth waters of the Arctic Ocean, in *The Polar Oceans and Their Role in Shaping the Global Environment*, *Geophys. Monogr. Ser.*, vol. 85, edited by O. M. Johannesen et al., pp. 33–46, AGU, Washington, D. C., doi:10.1029/GM085p0033.

Rudels, B., L. G. Anderson, and E. P. Jones (1996), Formation and evolution of the surface mixed layer and halocline of the Arctic Ocean, *J. Geophys. Res.*, *101*, 8807–8821, doi:10.1029/96JC00143.

Rudels, B., E. P. Jones, U. Schauer, and P. Eriksson (2004), Atlantic sources of the Arctic Ocean surface and halocline waters, *Polar Res.*, *23*, 181–208, doi:10.1111/j.1751-8369.2004.tb00007.x.

Screen, J. A., and I. Simmonds (2010), Increasing fall-winter energy loss from the Arctic Ocean and its role in Arctic temperature amplification, *Geophys. Res. Lett.*, *37*, L16707, doi:10.1029/2010GL044136.

Smedsrud, L. H., et al. (2013), The role of the Barents Sea in the Arctic climate system, *Rev. Geophys.*, *51*, 415–449, doi:10.1002/rog.20017.

Steele, M., and T. Boyd (1998), Retreat of the cold halocline layer in the Arctic Ocean, *J. Geophys. Res.*, *103*, 10,419–10,435, doi:10.1029/98JC00580.

Steele, M., J. H. Morison, and T. B. Curtin (1995), Halocline water formation in the Barents Sea, *J. Geophys. Res.*, *100*, 881–894, doi:10.1029/94JC02310.

Sundfjord, A., I. Fer, Y. Kasajima, and H. Svendsen (2007), Observations of turbulent mixing and hydrography in the marginal ice zone of the Barents Sea, *J. Geophys. Res.*, *112*, C05008, doi:10.1029/2006JC003524.

Sundfjord, A., I. Ellingsen, D. Slagstad, and H. Svendsen (2008), Vertical mixing in the marginal ice zone of the northern Barents Sea—Results from numerical model experiments, *Deep Sea Res., Part II*, *55*(20–21), 2154–2168, doi:10.1016/j.dsr2.2008.05.027.

Graphic design: Communication Division, UiB / Print: Skipnes Kommunikasjon AS

uib.no

ISBN: 978-82-308-3769-6